



**Utrecht
University**

Effect of vegetation on evolving channel patterns in experimental salt marshes

**Faculty of Geosciences
Department of
Physical Geography
MSc programme
Earth Surface and Water**

Master Thesis

**Jan-Eike Rossius
7062052**

**First supervisor:
Prof. Maarten G. Kleinhans**

**Second supervisor:
Dr. Jana Eichel**

August 12, 2022

Abstract

Salt marshes are highly valuable habitats and offer many important ecosystem services. They protect the coast from erosion and serve as pollution filters and nursery ground for fish. Furthermore, they are capable of storing a very high amount of carbon in a relatively short time. Their protection and restoration is therefore crucial for the mitigation of global warming. Salt marshes are shaped by a variety of biogeomorphic feedbacks which depend on many different biotic and abiotic aspects. In order to clarify the conditions needed for such biogeomorphic interactions and the effect of different vegetation colonisation patterns on it, four scaled landscape experiments were conducted in the tidal flume "The Metronome". Two experiments were unvegetated control experiments and two included vegetation. In one of these, the seeds were spread by the flowing water and in the other, circular patches were sown and expanded manually at random locations.

Vegetation focused the flow more effectively and led to a split-up into several channels further from the inlet, resulting in a longer and straighter main channel and an overall further landward expansion of the system. Despite these clear morphological differences, quantitative measures of the system, like eroded volume or drainage density, were very similar in all experiments, showing that these are mainly shaped by the hydrodynamic boundary conditions and that the experiments are very comparable.

The vegetation-induced morphological differences described above were more pronounced in the experiment with hydrochorous seed spreading than in the experiment with patchy seeding. This is a result of the patch locations being pre-determined randomly. This disables the biogeomorphic feedback between low flow velocities and vegetation establishment, causing further reduction of flow velocities. The completeness of this positive feedback loop is crucial for the emergence of a self-organised landscape. Even though the patches were very dense and covered a larger area of the system than the vegetation in the experiment with hydrochorous seed spreading, they were not able to foster the evolution of a self-organised landscape in a similar way.

Only locally, the patches sometimes had strong biogeomorphic effects. Their density enables them to show such effects, like the stabilisation of features or the initiation of channels around them, very clearly, but only if they are in the locally favourable position for that. Since this was not the case everywhere, the overall morphology in the experiment with patchy seeding was less self-organised and more similar to the unvegetated control experiments even though the biogeomorphic feedbacks were more pronounced in some locations. The feedback loops of biogeomorphic feedbacks thus need to be complete to enable the emergence of a fully self-organised landscape.

Samenvatting

Schorren zijn waardevolle habitats en bieden vele belangrijke ecosystemendiensten. Ze beschermen de kust tegen erosie en dienen als ontreinigingsfilter en kweekplaats voor vissen. Verder kunnen ze grote hoeveelheden koolstof binden. Hun bescherming en herstel is daarom cruciaal voor de beperking van klimaatverandering. Schorren worden door verschillende biogeomorfologische feedbacks gevormd, die van veel biotische en abiotische factoren afhankelijk zijn. Om de benodigde condities voor deze biogeomorfologische interacties en de invloed van verschillende kolonisatiepatronen van vegetatie daarop op te helderen, werden vier geschaalde landschapsexperimenten in de getijdenstroomgoot "Metronoom" uitgevoerd: Twee onbegroeide controle experimenten en twee experimenten met vegetatie. In één van deze experimenten werden de zaaides door het stromende water verspreid, in de andere werden handmatig ronde patches op toevallige locaties gezaaid.

Vegetatie leidde tot een efficiëntere concentratie van de stroming en een meer bovenstroomse opsplitsing van verschillende geulen. Dit resulteerde in een langere rechte hoofdgeul en een algeheel grotere landwaartse expansie van het systeem. Ondanks deze duidelijke morfologische verschillen waren kwantitatieve maten van het systeem, zoals geërodeerd volume of afwateringsdichtheid, zeer gelijkaardig in alle experimenten. Dit toont aan dat deze hoofdzakelijk worden gevormd door de hydrodynamische randvoorwaarden en dat de experimenten zeer vergelijkbaar zijn.

De hierboven beschreven en door vegetatie veroorzaakte morfologische verschillen waren in het experiment met hydrochore zaadverspreiding duidelijker dan in het experiment met gezaaide patches. De toevallig en van tevoren bepaalde locaties van de patches stellen de biogeomorfologische feedbacks tussen lage stroomsnelheden, de kolonisatie door vegetatie en vervolgens verder afnemende stroomsnelheden buiten werking. De volledigheid van deze positieve terugkoppeling is cruciaal voor de vorming van een zelf-georganiseerd landschap. Hoewel de patches heel dicht waren en een grotere oppervlakte bedekten dan de vegetatie in het experiment met hydrochore zaadverspreiding, waren ze niet in staat om op een vergelijkbare manier tot een zelf-georganiseerd landschap te leiden.

Alleen lokaal hadden de patches soms sterke biogeomorfologische effecten. Hun dichtheid maakt het mogelijk om zulke effecten, zoals de stabilisatie van kenmerken of de initiatie van geulen eromheen, duidelijk te laten zien, maar alleen als ze daarvoor op een lokaal geschikte plek zaten. Omdat dit niet overal het geval was, leek het experiment met gezaaide patches qua algemene morfologie meer op de controle experimenten en was minder zelf-georganiseerd, ondanks de duidelijkere biogeomorfologische feedbacks op sommige plekken. De terugkoppelingen van biogeomorfologische feedbacks moeten dus compleet zijn om een zelf-georganiseerd landschap te kunnen vormen.

Zusammenfassung

Salzwiesen sind wertvolle Habitate und erfüllen zahlreiche wichtige Ökosystemdienstleistungen. Sie schützen die Küste vor Erosion und dienen als Filter für Verschmutzungen und Kinderstube für Fische. Außerdem können sie große Mengen Kohlenstoff in kurzer Zeit binden. Ihr Schutz und ihre Renaturierung sind daher essenziell für die Abschwächung der globalen Erwärmung. Salzwiesen werden von einer Vielzahl biogeomorphologischer Feedbacks geformt, die von verschiedenen biotischen und abiotischen Faktoren abhängen. Um die Bedingungen, die für die biogeomorphologischen Wechselwirkungen nötig sind, und den Einfluss verschiedener Besiedlungsmuster der Vegetation darauf aufzuklären, wurden vier Landschaftsexperimente im Labormaßstab im Gezeitensimulator "Metronom" durchgeführt: zwei unbewachsene Kontrollexperimente und zwei Experimente mit Vegetation. In einem dieser Experimente wurden die Samen mit der Strömung verteilt und in anderen wurden händisch runde Patches an zufälligen Stellen gesät und erweitert.

Die durch Vegetation effektiver fokussierte Strömung im dadurch längeren und geraderen Hauptpriel führte zu einer Aufspaltung in mehrere Priele und generellen Ausbreitung des Systems weiter landwärts. Trotz dieser klaren morphologischen Unterschiede waren die Experimente untereinander gut vergleichbar, was sich in der Ähnlichkeit quantitativer, vor allem durch die Hydrodynamik bestimmter Kenngrößen des Systems, wie des erodierten Volumens oder der Einzugsdichte, zeigt.

Die oben beschriebenen, durch Vegetation verursachten morphologischen Unterschiede waren aufgrund der im Vorhinein zufällig festgelegten Patchpositionen ausgeprägter im Experiment mit hydrochorer Samenverteilung als im Experiment mit gesäten Patches. Das biogeomorphologische Feedback zwischen niedrigen Strömungsgeschwindigkeiten und Vegetationsansiedlung, die Strömungsgeschwindigkeiten weiter reduziert, ist durch die Bestimmung der Positionen unterbunden. Die Vollständigkeit dieser positiven Rückkopplung ist essenziell für das Entstehen einer selbstorganisierten Landschaft. Obwohl die Patches sehr dicht waren und eine größere Fläche bedeckten als die Vegetation im Experiment mit hydrochorer Samenverteilung, konnten sie die Entstehung einer selbstorganisierten Landschaft nicht im gleichen Maße fördern.

Nur lokal hatten die Patches aufgrund ihrer Dichte teilweise starke biogeomorphologische Effekte, wie die Stabilisierung von Merkmalen oder die Prielinittierung. Trotz dieser teils deutlicheren Effekte, war die Morphologie im Experiment mit gesäten Patches weniger selbstorganisiert und den Kontrollexperimenten ähnlicher, da sich nicht alle Patches an geeigneten Stellen befanden. Für die Entstehung einer selbstorganisierten Landschaft müssen die Rückkopplungen in biogeomorphologischen Wechselbeziehungen daher vollständig sein.

Contents

List of Figures	VI
List of Symbols	VIII
1. Introduction	1
2. Background	2
2.1. Concepts on biogeomorphic interactions of vegetation	2
2.2. Biogeomorphology of salt marshes	6
2.2.1. Occurrence of salt marshes	6
2.2.2. Salt marsh zonation	8
2.2.3. Channel networks on tidal flats and marshes	9
2.2.4. Human use and impact	12
2.2.5. Knowledge gap	14
2.3. Research questions and hypotheses	15
3. Methods	17
3.1. General experimental set-up in the Metronome	17
3.2. Experimental scenarios	19
3.2.1. Control experiments	19
3.2.2. Experiment with hydrochorous seed spreading	19
3.2.3. Experiment with patchy seeding	19
3.3. Data acquisition	21
3.4. Data analysis	22
3.4.1. DEM processing	22
3.4.2. Erosion and sedimentation	23
3.4.3. Vegetation detection	23
3.4.4. Water level measurements and maps of sub-, inter- and supratidal area	23
3.4.5. Channel network	24
4. Results	25
4.1. Morphological development	25
4.1.1. General development in all experiments	25
4.1.2. Control experiments	25

4.1.3. Experiment with hydrochorous seed spreading	30
4.1.4. Experiment with patchy seeding	33
4.2. Comparison of the system development	36
4.3. Vegetation cover and biogeomorphic interactions	39
4.4. Channel network	44
4.5. Water level measurements	48
5. Discussion	51
5.1. Role of initial conditions and experiment comparability	51
5.2. Biogeomorphic feedback window in experimental salt marshes	52
5.2.1. Integration of concepts	52
5.2.2. Quantified conceptual representation of the experiments	55
5.3. Water levels and tidal frame	59
5.4. Comparison and evolution of channel networks	59
5.5. Comparison with natural salt marshes	61
5.6. Implications for salt marsh restoration and future research	63
6. Conclusion	65
A. Channel network maps	67
B. Maps of sub-, inter- and supratidal area	72
C. Positions and reliability of water level measurements	77
References	82
Acknowledgements	90
Statement of originality	92

List of Figures

2.1. Concept of the biogeomorphic feedback window on lateral moraine slopes by Eichel et al. (2016)	4
2.2. Concept on conditions for salt marsh self-organisation, edited after Schwarz et al. (2018)	5
2.3. Satellite images of salt marshes in different settings	7
2.4. Plants species in the lower zones of European salt marshes	8
3.1. Initial conditions of the system in all experiments	18
3.2. Individual plants of <i>Lotus pedunculatus</i> at different growth stages	20
3.3. Spatial distribution and growth of the theoretically planned vegetation patches over the course of the eight sowing events	21
4.1. Morphological development of the first unvegetated control experiment	26
4.2. Erosion and sedimentation during the first unvegetated control experiment with respect to the respective previous DEM	27
4.3. Morphological development of the second unvegetated control experiment	28
4.4. Erosion and sedimentation during the second unvegetated control experiment with respect to the respective previous DEM	29
4.5. Morphological development of the experiment with hydrochorous seed spreading	31
4.6. Erosion and sedimentation during the experiment with hydrochorous seed spreading with respect to the respective previous DEM	32
4.7. Morphological development of the experiment with patchy seeding	34
4.8. Erosion and sedimentation during the experiment with patchy seeding with respect to the respective previous DEM	35
4.9. Eroded volume, eroded surface area and average erosion depth over time in the different experiments	37
4.10. Eroded volume, eroded surface area and average erosion depth along the flume in the different experiments	38
4.11. Map of vegetation age and type in both vegetated experiments	40
4.12. Vegetation cover of different types over time	41
4.13. Different local effects of vegetation	43
4.14. Exemplary maps of the channel network at different stages in all experiments	45
4.15. Evolution of different variables characterising the channel network over time	46

4.16. Different variables characterising the channel network along the flume	47
4.17. Water surface elevation at different stages during the experiments	49
4.18. Exemplary maps of sub-, inter- and supratidal areas from different stages of the experiments	49
4.19. Evolution of sub-, inter- and supratidal area over time in all experiments	50
5.1. Concept on the conditions for biogeomorphic interactions	53
5.2. Quantitative representation of the experiments in the concept on the conditions for biogeomorphic interactions	56
5.3. Evolution of the total network length in the experiments and at Skallingen, Denmark	60
A.1. Channel network maps of the first unvegetated control experiment	68
A.2. Channel network maps of the second unvegetated control experiment	69
A.3. Channel network maps of the experiment with hydrochorous seed spreading	70
A.4. Channel network maps of the experiment with patchy seeding	71
B.1. Tidal maps of the first unvegetated control experiment	73
B.2. Tidal maps of the second unvegetated control experiment	74
B.3. Tidal maps of the experiment with hydrochorous seed spreading	75
B.4. Tidal maps of the experiment with patchy seeding	76
C.1. Positions and reliability of water level measurements in the first unvegetated control experiment	78
C.2. Positions and reliability of water level measurements in the second unvegetated control experiment	79
C.3. Positions and reliability of water level measurements in the experiment with hydro- chorous seed spreading	80
C.4. Positions and reliability of water level measurements in the experiment with patchy seeding	81

List of Symbols

Symbol	Description	Unit	Pages
A	watershed area	m^2	9, 11
B	blue image band	–	23
D_{10}	10 % of the sediment is finer than this grain size	m	17
D_{50}	median grain size	m	17
D_{90}	10 % of the sediment is coarser than this grain size	m	17
D_d	drainage density	m^{-1}	11, 15, 24, 44, 46, 59
e_g	geometric efficiency	–	12, 14, 15, 24, 44, 46, 47, 48, 59, 60
G	green image band	–	23
GCC	green chromatic coordinate	–	23
l_H	Hortonian length	m	11, 12
m_{UPL}	mean unchannelled path length	m	11, 12, 15, 24, 44, 46, 47, 48, 59, 60
P	tidal prism	m^3	9
R	red image band	–	23
ΣL	total length of channels	m	11, 44, 46, 47, 48, 59, 60

1. Introduction

Salt marshes are "areas of land covered chiefly by halophytic vegetation which are regularly flooded by the sea" (Allen, 2000). They form a unique ecosystem and are home to many highly specialised plant species. They are exposed to significant tidal energy and often strong water level fluctuations. Additionally, waves and storm surges can affect salt marshes as well, as they are connected to the open sea. This setting suggests that these environments are shaped by the hydrodynamics. The plant species living there must be well adapted to these circumstances. However, it is not only adaptation that enables the plants to live in salt marshes. The salt marsh vegetation has a significant effect on the surrounding landscape as it slows down flow over it (Baptist et al., 2007) and can thus enhance channel formation elsewhere (Schwarz et al., 2014; Temmerman et al., 2007). Consequently, not only hydrodynamics shape the morphology of salt marshes but vegetation is a significant factor as well. Studies on salt marsh morphology therefore must not ignore vegetation effects, especially if they examine the channel network.

Due to the large variety of aspects influencing the morphology of salt marshes and the often lacking long-term field data, the identification and quantification of different factors' effects has proven to be difficult (Wiberg et al., 2020). The exact conditions under which biogeomorphic feedbacks can significantly shape salt marsh landscapes are not entirely clear, neither is the exact extent of these effects.

Within this thesis, the biogeomorphic interactions in salt marshes will be examined by analysing scaled landscape experiments. A total of four experiments were conducted among which two unvegetated control experiments and two experiments with vegetation. This vegetation colonised the system differently. In one experiment, the seeds were spread by the flowing water whereas they were sown manually in patches in the other. The boundary conditions were otherwise constant. This makes the direct comparison of different colonisation strategies and the emerging biogeomorphic feedbacks possible. Their effect on the morphology and channel network as well as on quantitative measures of the system will be studied in this thesis and related to the existing scientific knowledge.

2. Background

2.1. Concepts on biogeomorphic interactions of vegetation

Many different landscapes are shaped not only by abiotic boundary conditions but also by the organisms living in it. Prominent examples are termites, beavers or corals that build mounds, dams and reefs. By creating these large solid structures, they create their own habitat. This has significant impacts on the surrounding landscape or even creates entirely new landscapes. Other species find a habitat in these as well and are thus dependent on the species that actively shape their environment. This principle was described by Jones et al. (1996) and was called eco-engineering.

Not only animals can act as eco-engineers but also many plants. Strong biogeomorphic effects of plants are for example reported from dunes (Reijers et al., 2019). Here, the marram grasses like *Calamagrotis arenaria* or *Ammophila breviligulata* enhance the deposition of aeolian sand and thereby shape their environment in such a way that it provides the best habitat for themselves (Reijers et al., 2019). Also in fluvial systems, vegetation significantly affects the landscape development (Braudrick et al., 2009; Corenblit et al., 2011; Oorschot et al., 2016; Tal & Paola, 2010; van Dijk et al., 2013). The stabilising effect of plants on river banks even is the main driver of the emergence of meandering rivers from braided systems (Braudrick et al., 2009; McMahon & Davies, 2018).

Vegetation can also act as eco-engineer in very harsh environments as for example moraine slopes in glacier forelands (Eichel et al., 2016; Eichel et al., 2013). When these areas are first colonised, only pioneer species with a high resilience can settle here as the geomorphic processes of high severity, like for example debris flows, occur regularly. Engineering species like *Dryas octopetala* cannot settle yet at this stage as severe geomorphic processes take place that inhibit their growth. Only when process magnitude further decreases, they can establish. If their cover is high enough, in this specific case roughly 35 %, they start to act as eco-engineer (Eichel et al., 2016). Their roots stabilise the slope and bound solifluction becomes the dominant process over other processes. The processes taking place now are generally less severe but occur more often or even continuously, also due to the eco-engineering vegetation. *Dryas octopetala* has flexible roots and is therefore well adapted to bound solifluction and now finds itself in an ideal habitat (Eichel et al., 2013). When the bed is further stabilised, also other species can establish (Eichel et al., 2016). These often have competitive advantages over *Dryas octopetala* on a stable ground and can thus become dominant now. The landscape is then not further shaped by biogeomorphic interactions (Eichel et al., 2016).

Generally, plants need certain conditions under which they can establish and grow. Especially when they are juvenile, they are sensitive to disturbances and need the right environment to develop into a mature plant. Such conditions are not found everywhere, as most landscapes are characterised by gradual or abrupt changes, so that conditions can vary already locally. They can also change in time since many landscapes follow an evolution over time or certain features migrate, like for example meander bends in rivers. Disturbances for vegetation are formed by geomorphic processes of different magnitudes and frequencies. The most severe processes often occur only rarely whereas processes with a lower impact occur more often or even happen gradually. Depending on the plant species and its adaptations, these processes or different kinds of stress can hinder the vegetation establishment or can be a reason for mortality. If conditions are very favourable over a sufficient time span, a landscape fully covered in vegetation emerges, whereas it stays or becomes bare if conditions do not allow for the long-term settling of vegetation.

Many of these general limitations to and conditions for plant growth were integrated in a concept by Eichel et al. (2016) that was developed based on the observations of biogeomorphic interactions on lateral moraine slopes. (see fig. 2.1). In the landscape evolution, different thresholds or threshold ranges were identified. The first settling opportunity for the engineering species is called establishment threshold (see fig. 2.1). The beginning of landscape shaping biogeomorphic interactions with a sufficient vegetation cover marks the engineering threshold (see fig. 2.1). When other plants finally suppress the further growth of the engineering species, the so-called competition threshold is crossed (see fig. 2.1). The engineering and competition threshold define the zone in which biogeomorphic interactions shape the landscape. This zone is called biogeomorphic feedback window (see fig. 2.1) (Eichel et al., 2016). If the geomorphic boundary conditions lie within this window, biogeomorphic interaction can occur if the right plant species colonise the landscape.

Similar aspects can be found in salt marshes. The hydrodynamic energy often is a limiting factor for vegetation settlement here. Tidal inundation takes place regularly and causes long inundation periods of the plants which imposes stress on them, especially because the water is usually saline. Also the currents can form a limitation for vegetation establishment. Only when the hydrodynamic energy input is low enough, vegetation establishment is possible, in other words, the establishment threshold is crossed. For a large part, biogeomorphic interactions on salt marshes take place via flow velocities and their alterations. Vegetation slows down flow over it by inducing extra friction. To maintain the same discharge over a certain marsh platform section, flow is then accelerated in adjacent unvegetated areas (Temmerman et al., 2007). If this effect is large enough, vegetation starts to act as eco-engineer, so the engineering threshold is crossed and the biogeomorphic feedback window is entered. The competition threshold is less applicable to salt marshes, as other species than the pioneer species, that also act as engineering species here, barely ever settle on the marsh edges due to the frequent inundation and high salinity. Significant aggradation and/or coastline progradation would therefore be the only possibility.

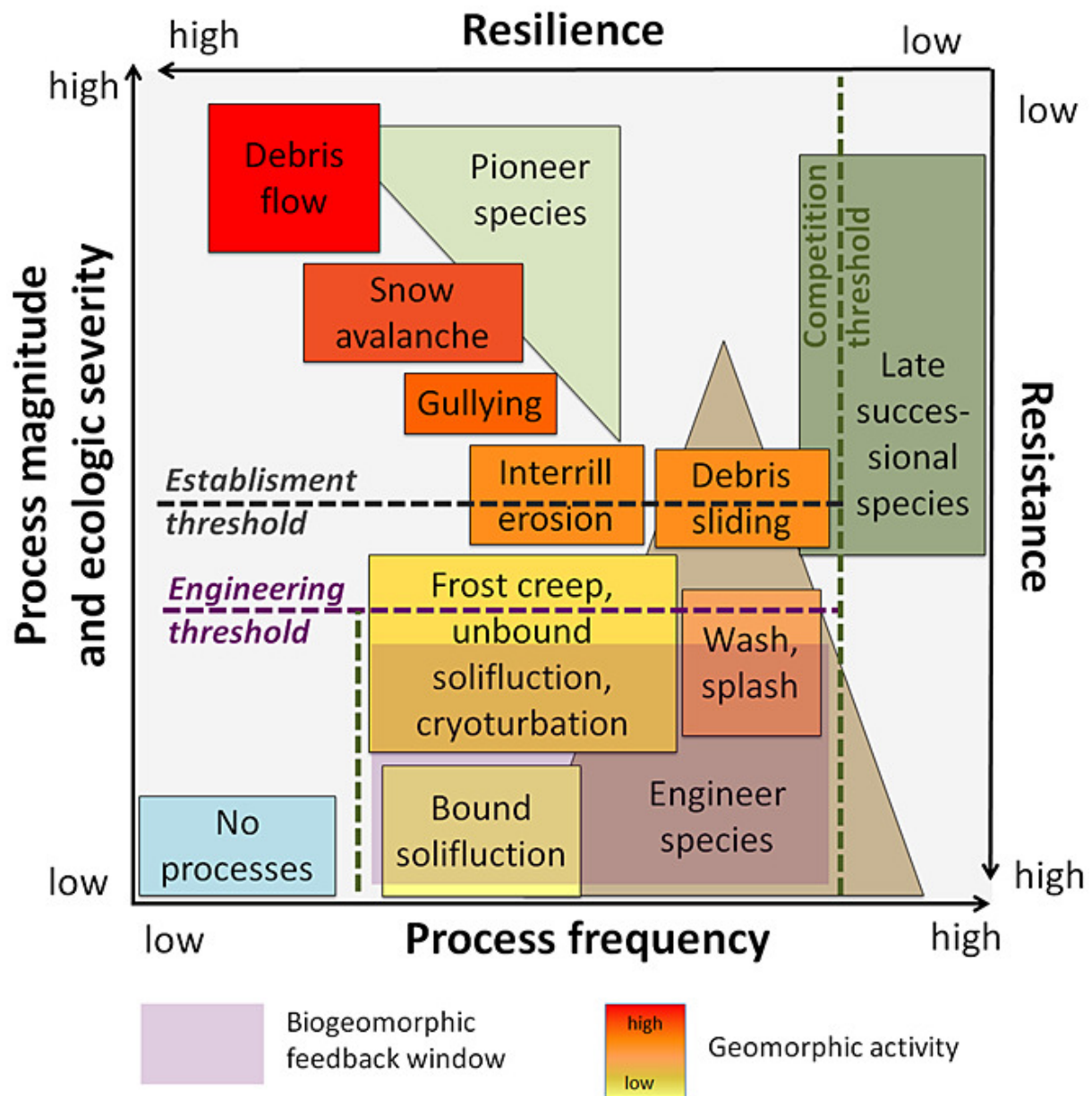


Figure 2.1.: Concept of the biogeomorphic feedback window and different thresholds on lateral moraine slopes depending on geomorphic process frequency and intensity as well as plant resilience and resistance. By Eichel et al. (2016)

These biogeomorphic interactions were summarised in a concept by Schwarz et al. (2018) (see fig. 2.2). In this concept, the degree of biogeomorphic self-organisation is coupled to the respective timescales of hydrogeomorphic development and vegetation colonisation. Only if these are similar, biogeomorphic feedbacks shape the landscape (Schwarz et al., 2018). This zone of self-organisation of the landscape (see fig. 2.2) can be seen as biogeomorphic feedback window (see fig. 2.1) and its boundaries as thresholds for establishment/engineering and stabilisation. Stabilisation in this case takes place via higher vegetation density and slower hydrogeomorphic development rather than by the colonisation through successive plant species.

This concept implies that, if vegetation colonisation takes place on a slower timescale than the geomorphic evolution purely driven by abiotic hydrodynamic forcings, these dominate the landscape evolution and vegetation settlement is hindered, sometimes causing the landscape to stay bare (see fig. 2.2). If the opposite is the case and vegetation colonisation happens much faster than geomorphic evolution driven by abiotic factors, the emerging vegetation cover stabilises the existing landscape, which will therefore also under these circumstances not be shaped by biogeomorphological feedbacks (see fig. 2.2). The speed of colonisation also often correlates with the pattern. Species growing in a patchy pattern tend to cover an area more slowly than species which grow more homogeneously spread (Schwarz et al., 2018). A similar dependency of the emerging landscape on the respective timescale of vegetation settling and morphodynamics was also found for meandering rivers (Oorschot et al., 2016).

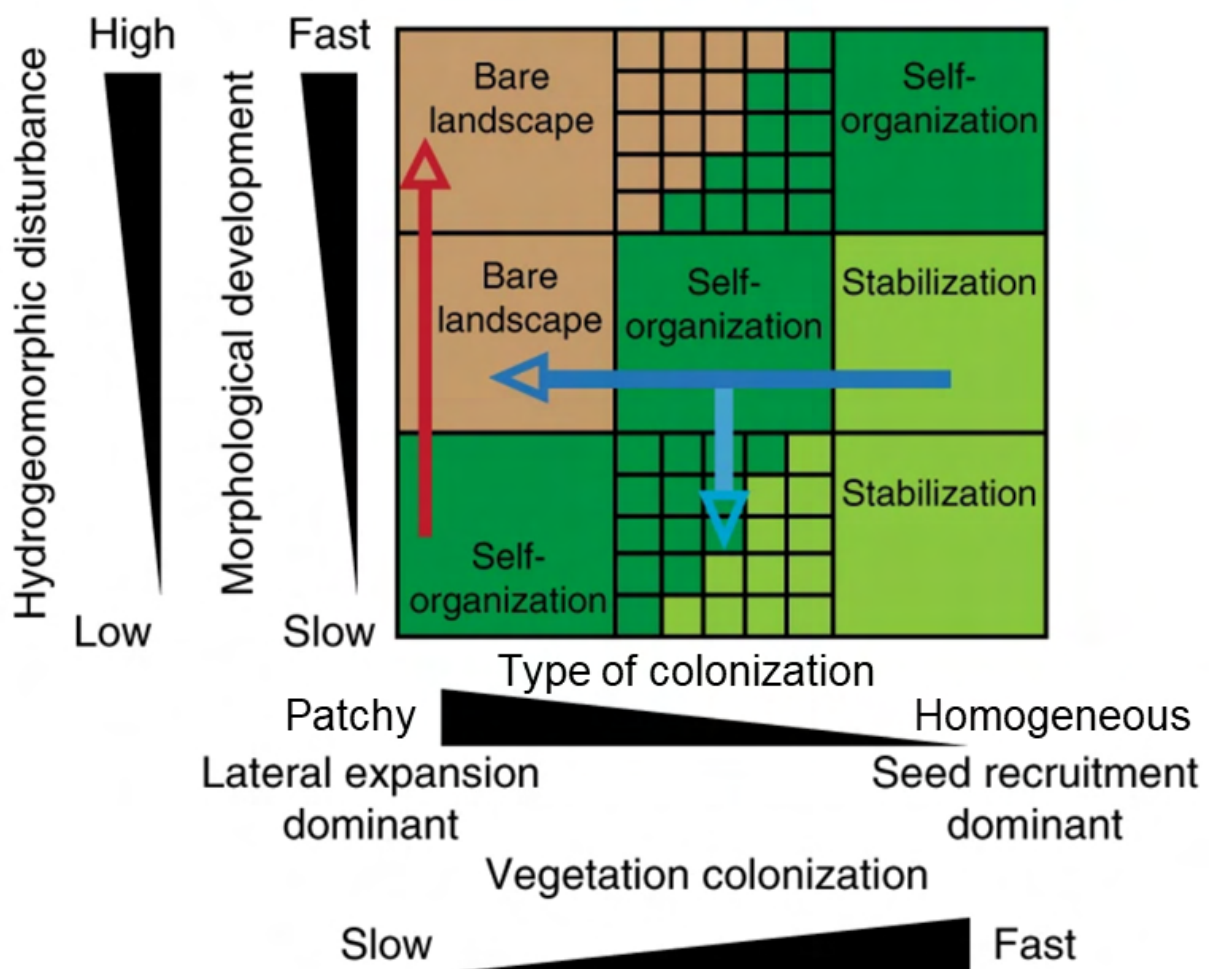


Figure 2.2.: Concept on conditions for salt marsh self-organisation depending on speed and dynamics of morphological development and speed and type of vegetation colonisation resulting in a self-organised landscape if these processes are balanced, or a bare landscape if hydromorphodynamics dominate, or a stabilised landscape if vegetation colonisation dominates. Red and blue arrows indicate transitions that can occur if hydromorphodynamics change or shifts in colonising species takes place. Edited after Schwarz et al. (2018)

Both concepts, the one by Eichel et al. (2016) and the one by Schwarz et al. (2018), show that biogeomorphic feedbacks act as major factor in landscape evolution only under certain conditions. They indicate whether this is the case, or if either biological stabilisation or an (almost) bare landscape occur, and if so, why. The concepts provide a way to simplify the various interactions in nature and give a clear overview of the conditions and main drivers of biogeomorphic interactions. They allow for an integration of new findings into the existing knowledge about the system and therefore lead to a better understanding. They also indicate where further research is needed, for example a quantification of thresholds.

Even though both concepts were developed for different landscapes, they have many aspects in common, even if they are named differently. The concept on the biogeomorphic feedback window (Eichel et al., 2016) is a bit more general as it includes many different processes of various magnitudes and frequencies whereas all geomorphic processes are reduced to hydrodynamic disturbance in the concept of Schwarz et al. (2018). But since tides play the most important role in these landscapes, this is a reasonable simplification. Another difference is that pioneer species mostly already act as eco-engineer in many coastal environments while this is not the case on high mountain slopes (Eichel et al., 2016). This shows how prone coastal environments are to biogeomorphic feedbacks and therefore highlights the importance of their study.

2.2. Biogeomorphology of salt marshes

2.2.1. Occurrence of salt marshes

Salt marshes occur on almost all continents in tropical to arctic climates (Kelleway et al., 2017; Mcowen et al., 2017). However, in tropical and subtropical climates, mangroves often prevail in environmental settings suitable for salt marshes (Kelleway et al., 2017). The total area of salt marshes in the world is estimated at 54 951 km² (Mcowen et al., 2017). In Europe, salt marshes mainly occur along the North Sea and Atlantic coast, as they are characterised by tidal influence and saline conditions (Allen, 2000). But they also occur in the Mediterranean, e.g. in the Venice Lagoon (Kearney & Fagherazzi, 2016).

Several types of salt marshes exist in different local geographical settings. Dijkema (1987) distinguished three different types of salt marshes: Barrier-connected salt marshes, foreland salt marshes and estuarine salt marshes. Allen (2000) used a total of seven categories of which some are sub-categories of the ones used by Dijkema (1987): Open coast marshes (see fig. 2.3 d)), marshes enclosed by barrier spits along open coasts (see fig. 2.3 a)), marshes in open (see fig. 2.3 c)) and restricted embayments, marshes in either open estuaries (see fig. 2.3 b)) or such restricted by spits and marshes in rias and lochs (see fig. 2.3 f)).

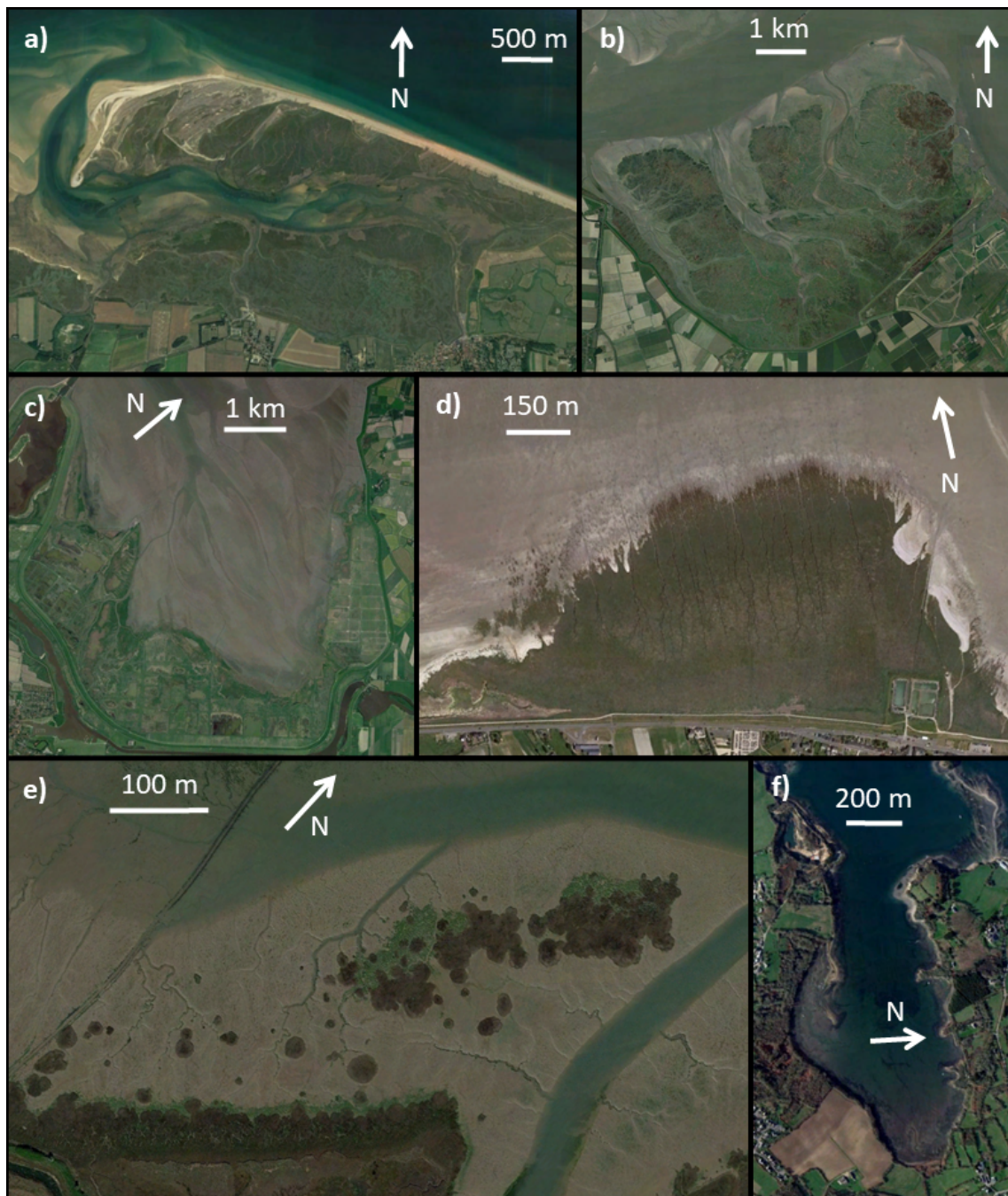


Figure 2.3.: Satellite images of salt marshes in different settings. The seaward edge is always at the top. (a) Salt marsh enclosed by Blakeney Point spit, Norfolk, UK; (b) Estuarine salt marshes "Verdrongen Land van Saeftinghe", Zeeland, NL; (c) Foreland salt marshes in the Leybucht embayment, East Frisia, DE; (d) Open coast marsh near Le Vivier-sur-Mer, Brittany, FR; (e) Patchy colonisation of mudflat in Hamford Water tidal basin, Essex, UK; (f) marshes in ria "Anse de Penn Foul", Brittany, FR. All images were retrieved from Google Earth in April 2022.

2.2.2. Salt marsh zonation

Tidal marshes form around the mean high water line in the high intertidal to low supratidal area. The lower and more seaward parts of the marsh are flooded every tidal cycle. This pioneer zone is colonised by only few species with high salinity and inundation tolerance (Boorman, 1999). In European salt marshes, this zone is usually dominated by the perennial *Spartina anglica* (see fig. 2.4 a)), the annual *Salicornia europaea* (see fig. 2.4 b)) and/or the perennial *Suaeda maritima* (see fig. 2.4 c)) (Boorman, 1999).

With increasing elevation, inundation times and frequencies as well as soil salinity and hydrodynamic energy usually decrease. Consequently, the species composition becomes more diverse, as the environment is less extreme and therefore asks less specialisation (Boorman, 1999). Examples of genera occurring in the higher areas of tidal marshes are *Juncus*, *Puccinellia*, *Limonium*, *Plantago* or *Elymus* (Rupprecht et al., 2017; Wolters et al., 2005).

Almost all different plant species occur in certain zones where they are the dominant species. These zones are mainly characterised by elevation relative to the tidal frame, but also distance to channels and soil salinity play a role (Allen, 2000; Boorman, 1999; Townend et al., 2011). Some studies even suggest that elevation is not the major factor determining the species assemblage. Instead, soil salinity seems to play a more important role as the elevation range in which a certain species occurs is locally constant but significantly varies between different marsh sites (Silvestri et al., 2005). However, close to the shoreline, elevation still seems to play an important role as

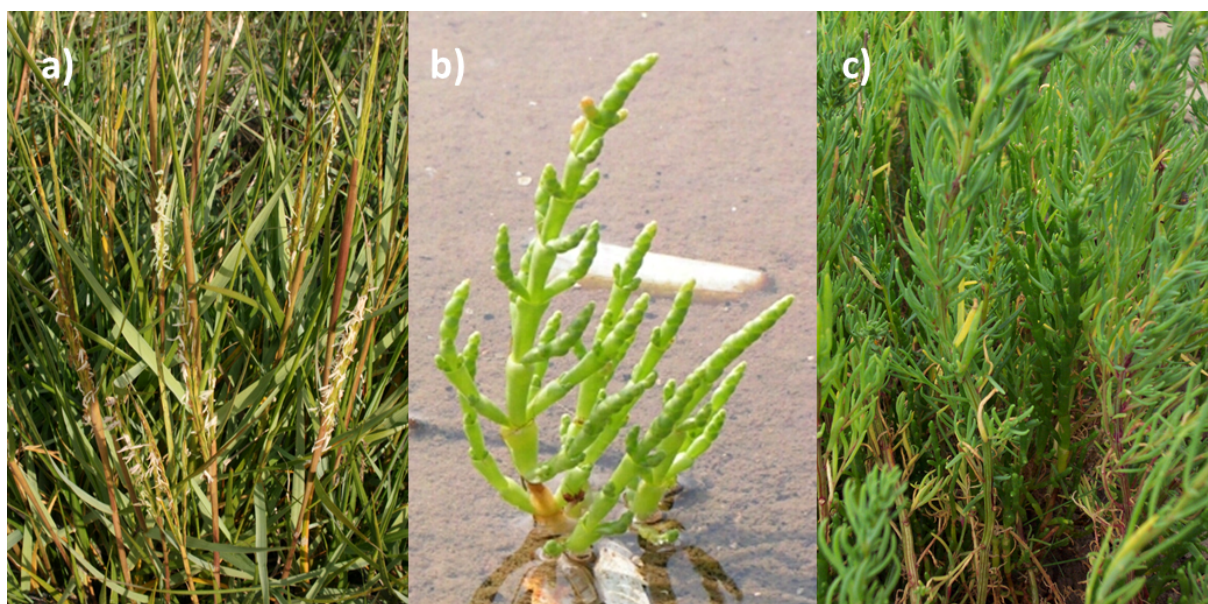


Figure 2.4.: Plants species in the lower zones of European salt marshes: (a) *Spartina anglica*, (b) *Salicornia europaea* and (c) *Suaeda maritima* (Sources: (a) Sten - Own work, CC BY-SA 3.0, <https://commons.wikimedia.org/w/index.php?curid=4833986>, (b) M.Buschmann - Germany, CC BY-SA 3.0, <https://commons.wikimedia.org/w/index.php?curid=269039>, (c) Vatadoshu - Own work, CC0, <https://commons.wikimedia.org/w/index.php?curid=39536724>, all retrieved on 8 April 2022)

it is the main variable determining inundation time and frequency, which can prevent settling and cause mortality.

Plants are not only adapted to the corresponding elevation range but also actively shape them (Marani et al., 2013). Through organic sedimentation, they control the marsh elevation. This elevation is found to be slightly above the theoretically ideal elevation for biomass production of a certain species. This increases the resilience of the ecosystem as biomass production and therefore organic sedimentation is increased if the elevation drops under that of the equilibrium state (Marani et al., 2013).

This biomass-elevation feedback results in multi-modal elevation distribution of salt marshes with highly specialised plant species. Microcliffs often occur between the terrace-like platforms that are dominated by a certain species (Marani et al., 2013). In many cases, continuous accretion occurs seaward of the lowest microcliff until this newly created platform reached a higher elevation. Storms can erode this again and the salt marsh edge lies further landward. After this, the lower parts are recolonised by pioneer species and the marsh elevation increases again by sedimentation. When this behaviour occurs, the marsh is a so-called cyclic salt marsh. (Allen, 2000).

2.2.3. Channel networks on tidal flats and marshes

Hydrodynamic control

Intertidal mudflats and salt marshes are characterised by distinct channel networks. The number and size of channels is generally assumed to be dependent on hydrodynamic parameters like the tidal prism P (D'Alpaos et al., 2010). This is based on the assumption that the entire tidal prism P is exchanged via the channel network (Rinaldo et al., 1999; Vandenbruwaene et al., 2013) and therefore determining its cross-sectional area, similarly to tidal inlets (Hughes, 2002). This is an assumption in many (modelling) studies on tidal channel networks (D'Alpaos et al., 2007; Kirwan & Murray, 2007). However, field studies suggest that is not always the case (Temmerman et al., 2005; Vandenbruwaene et al., 2013). Instead, sheetflow occurs over the entire marsh area when water levels are higher, especially when the vegetation is overtopped and inundated completely. This is mainly important for the lower seaward parts of marshes, as the inundation height is larger here. This implies that not the entire tidal prism P determines the channel dimensions. Only the part of P that is drained through the channel networks has morphological effects on it (Vandenbruwaene et al., 2013). This is supported by the findings of Kleinhans et al. (2009) that the main erosion work in the channel network is done in the late ebb phase when drainage only takes place via channels and not via the entire marsh. It further implies that major effects take place in the transition from a bare tidal flat to a vegetated marsh but not in the transitions from a low vegetated marsh to a high vegetated marsh (Vandenbruwaene et al., 2013). Tidal watershed area A , determined by water surface gradients instead of topography, was found to have an effect on tidal channel dimensions as well (Marani et al., 2003; Rinaldo et al., 1999).

Vegetation effects

Nowadays, the important role of vegetation in the initiation and development of channel networks on tidal marshes is widely recognised (Bij de Vaate et al., 2020; Kearney & Fagherazzi, 2016; Schwarz et al., 2014; Schwarz et al., 2018; Temmerman et al., 2007; Townend et al., 2011; Vandenbruwaene et al., 2013). Generally, vegetation is known to stabilise banks and locally limit erosion, for example in fluvial systems (Braudrick et al., 2009; Oorschot et al., 2016; Tal & Paola, 2010; van Dijk et al., 2013). Here, it is also crucial for the emergence of meandering channels (Braudrick et al., 2009; McMahon & Davies, 2018). Tidal networks are often characterised by meandering channels as well. However, the mechanisms causing this kind of meandering and the migration of channels are different from those in meandering rivers (Kleinhans et al., 2009). Deepening of the channels happens via backward eroding steps in the final ebb stage. This is due to the cohesive nature of the fine sediment that is usually present on mudflats and salt marshes, which prevents erosion except in the most energetic flow stage of the tidal cycle (Kleinhans et al., 2009).

Vegetation has a crucial role in the initiation of channels when previously bare mud flats are colonised (Bij de Vaate et al., 2020; Schwarz et al., 2014; Schwarz et al., 2018; Temmerman et al., 2007). As Temmerman et al. (2007) found, the specific effects of vegetation are scale-dependent: Plants do not only prevent erosion locally and stabilise the sediment and channel banks, but also enhance erosion further away as the flow is hindered by vegetation patches and is therefore concentrated between them. This leads to vegetation-induced channel initiation. Whether this process is dominant in the formation of a channel network also depends on the initial bathymetry (Schwarz et al., 2014). A homogeneous bare mud flat is much more prone to vegetation-induced channel erosion when it is colonised than heterogeneous mud flats with a pre-existing channel network. Here, vegetation-stabilised channel network inheritance is more likely to happen (Schwarz et al., 2014).

Effects of different colonisation strategies

The biogeomorphic effects are not the same for all halophytic marsh vegetation. Instead, they are highly species dependent (Bij de Vaate et al., 2020; Schwarz et al., 2018). This is not only because different species settle at different elevations, but also because of different plant life-history traits, as observed by Schwarz et al. (2018).

The annual pioneer species *Salicornia europaea* spreads via hydrochorous distribution of seeds and is characterised by a high seed recruitment. This leads to a relatively homogeneous colonisation of tidal flats. In consequence, vegetation induced flow resistance and bank stabilisation is relatively constant in space. This favours the stabilisation of an existing channel network (Schwarz et al., 2018).

In contrast, *Spartina anglica*, another important pioneer species in European salt marshes, is characterised by a low seed recruitment and therefore settles in only few locations. However, it can clonally expand laterally via tillering. This results in dense patches of vegetation with bare areas in between (see also fig. 2.3 e)). These patches promote the erosion of channels in between where flow is concentrated (Schwarz et al., 2018; Temmerman et al., 2007). If vegetation expansion and morphodynamic development take place on similar time scales, a self-organised landscape emerges (Schwarz et al., 2018).

Quantitative measures of tidal channel networks

Channel networks can be described by several quantitative measures. The oldest and most widely applied measures were introduced by Horton (1932, 1945). A main variable is the drainage density D_d (Horton, 1932). It describes how well or poorly a basin is drained by its channel network. It is defined as:

$$D_d = \frac{\Sigma L}{A} \quad (2.1)$$

with ΣL being the total length of all channels within the watershed area A . The inverse of the drainage density D_d defines the Hortonian length l_H .

Another important measure is the overland flow introduced by Horton (1932). In more recent publications on tidal networks (Kearney & Fagherazzi, 2016; Liu et al., 2020; Schwarz et al., 2018), it is usually referred to as the unchannelled path length of which the mean value m_{UPL} is mainly used to characterise channel networks. m_{UPL} describes the average distance a drop of water has to travel over the unchannelled ground/marsh platform before it reaches a channel. Even though m_{UPL} often correlates with D_d , it forms an independent variable (Horton, 1945; Kearney & Fagherazzi, 2016). As it measures the average proximity of a channel, it shows how dissected a basin is by its channel network. Close proximity to channels is important for many species inhabiting salt marshes (Temmerman et al., 2005; C. Wang et al., 2021), as sediment and nutrient availability is often the highest here, which also leads to higher elevations; many marshes show a distinct levee-basin topography (C. Wang et al., 2021).

Tidal channel networks not only drain the water from the basin during ebb but also supply the marsh with water during flood. This water includes nutrients and sediment which is necessary for the plants and the marsh to grow. As the sediment deposition usually decreases with distance from a channel (Temmerman et al., 2005). An efficient network is therefore characterised by a low m_{UPL} , but also by an, in relation, low drainage density D_d and therefore high Hortonian length scale l_H as the lower m_{UPL} should not be achieved by many more channels since this decreases the marsh platform area and thus the suitable habitat for plants. To compare this also across differently sized marshes and scales, measures like the Hortonian length l_H or the mean unchannelled path length

m_{UPL} alone are unsuitable as they are both dimensional and vary with scale (Kearney & Fagherazzi, 2016). A dimensionless variable serving this purpose independent of scale is the geometric efficiency e_g (Kearney & Fagherazzi, 2016), defined as the ratio of Hortonian length and mean unchannelled path length:

$$e_g = \frac{l_H}{m_{UPL}} \quad (2.2)$$

When unvegetated and vegetated systems are compared, it can be observed that vegetated systems have significantly more efficient networks than unvegetated systems (Kearney & Fagherazzi, 2016). This is due to the more meandering configuration that is usually found in vegetated systems. A higher sinuosity generally reduces m_{UPL} (Kearney & Fagherazzi, 2016). Exemplary values for e_g found by Kearney and Fagherazzi (2016) are values around 1 for unvegetated systems and values around 2-3 for vegetated systems.

The delineation of watersheds and the flow paths over the platform need to be determined based on water surface gradients and therefore flow directions. These are not necessarily the same as if they were determined based solely on topography (Fagherazzi et al., 1999; Kearney & Fagherazzi, 2016; Rinaldo et al., 1999). However, based on the assumption that gradients on the marsh platform are relatively constant in space, the shortest distance to a channel can be used as approximation (Vandenbruwaene et al., 2012).

2.2.4. Human use and impact

Salt marshes are of high importance for humans even though they are often only indirectly used for human activities. Small-scale agricultural use does occur by using salt marshes as grazing location for livestock (Davidson et al., 2017) or by harvesting certain plants that are suitable for human consumption (Loconsole et al., 2019). A more important modern-day use of salt marsh areas is recreation. The beauty of the natural landscape and the biological diversity attract many tourists to these coastal areas (Kelleway et al., 2017).

Tidal marshes also serve as a habitat, breeding ground and shelter for many species of for example birds and fish, which are then exploited by humans elsewhere (Baker et al., 2020). Salt marshes ensure a high biodiversity in coastal areas and also act as a filter for pollutants in coastal waters, thereby also benefiting the water quality in adjacent estuarine and coastal water as well as deeper parts of the ocean (Nelson & Zavaleta, 2012).

From a human perspective, probably the most important function of salt marshes is the coastal protection effect they provide. Vegetated marshes significantly reduce the wave energy during storm surges and thereby protect the adjacent land (Leonardi et al., 2018; Möller et al., 2014; Rupprecht et al., 2017). They even provide this effect when they are totally flooded (Möller et al., 2014). Additionally, they stabilise the sediment and thereby decrease or even prevent coastal

erosion (Leonardi et al., 2018; Möller et al., 2014). The presence of a marsh at the seaward side of a dike will result in lower height requirements (Möller et al., 2014; Rupprecht et al., 2017).

All these functions are ecosystem services that salt marshes provide to humans. They are of an extremely high value for society. Salt marshes and their tropical counterpart, mangroves, are estimated to provide (2007) US\$ 24.8 trillion worth of ecosystem services annually (Costanza et al., 2014; de Groot et al., 2012), which is roughly a third of the global GDP (Costanza et al., 2014). Coastal wetlands provide, after coral reefs, the second highest value of ecosystem services per unit area (Costanza et al., 2014).

In spite of this high value of salt marshes for humans, their area shows a decreasing trend (Costanza et al., 2014; Duarte et al., 2008). Especially in north-western Europe, there is a long history of embankments of salt marshes (Allen, 2000). Man-made structures and alterations are still visible and actively implemented in modern-day salt marshes, especially along the Wadden Sea (see fig. 2.3 c)). This is done for stabilisation of the salt marsh and coastal protection. Salt marshes were usually claimed and embanked for the agricultural use of the land. This land-claim often occurred in several stages (Allen, 2000). As the embanked areas are not flooded anymore, they also do not receive any sediment input anymore. Natural compaction and drainage then cause subsidence which makes the areas more prone to severe flooding in case of dike breaches (Allen, 2000). The areas that were embanked the earliest are nowadays usually the most low-lying (Allen, 2000).

As the ecological value and the function as coastal protection is more recognised nowadays, there are plans and projects of de-embankments of certain areas to restore salt marshes (Gourgue et al., 2021; Vandenbruwaene et al., 2012). Accidentally, such de-embankments also happened in earlier times as a consequence of dike failure. Wolters et al. (2005) found that the success of marsh restoration can vary significantly from site to site. Many factors affect the marsh development and species assemblages. Especially on sites with compacted sediment, an artificially created channel system proved to be beneficial for the initial settling of plants and sediment accretion (Wolters et al., 2005). This is closely connected with the fact that a more heterogeneous topography favours seedling establishment and survival due to better drainage (Cao et al., 2021). Salt marsh systems with a more efficient channel network also proved to be more resilient with respect to droughts (Liu et al., 2020). A grazing-regime can lead to a higher biodiversity as one species often becomes dominant otherwise (Wolters et al., 2005). Pre-existing ditches developed to channels in equilibrium with tidal flow already rather fast (Vandenbruwaene et al., 2012). Lower elevations are generally favourable for the initiation of a natural channel network (Vandenbruwaene et al., 2012; Wolters et al., 2005).

Salt marshes also have a very high potential of carbon storage (Mcleod et al., 2011; Mossman et al., 2021; Ouyang & Lee, 2014). The sequestration of CO₂ in coastal and marine ecosystems, so-called "blue carbon" has a much higher potential than CO₂-uptake by, for example, forests and other terrestrial ecosystems. Salt-marsh restoration therefore is a suitable measure not only for coastal protection but also for the sequestration of man-made CO₂-emissions and climate change

mitigation (Mcleod et al., 2011; Mossman et al., 2021). With ongoing climate change and sea-level rise, the potential of coastal wetlands as a carbon sink, might even increase (F. Wang et al., 2021).

At the same time, climate change and accelerated sea-level rise pose a serious threat for many salt marsh ecosystems worldwide (Valiela et al., 2018). The potential of salt marshes to keep up with sea-level rise is highly dependent on sediment availability (Fagherazzi et al., 2020) but also limited by "coastal squeeze" in many locations (Schuerch et al., 2018; Valiela et al., 2018). Next to sediment availability, the existence of sufficient (lateral) accommodation space is crucial for the fate of coastal wetlands (Schuerch et al., 2018). The resilience of salt marshes with respect to sea-level rise is also found to increase with tidal range and biodiversity (D'Alpaos et al., 2012). Due to these different factors, estimates for tidal wetland area change until the end of the century show a huge variety, ranging from a 95 % loss (Valiela et al., 2018) up to a 60 % gain (Schuerch et al., 2018).

2.2.5. Knowledge gap

Even though salt marsh morphology and its dependence on biogeomorphic feedbacks and hydrodynamic boundary conditions receive a lot of scientific attention in recent years (Bij de Vaate et al., 2020; Fagherazzi et al., 2020; Schuerch et al., 2018; Schwarz et al., 2018), many things still remain unclear. Despite the high value of ecosystem services they provide, salt marshes still receive relatively little attention compared to other coastal ecosystems like coral reefs (Duarte et al., 2008). Quantification of certain thresholds is lacking and also the dependence on colonisation patterns is not yet entirely clear. The effects of the colonisation pattern on channel network properties like the geometric efficiency e_g is unexplored as well, just like the evolution of such measures during the colonisation of a marsh.

The strong variations in boundary conditions like tidal range cause significant differences between field sites which makes it difficult to draw general conclusions that are valid for all salt marshes (Wiberg et al., 2020), as for example concerning the influence of tidal prism on channel dimensions (D'Alpaos et al., 2010; Vandenbruwaene et al., 2013). Additionally, long-term field observations are rare as they require a lot of time and data. Individual effects cannot be isolated which makes the identification of causes less straight-forward.

This is something that can be done with numerical models. However, these also have drawbacks, as they only model the processes that were implemented and are therefore limited by the already existing knowledge, underlying assumptions and model capabilities, resulting in certain processes often being excluded from models (Wiberg et al., 2020).

Experiments provide a possibility to study certain landscapes in a controlled setting without being dependent on the correct representation of all processes in a numerical model. Scaled landscape experiments can therefore be a powerful tool to study coastal landscapes (Kleinhans et al., 2017;

van Dijk et al., 2021; Weisscher et al., 2022). However, experiments on salt marshes are rare (Kearney & Fagherazzi, 2016) and mainly focus on wave attenuation of a salt marsh cross-section (Baptist et al., 2007; Möller et al., 2014; Rupprecht et al., 2017). Previous scaled landscape experiment of tidal systems often had problems with scale effects and lack vegetation (Stefanon et al., 2012) or were focused on entire estuaries (Kleinhans et al., 2022; van Dijk et al., 2021; Weisscher et al., 2022).

2.3. Research questions and hypotheses

The main goal of this research is to examine the effects of biogeomorphic feedbacks in salt marshes and the resulting effects of vegetation in general and of different colonisation patterns in particular. The occurring biogeomorphic feedbacks and the evolving channel network and the morphology in experimental systems will be analysed. This is of high importance for the understanding of marsh development in general, but especially for the restoration of marshes in previously embanked areas, as new channel networks develop here and are affected by the establishing vegetation. The following questions form the main objectives of this thesis:

- How does vegetation and its colonisation pattern affect the channel network development and morphology?
- Which biogeomorphic feedbacks occur depending on the colonisation pattern of vegetation?
- What are the effects of a certain colonisation pattern on the conditions for biogeomorphic interactions and how can this be conceptualised?
- How does vegetation and its colonisation pattern affect channel network measures like drainage density D_d , mean unchannelled path length m_{UPL} and geometric efficiency e_g ?
- How are inter- and supratidal area affected by vegetation and its colonisation pattern?

In order to answer these questions, the first scaled landscape experiments of salt marshes including living vegetation will be conducted. Four experiments will be analysed: two unvegetated control experiments, an experiment with hydrochorous seed spreading and an experiment with patchy seeding.

Hypotheses are that vegetation enhances channel initiation and development (Temmerman et al., 2007) and promotes more efficient networks, as observed in nature (Kearney & Fagherazzi, 2016). As a patchy vegetation pattern shows more biogeomorphic feedbacks and results in more self-organised landscape in nature (Schwarz et al., 2018; Temmerman et al., 2007), it is expected to show the vegetation effects more clearly. Moreover, it is hypothesised that morphological and vegetation colonisation time scale need to be suitable for biogeomorphic interactions and that these interactions might be stronger or weaker over the course of the experiments, as development speed is not constant. As the findings from mountain areas (Eichel et al., 2016) are the only ones

quantifying vegetation cover for the engineering threshold, it can only be hypothesised that values for salt marshes might be similar, but of course there are a lot of reasons that can cause a different quantification since it is a different landscape. Concerning the interaction with hydrodynamics, it is hypothesised that vegetation will result in higher intertidal and especially supratidal area, as observed in previous experiments on estuaries (Weisscher et al., 2022).

3. Methods

3.1. General experimental set-up in the Metronome

In order to investigate the channel networks on salt marshes and how this depends on different vegetation patterns, four scale experiments were conducted in the laboratory. Experimental salt marshes were never successfully created in a laboratory before. The experiments were conducted in the flume 'The Metronome', a unique facility in which tidal systems can be created by tilting the flume periodically (Kleinhans et al., 2012; Kleinhans et al., 2017). It was successfully used to simulate different kinds of estuaries with and without vegetation in the past (Braat et al., 2019; Kleinhans et al., 2022; Leuven et al., 2018; van Dijk et al., 2021; Weisscher et al., 2022).

The Metronome is a 20 m by 3 m flume which can be tilted over an axis in the middle at 10 m. In the four salt marsh experiments, that are studied in this thesis, the initial conditions and some general settings were the same. Only one half of the flume was used, so that the tilting axis is located at the landward end of the system. The landward 7.4 m were filled with sand up to 11.5 cm above the flume bottom. The sand used was a poorly sorted sand with a unimodal grain size distribution and a median grain size D_{50} of 0.55 mm and a D_{10} and D_{90} of 0.32 mm and 1.2 mm, respectively (Kleinhans et al., 2017). At the edges of the system, the sand bed was 3 cm higher than the basin in the centre for 30 cm from both sides of the flume (see fig. 3.1).

This system is separated from the 'sea' by two barriers with an inlet with a width of roughly 55 cm in the middle (see fig. 3.1). The barriers consist of a wooden framework with inclined sides that was filled with sand. The round heads of the barriers at the inlet were formed with bubble-wrap and filled with sand as well. Also the wooden framework was covered in bubble-wrap to increase the hydraulic roughness (see fig. 3.1). Seaward of the barriers, no sand was present at the initial stage, so that the artificial grass at the bottom and sides of the flume was exposed. The inside of the flume is covered with this artificial grass because it has a similar hydraulic roughness as the sand. At the seaward end, a wave generator is present which is active during the flood phase (Leuven et al., 2018). Behind that, a weir regulates the water level. Water is continuously pumped into the flume and flows out over this weir.

At the landward end, the system was limited by a barrier of sand, similar to the edges along the sides (see fig. 3.1). Behind this sandy barrier, a wooden plank is placed in the sand bed to limit ground water flow.

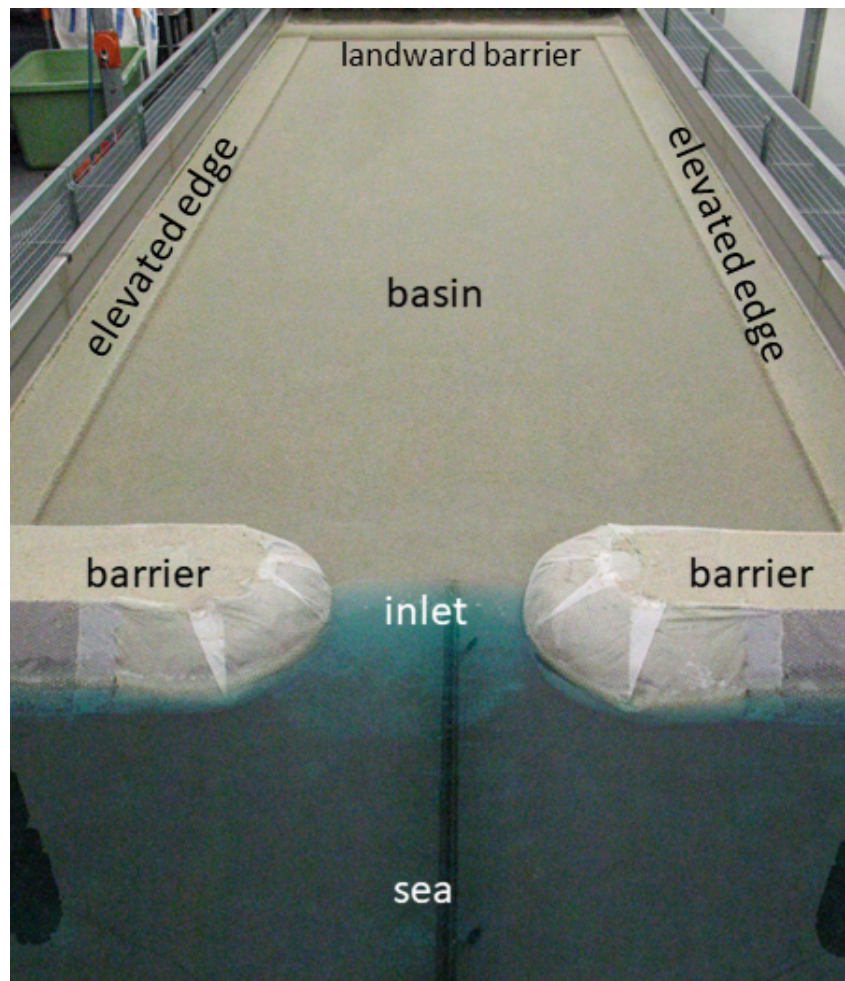


Figure 3.1.: Initial conditions of the system in all experiments

The general settings of the flume tilting etc. were the same in all experiments. The tilting was asymmetrical with an M4-component, so that the flow-conditions are flood-dominant (Weisscher et al., 2022). The duration of one tidal cycle was set to 40 s. The tilting amplitudes of the M2-component and the M4-amplitude were 75 mm and 15 mm (20%), respectively. This resulted in a maximum slope of 0.009 m m^{-1} during the shorter flood phase and a maximum slope of 0.006 m m^{-1} during the longer ebb phase. This is a slightly higher tidal amplitude than in Weisscher et al. (2022), who used tilting amplitudes of 60 mm and 12 mm, respectively. The amplitude of the weir was adjusted accordingly. The mean sea-level was determined by an offset of 92 mm of the weir above the flume bottom. This implies that the mean sea-level is lower than the initial sand bed height (see also fig. 3.1). These settings were found to be suitable for creating the desired morphology during twelve pilot experiments prior to the control experiment.

Such high slopes induced by the tilting are necessary for reaching similar values as in nature for different important force ratios. Shield's numbers should be similar despite the lower water depth in the experiments in order to create comparable sediment transport. The dynamic scaling ensures that. Extensive work on the scaling of the experiment has been done by Kleinhans et al. (2017).

3.2. Experimental scenarios

3.2.1. Control experiments

The first experiment was the first control experiment in which no vegetation was used. 5000 cycles were run in this experiment. Since later experiments with vegetation were run longer, a second control experiment was conducted as fourth experiment after the ones with vegetation. This second control experiment was run until 10 000 cycles.

3.2.2. Experiment with hydrochorous seed spreading

In the second experiment, vegetation was used. The seeds were sown during nine sowing events and were distributed by the flow. Sowing events took place every 500 cycles and were started at 1000 cycles. Every sowing event consisted of 60 cycles. The first 10 cycles were run as spin-up for the normal flow pattern to establish after the system was dry. During the next 25 cycles, the seeds were added at the inlet during the flood phase, so that they spread hydrochorously throughout the system. During the final 25 cycles, no further seeds were added but the already sown seeds could still be transported further by the flow. After this, the flume stood still for four consecutive days, so that the newly sown seeds could germinate and start to grow. For every of the nine sowing events, 200 g of seeds of *Lotus pedunculatus* were used. This species proved to be suitable for laboratory experiments at this scale and was used successfully in the past (Kleinhans et al., 2022; Lokhorst et al., 2019; Weisscher et al., 2022). It germinates relatively fast but does not grow extremely tall or in unsuitable places (Lokhorst et al., 2019)(see fig. 3.2). The 200 g of seeds amount to approximately 160 000 seeds per sowing event. The seeds were soaked for one day before they were used in the experiment to speed up the germination. During the last sowing event at 5000 cycles, not only *Lotus pedunculatus* was added but also 180 g of seeds of *Veronica beccabunga* and 300 ml of crushed walnut shell of different grain sizes as a mud simulant in order to test where these settle. After this last sowing event, the flume stood still for six instead of four days. This experiment was run until 5500 cycles were reached.

3.2.3. Experiment with patchy seeding

In the third experiment, a different vegetation pattern was used. The vegetation was sown manually in patches. There were eight sowing events and sowing took place every 500 cycles, starting at 1000 cycles. Each sowing event a number of new patches with an initial radius of 2.5 cm were added and the already existing patches from previous sowing events were expanded with a radius expansion of 5 cm. The number and growth rate of patches was determined in such a way that it is practically feasible and a vegetation cover of 60 % of the basin would be reached at the eighth sowing event in case that no vegetation is eroded during the course of the experiment. This results in usually 13 patches that need to be added during one sowing event. However, if these patches



Figure 3.2.: Individual plants of *Lotus pedunculatus* at different growth stages. The approximate age is indicated. The scale below is in centimetres.

would be placed in a channel or within an existing patch, they are not sown. The placement of the patches was determined by a random algorithm, but one of the realisations was chosen as not all random realisations give a useful distribution of the patches. Figure 3.3 gives an overview of the placement and growth of the patches under the permission that no erosion takes place. But of course, erosion did take place and the final vegetation cover therefore was lower, as new patches were not placed in channels and existing patches also were not expanded into channels.

After the sowing events, the flume stood still again for four consecutive days to allow for the germination and growth of the plants. Again, *Lotus pedunculatus* was the species used. The number of seeds used per sowing event varied due to the growing number and size of patches. The amount of seeds was determined by the surface area that needed to be sown. It was aimed at a seeding density of 10 seeds/cm². It was assumed that roughly half of the seeds would germinate, to ensure a density of about 5 plants/cm² in the end. The total number of seeds that were added was therefore lower than in the experiment with hydrochorous seeds distribution but the manual sowing prohibited the large scale export of seeds out of the system to the delta. The seeds were soaked for one day and then dried again for one day before they were sown. The soaking speeds up the germination and the drying is necessary for the manual sowing since adhesion would otherwise prevent the seeds being sown loose from each other. This procedure was tested to not have significant differences in germination speed compared to soaking only, as done in the experiment with hydrochorous seed distribution.

10 000 cycles were run in this experiment but the last sowing event took place after 4500 cycles. The later cycles were run shortly after each other, so that the vegetation did not have the time to grow new roots in places where it was deposited.

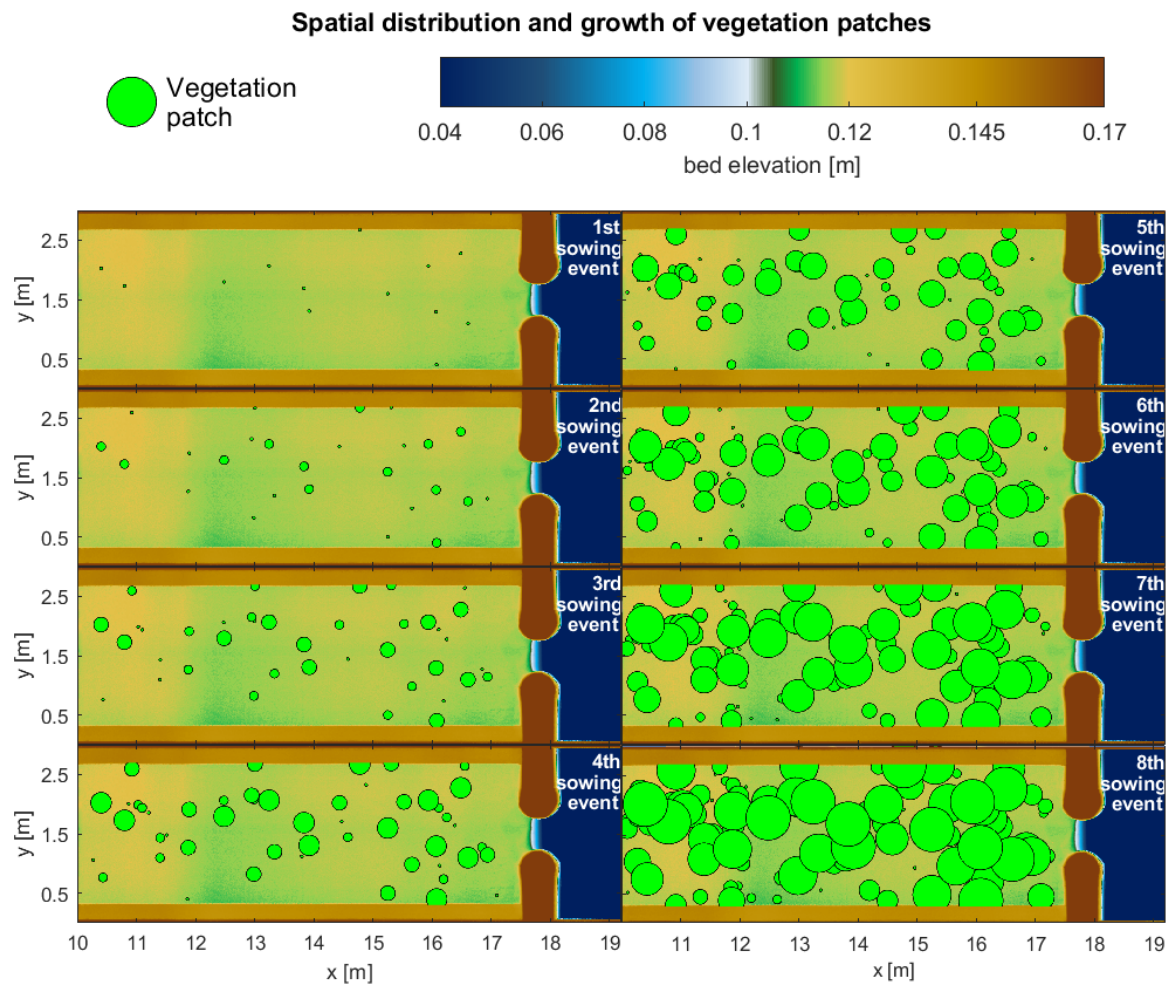


Figure 3.3.: Spatial distribution and growth of the theoretically planned vegetation patches over the course of the eight sowing events

3.3. Data acquisition

During all experiments, the evolution of the system was surveyed with different instruments. Some instruments were only available and/or used for parts of the experiments and not the full four experiments.

The digital elevation models (DEMs) of all experiments were made with a laser scanner above the flume. The laser line is as wide as the flume and is registered by a camera. This set-up is mounted on rails and moves over the entire length of the flume to capture whole system. From the height and position of the laser line in the camera photos, the elevation of the sand bed can be calculated. The horizontal and vertical accuracy are approximately 1 mm and 0.2 mm, respectively. DEMs were usually taken every 500 cycles in all experiments, only in the later stages of the experiment with patchy seeding after the seeding was done and after 5000 cycles in the second control experiment, sometimes 1000 cycles were run between two consecutive DEMs.

On the movable laser scanner gantry above the flume, a single-lens reflex camera is mounted as well. With this camera, overhead photos with a high resolution can be taken. This was, however, not possible during the first control experiment and the first 2000 cycles of the experiment with hydrochorous seed spreading. This camera was always used when a DEM was taken and after the four days of vegetation growth before the continuation of the experiment.

Overhead photos by four cameras above the flume were triggered by the flume tilt. These cameras take a photo once every tidal cycle. Their resolution is however much lower compared to the single-lens reflex camera on the laser gantry. These cameras became available at 2500 cycles into the experiment with hydrochorous seed distribution.

A digital camera mounted on a special set-up aimed at a similar function. It took a photo roughly every tidal cycle, however not as precise since it is not directly coupled to the tilt. With these photos, time-lapse videos of the system's evolution can be created. This camera was used during the first control experiment and the two vegetation experiments.

Photos were also taken manually with a single-lens reflex camera from the sides of the flume during all experiments. Such photos were taken every time a DEM was taken as well and, in the experiments with vegetation, after sowing to document the locations of the seeds and after the four days of vegetation growth to document the plant growth before the experiment is continued.

Furthermore, the water level was measured in all four experiments generally every 500 cycles, shortly after a DEM was taken. It was measured with three ultrasonic sensors on a bar above the flume. These measure the distance between the sensor and the water surface acoustically with a frequency of 10 Hz. The bar with the sensors was positioned at up to six locations along the flume, depending on the size of the system. One measurement was always done in the sea, one closely behind the inlet and the others were spread over the length of the system. The y-position of the sensors was occasionally adjusted to place them above interesting morphological features. The positions of the water level measurements can be found in Appendix C. The water level was measured for at least 2 min at every location, which covers three tidal cycles.

3.4. Data analysis

3.4.1. DEM processing

In order to create digital elevation models from the raw laser data, this data was corrected for different distortions resulting from the camera perspective and lens, so that they represent the correct elevation at the corresponding location. Afterwards, the data was gridded on a regular grid with a cell size of 3 mm by 3 mm. This implies, that one grid cell usually contains data from nine raw data points. In this way, the 10th and 90th percentile can be calculated as well, which can indicate vegetation.

The DEMs of difference were simply created by subtracting the respective DEMs from each other. No further error analysis was applied here, as the data quality is fairly constant in all DEMs because the same system was used. Some small differences only occurred due to some disturbances of the laser system between DEMs were taken that caused a change in camera position. These disturbances occurred between 1500 cycles and 3500 cycles in the experiment with hydrochorous seed spreading. Basic corrections for these were applied to ensure that the DEMs are comparable. However, the effect can still be visible in the DEMs of difference.

The processing and visualisation was done in MATLAB and involved the use of several functions created by others (Childress, 2021; Greene, 2022; Martínez-Cagigal, 2022).

3.4.2. Erosion and sedimentation

For the analysis of sedimentation and erosion, the DEMs from different stages were subtracted from the initial DEM. In the quantification of the eroded volume and surface area, only grid cells where the erosion exceeded a threshold of 3 mm were counted. This filters out noise which is especially necessary as the calibration of the DEMs changed several times during the course of the experiments. Furthermore, only the basin area was included in these calculations, so possible erosion of the elevated edges is not taken into account. Just like the threshold value, this is necessary to filter out noise.

3.4.3. Vegetation detection

Vegetation was detected in the images by the single-lens reflex camera on the laser gantry. The green chromatic coordinate GCC (Gillespie et al., 1987; Sonnentag et al., 2012; Woebbecke et al., 1995) was used as vegetation index to detect plants. It is calculated as follows:

$$GCC = \frac{G}{R + G + B} \quad (3.1)$$

R , G and B are the respective bands of red, green and blue in the images.

3.4.4. Water level measurements and maps of sub-, inter- and supratidal area

The water level measurements were filtered for outliers, slightly smoothed with a moving window median filter, averaged over the three measured cycles and subtracted from a reference to give actual water levels and not distances between sensors and water surface. High and low water levels were extracted as the 2nd and 98th percentile. All water level curves were visually evaluated whether they give reliable high and especially low water levels. In intertidal areas, the bed elevation would otherwise often be selected as low water level. Which measurements were evaluated as reliable, is indicated in Appendix C.

For the creation of maps of sub-, inter- and supratidal area, the reliable high and low water levels were interpolated with a cubic interpolation in the rectangular area of the system that is spanned up by the measurements. In order to have a high and low water surface covering the entire system, high and low water levels everywhere outside of the area covered by measurements were assumed to have the same value as the closest (interpolated) value in the area within the measuring locations. These planes were then put in relation to the elevation in the DEMs to create the maps of sub-, inter- and supratidal area.

3.4.5. Channel network

The channel networks were digitised manually in ArcGIS Pro. The total length of the line features was used as total network length. The unchannelled path length was calculated simply by the distance from such a line feature with the PathDistance tool. Further analysis of variables like D_d , m_{UPL} or e_g was done in in MATLAB.

4. Results

4.1. Morphological development

4.1.1. General development in all experiments

The four experiments resulted in a significantly different morphology, depending on the vegetation pattern that developed. All experiments showed a similar behaviour in the beginning and the effects of vegetation only played a major role in later stages when a significant vegetation cover became present in the system.

While the actual speed of development can differ between experiments, the general patterns that developed were very similar. At the very beginning, small channels started to form around the inlet that expanded by backward erosion. The number of these initial channels differed but one channel usually became dominant very fast. This channel expanded upstream in a straight line and developed small side channels. Side channels closer to the inlet were larger, so that a kind of triangular system shape developed. This kind of system grew during the ebb phases by backward erosion but also developed a depositional lobe at the upstream end where sediment was deposited during the flood phase. This caused the upper main channel to split up at some point, resulting in a more asymmetrical system which started to expand sideways in the upstream part. Curved channels then expanded to the sides and migrated downstream. In the space in between, a dynamic bar and channel pattern emerged. The most upstream part of the system was mainly unaffected by morphological change.

4.1.2. Control experiments

First control experiment

The first control experiment mainly showed the development described above. There was no vegetation present that affected the morphological change, so the sand bed could be easily eroded. Consequently, the curved channel at the sides expanded over the whole width of the system and also partially eroded the elevated edges (see fig. 4.1). They also moved downstream very far, so that the split-up into several channels already took place directly landward of the inlet (see fig. 4.1).

Figure 4.2 shows the morphological differences between the DEMs that were made. It clearly shows that the expansion of the system was based on backward erosion in the beginning (until

1500 cycles) and deposition outside the delta only occurred on the depositional lobe at the upstream end of the system. From 2000 cycles to 3500 cycles, the outward and seaward expansion of the curved channels on the sides took place. After 4000 cycles, the system was almost in a dynamic equilibrium as erosion and sedimentation within the system were very similar and the delta barely grew further (see fig. 4.2).

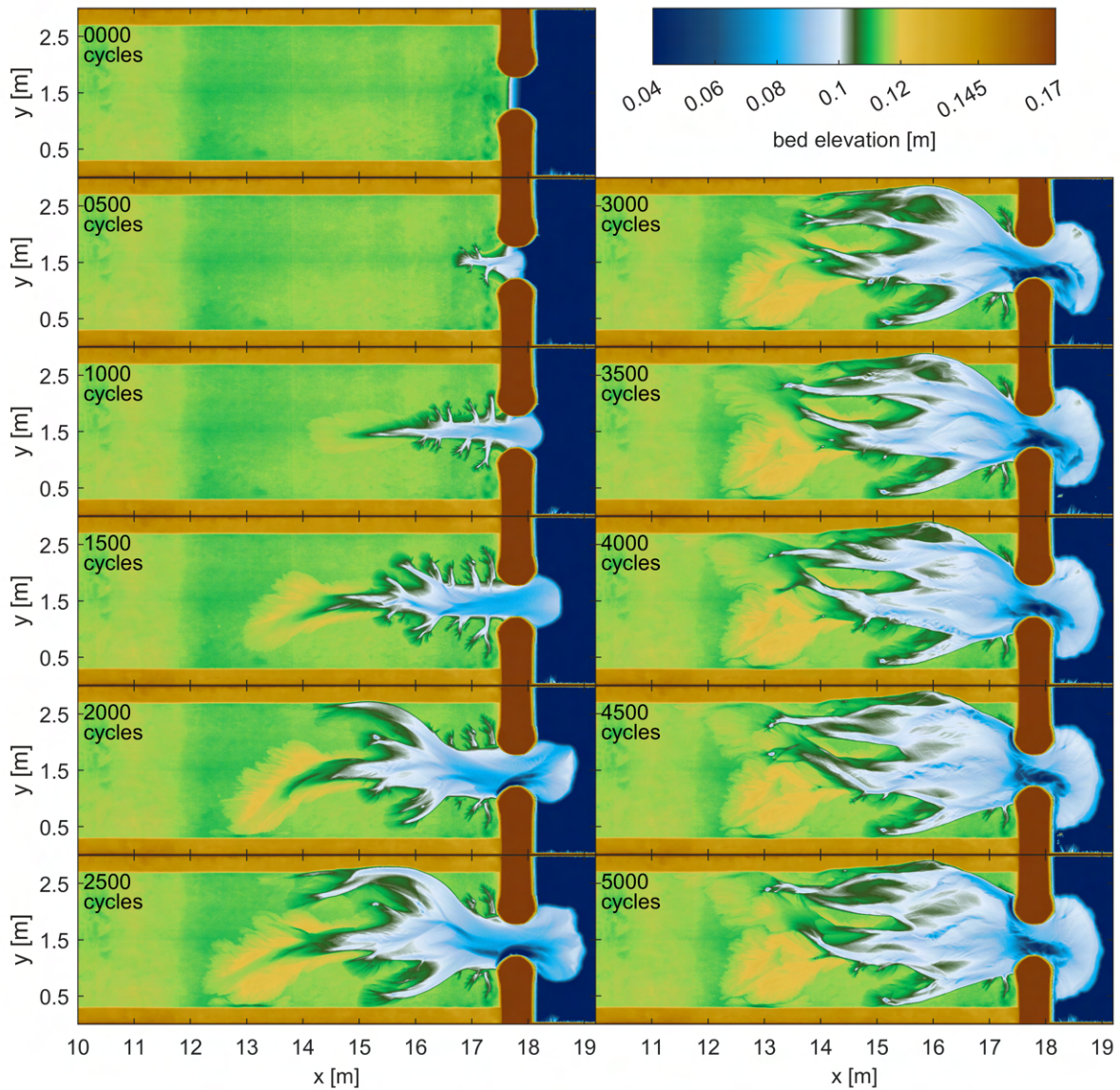


Figure 4.1.: Morphological development of the first unvegetated control experiment

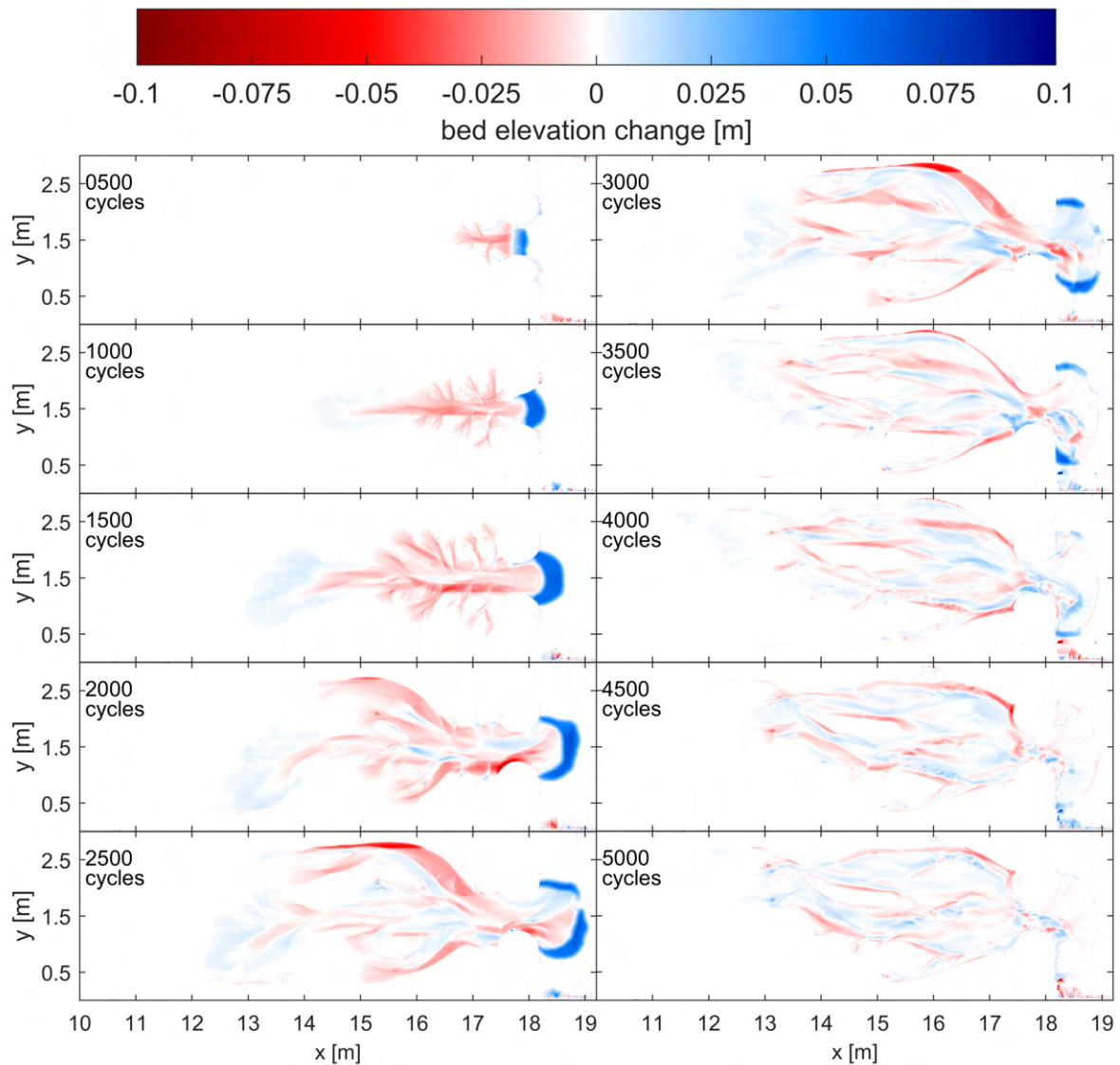


Figure 4.2.: Erosion and sedimentation during the first unvegetated control experiment with respect to the respective previous DEM

Second control experiment

The second control experiment showed a slower development in the early stages but still developed in a similar way (see fig. 4.3). Between 3500 cycles and 7000 cycles, the system was skewed to one side. In the latest stages, this was not as clear anymore. The split-up into several channels already occurred shortly behind the inlet, similar to the first control experiment and also the landward expansion was very comparable in both control experiments (see fig. 4.1 and 4.3).

Also the morphological differences between consecutive DEMs follow a similar pattern as in the first control experiment (see fig. 4.4). Backward erosion dominated in the early stages, followed by the further development of channels while the delta still grew and finally mainly re-distribution within

the system occurred as the delta reached its final size (see fig. 4.4). The only major difference between the two control experiments was the slower development and longer continuation of the second one to have a better representation of the final stages with mostly redistribution.

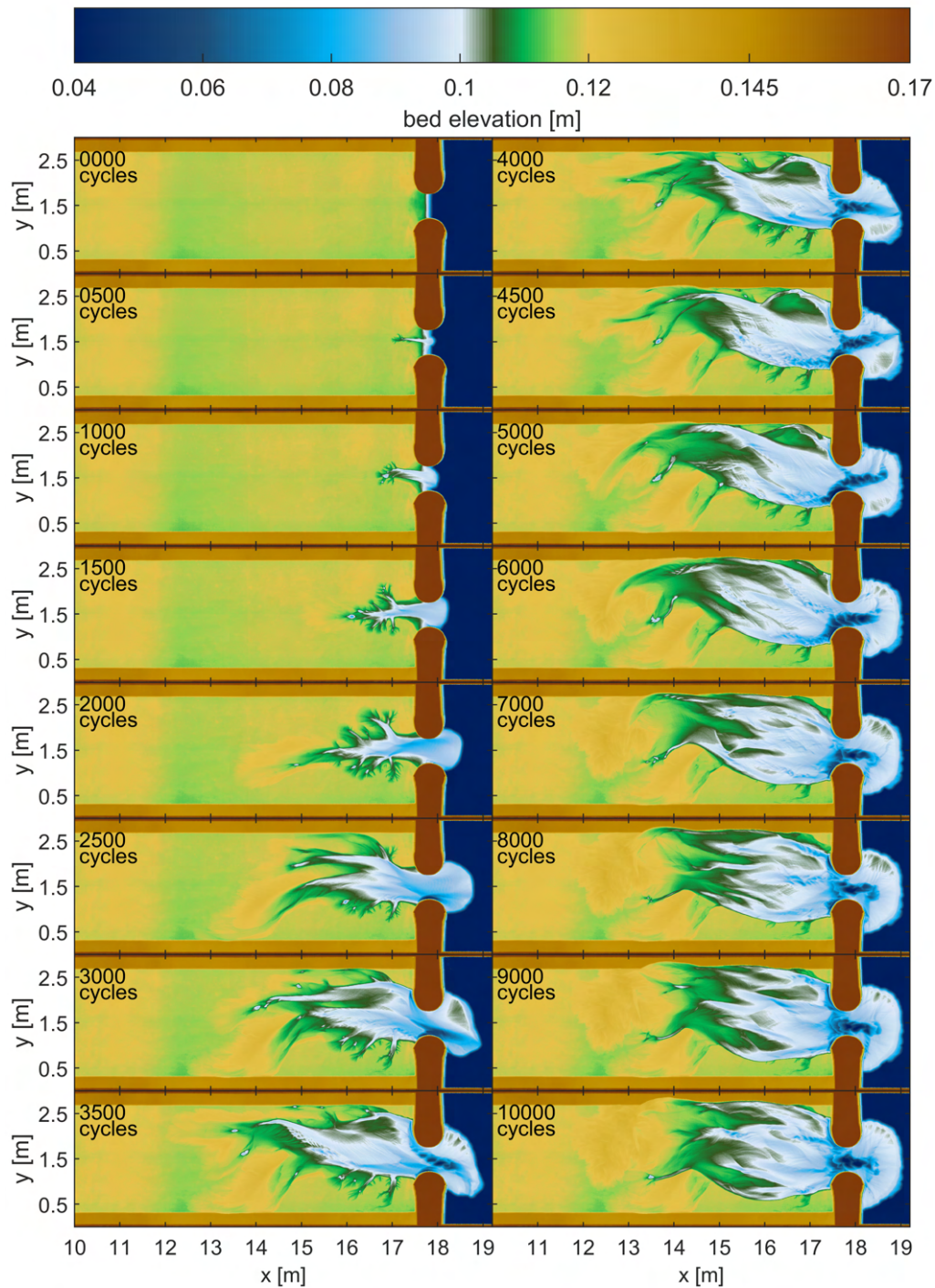


Figure 4.3.: Morphological development of the second unvegetated control experiment

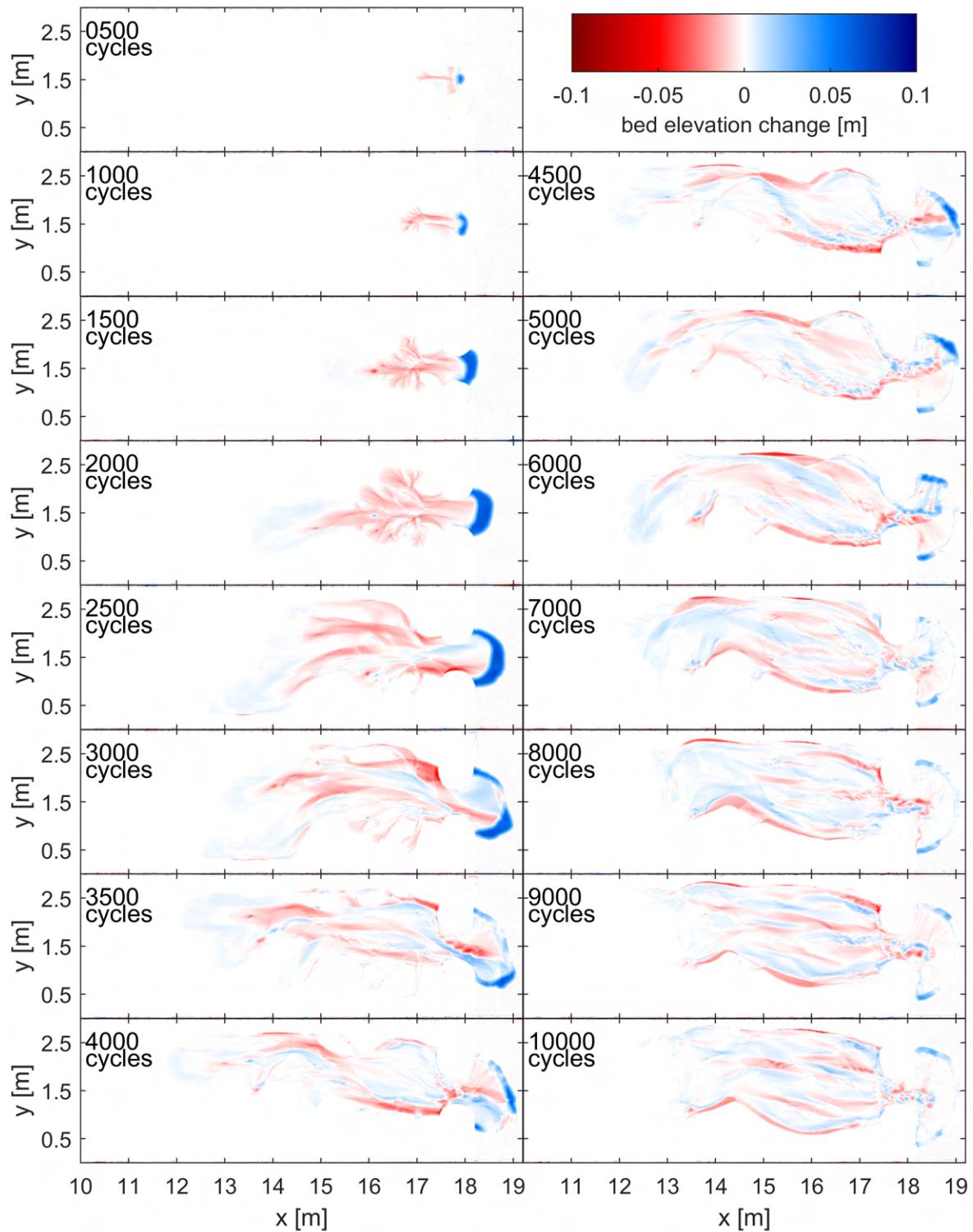


Figure 4.4.: Erosion and sedimentation during the second unvegetated control experiment with respect to the respective previous DEM

4.1.3. Experiment with hydrochorous seed spreading

The initial development in the experiment with hydrochorous seed spreading was somewhat slower than in the first control experiment but faster than in the second control experiment. The split-up of the main channels occurred later and further upstream (see fig. 4.5). The outward and seaward expansion was then much more limited than in the control experiments (see fig. 4.6). This can be attributed to the vegetation that was present on the banks and therefore hindered the erosion. The resulting morphology was, unlike in the control experiments, dominated by a wide, long and straight main channel which split up further upstream into several smaller channels (see fig. 4.5). The main channel continued to widen throughout the course of the experiment but the downstream part of the system never got as wide as in the control experiments (see fig. 4.6). However, the system expanded further upstream. In this area with several channels developed with bars in between that were vegetated, just like the banks along the main channel. The vegetation on the bars was generally younger and established later, also because the banks along the main channel became supratidal at a certain point because the drainage occurred only via the channels instead of the flat sand bed.

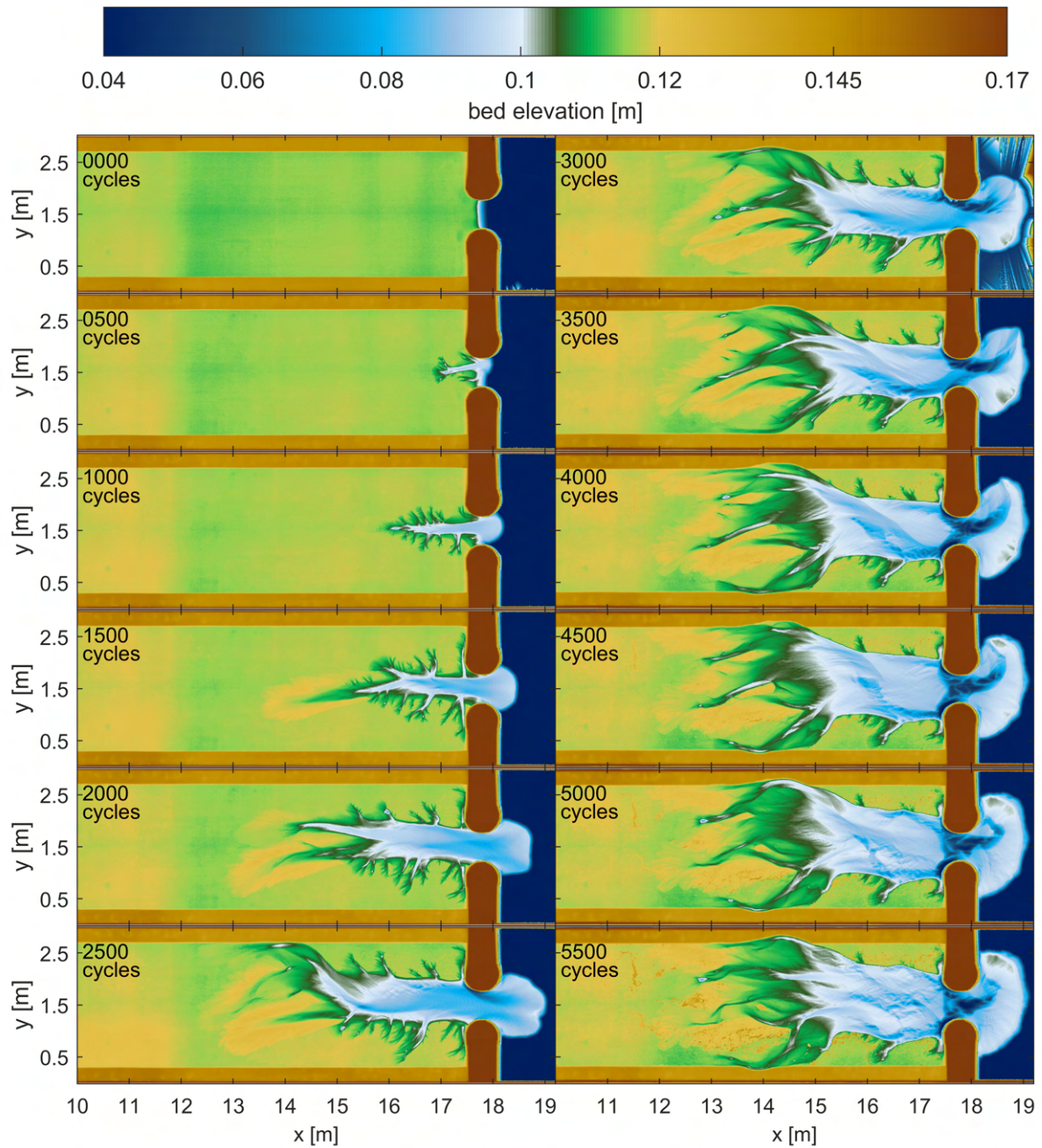


Figure 4.5.: Morphological development of the experiment with hydrochorous seed spreading. The major elevations in the sea at 3000 cycles are errors in the data.

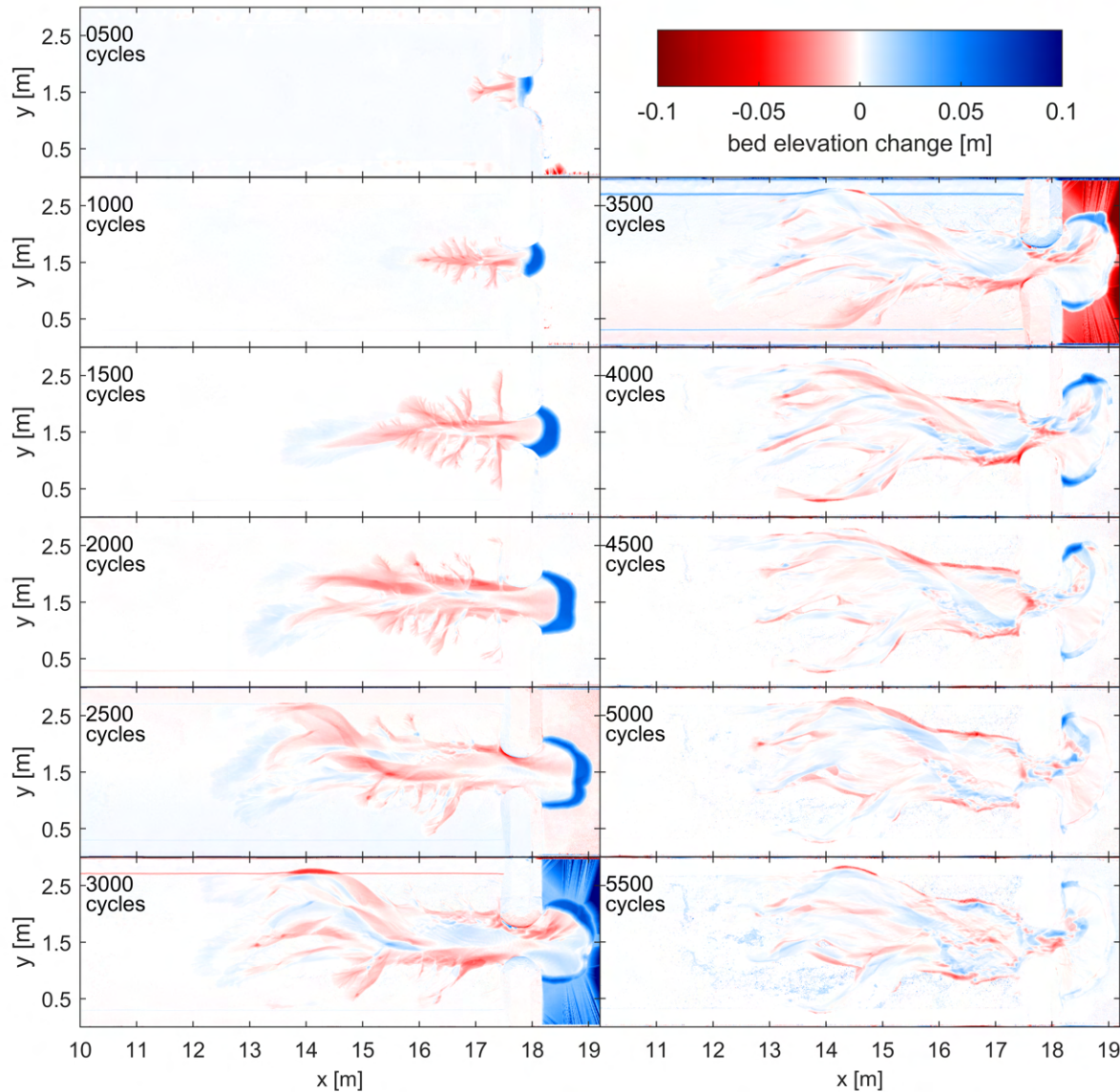


Figure 4.6.: Erosion and sedimentation during the experiment with hydrochorous seed spreading with respect to the respective previous DEM. The major differences in the sea at 3000 cycles and 3500 cycles are errors in the data. Some other small systematic differences between DEMs might be visible, these are due to the laser scanner configuration changing several times.

4.1.4. Experiment with patchy seeding

The initial development of the experiment with patchy seeding was a bit faster than in the other experiments. After the split-up of the main channel, the system developed a bit skewed (see fig. 4.7). It developed similarly branching channels as the experiment with hydrochorous seed spreading but the wide and straight main channel behind the inlet was shorter. This channel widened mainly on one side (see fig. 4.7) as the other channel bank was fixed by several vegetation patches. One patch kept a bifurcation in a stable place over several thousand cycles. In the upstream part, the central most developed one of the branching channels was limited by a row of vegetation patches on one of its banks. These patches determined the expansion direction of the channel but were eventually eroded by lateral channel migration.

The branching channels landward of the main channel were fewer than in the experiment with hydrochorous seed spreading. Especially from 5000 cycles onward, the two central branching channels became dominant while the channels at the sides became relatively inactive (see fig. 4.7). At this stage, after the last sowing event, vegetation blocked the flow over almost the entire width of the flume between 12 m and 13 m. This greatly affected the flow. In the two central channels, water level during flood rose much higher than in areas where the flow was blocked by vegetation. Channel migration caused significant erosion of vegetation in several places. The eroded plants were then mostly deposited close to other vegetation in the upstream part. Shortly after 8500 cycles, the continuous vegetation range breached and a channel could develop into the area lying behind (see fig. 4.7).

The dense vegetation had significant effects on the flow but this also happened vice-versa. Vegetation at the upstream end of channels, especially in areas where sand was deposited, was often uprooted but not removed. The plants were woven together densely with their roots and stems and then moved up and down with the rising and falling water levels but were not moved away laterally.

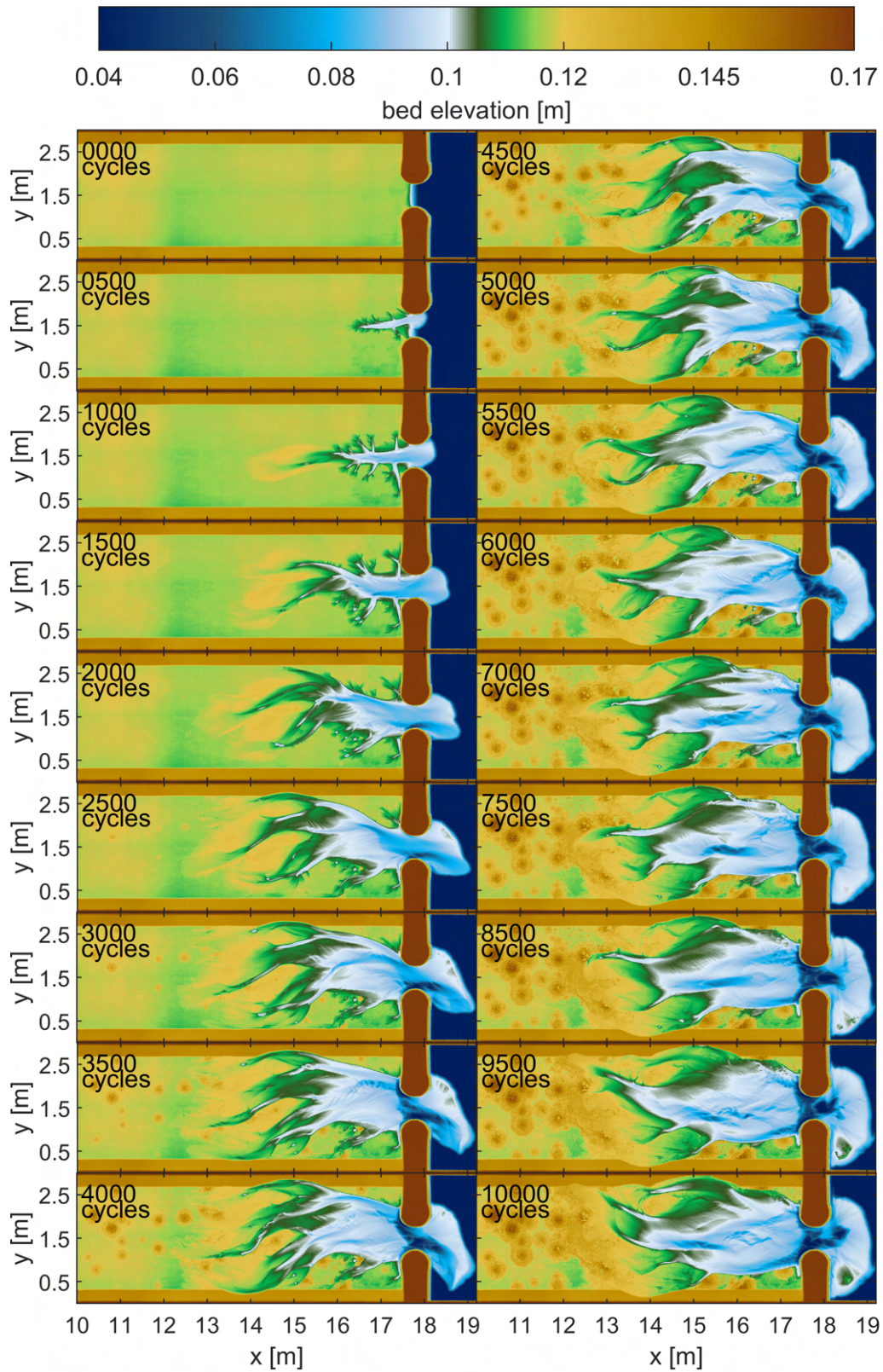


Figure 4.7.: Morphological development of the experiment with patchy seeding

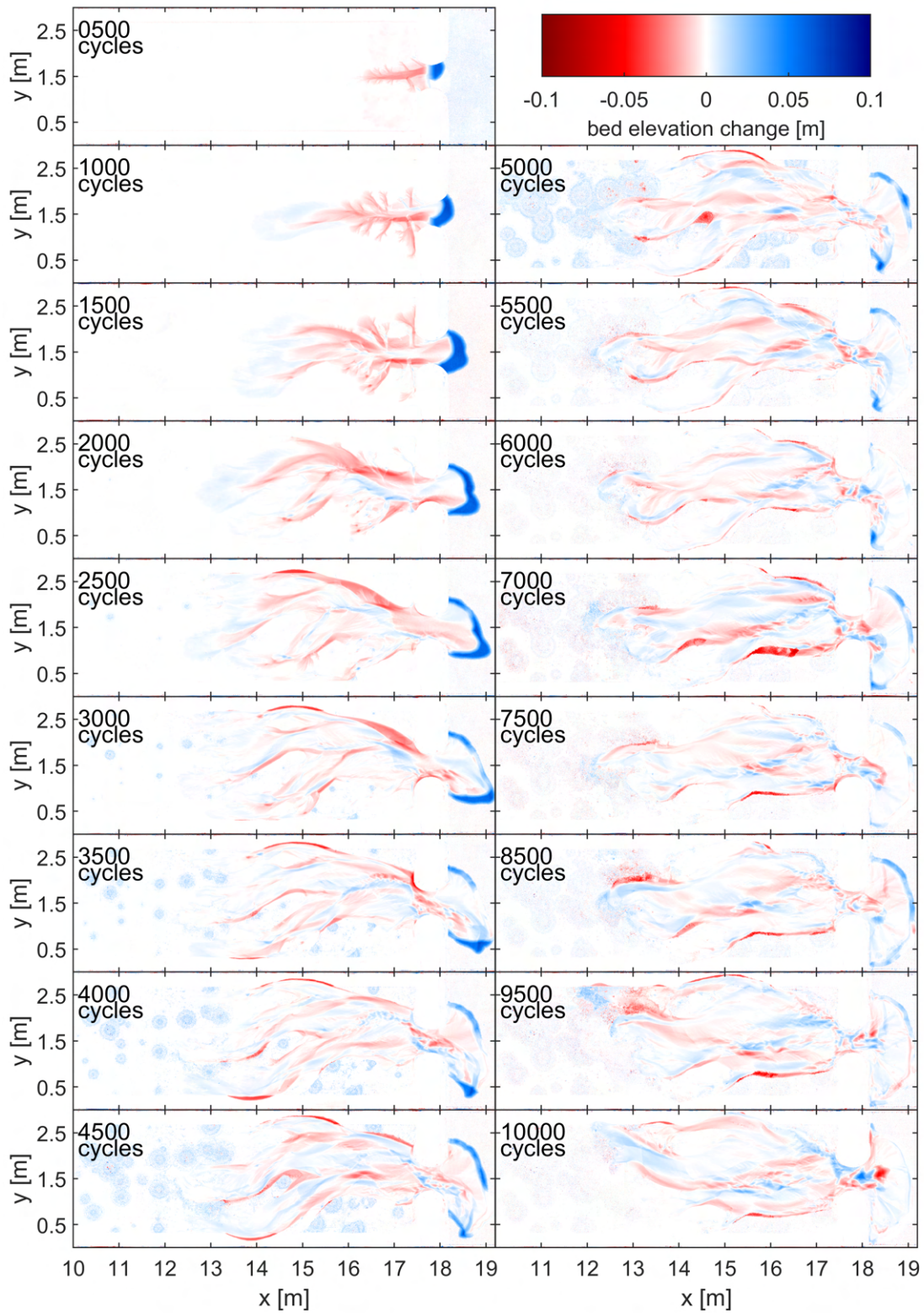


Figure 4.8.: Erosion and sedimentation during the experiment with patchy seeding with respect to the respective previous DEM

4.2. Comparison of the system development

All experiments have shown some similar characteristics and developments, especially in the early stages. They are therefore very comparable. Of course every experiment is unique and different from others, but they still show the same stages of development and the emerging pattern is similar. Especially the two control experiments show this very well.

Differences initially mainly occur due to the speed of the development. The evolution of the system shows an adjustment to the boundary conditions. This is very slow in the beginning as the initial conditions are very different from a morphology that would be in equilibrium with the boundary conditions. Not much water can flow over the bed in the beginning, so that only small changes take place. This also implies that perturbations and little disturbances in the initial bed can have a great effect. This is reflected in the diverging development speeds of the different systems in the beginning.

As the systems mainly grow by eroding the initial sand bed, the development speed of the system is reflected in the eroded sediment volume. Plotted over time, this shows a characteristic curve representing slow development at the beginning and a fast adaptation after that, which eventually transitions into a state close to equilibrium (see fig. 4.9 a)). The speed of the initial development can cause an offset between different experiments. However, there are still some differences visible. The experiment with hydrochorous seed spreading for example seemed to take longer until it reached equilibrium but eventually reached the eroded volume of the first control experiment despite the slower initial development (see fig. 4.9 a)). The experiment with patchy seeding showed an evolution very similar to the first control experiment until about 3000 cycles but then continued to grow slowly but steadily and did not seem to reach a clear equilibrium (see fig. 4.9 a)). This was different in the second control experiment which was run for 10 000 cycles as well. Here, the initial development was slower than in all other experiments but the curve still shows a similar shape. In the final stages, the curve is much flatter than the one of the experiment with patchy seeding (see fig. 4.9 a)), implying that the system was closer to an equilibrium.

A similar trend can be seen in the surface area that was affected by erosion (see fig. 4.9 b)). Here, the eroded area in the hydrochorous seed spreading experiment reached the eroded surface area of the first control experiment and the experiment with patchy seeding despite an initial offset. This highlights the expansion further upstream in this experiment. The experiment with patchy seeding again showed a slow but steady growth in later stages. The curve of the second control experiment always is a bit underneath the ones of the other experiments, highlighting the slow development in this experiment. At 7000 cycles, the eroded surface area in the second control experiment even seemed to decrease a bit (see fig. 4.9 b)). This can be due to deposition in enough areas, so that the threshold for erosion in the calculation was not reached anymore in these areas. This also correlates to a higher mean erosion depth (see fig. 4.9 c)), as the shallow areas were filtered out.

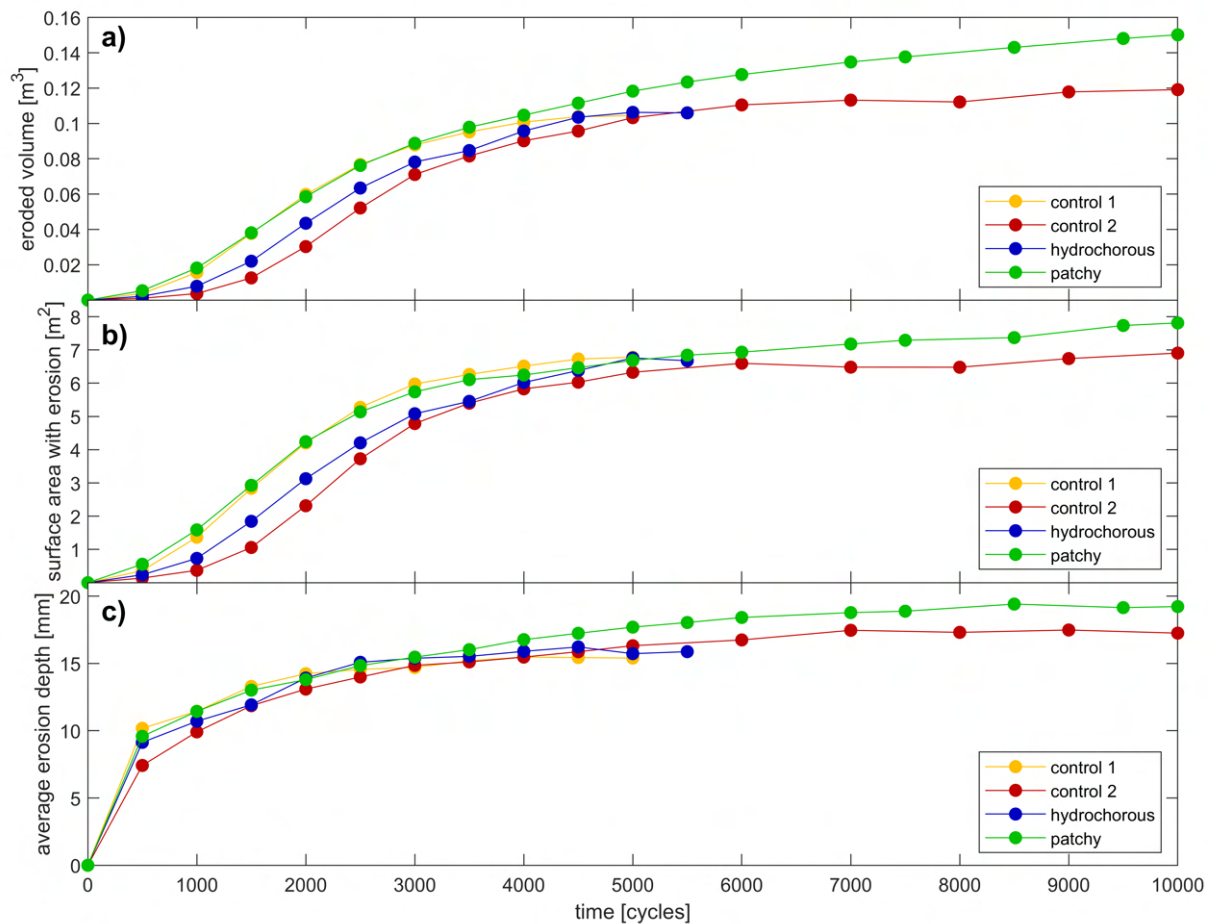


Figure 4.9.: (a) Eroded volume, (b) eroded surface area and (c) average erosion depth over time in the different experiments

Differences are also visible in the average erosion depth (see fig. 4.9 c)). The mean erosion depth generally increased fast in the beginning and more slowly in later stages. The first control experiment and the experiment with patchy seeding again showed a very similar development in the beginning (see fig. 4.9 c)), but after 2500 cycles, the mean erosion depth of the experiment with patchy seeding surpassed the one of the first control experiment. The slow development of the second control experiment is here again reflected in the overall lower values (see fig. 4.9 c)). The average depth in the experiment with hydrochorous seed spreading showed a less clear and consistent behaviour than the others with a slower increase in the beginning, followed by a faster increase and then a stabilisation (see fig. 4.9 c)).

The differences become even more clear when the variables explained above are investigated along the flume and not for the entire system. Figure 4.10 shows the eroded volume, surface area and mean erosion depth over the length of the flume for the different experiments, all at 5000 cycles and for the second control experiment and the experiment with patchy seeding at 10 000 cycles as well. The major erosion clearly took place further upstream in the experiments with vegetation, both in volume and especially in area. The vegetated experiments both showed a clear peak slightly

landward of 15 m where almost the entire cross-section of the flume is affected by erosion (see fig. 4.10 b)). The unvegetated experiment had their maximum roughly one metre further seaward and the peak was not as clear (see fig. 4.10 b)).

The erosion depth was generally similar and linearly decreased in upstream direction. In the vegetated experiments, it was a bit higher in the downstream part and a bit lower in the upstream part compared to the control experiments. This reflects the clear main channel that developed in the downstream part in both vegetation experiments. The only exception was the experiment with patchy seeding at 10 000 cycles (see fig. 4.10 c)). The mean erosion depth was significantly higher here than in the other experiments or at the earlier stage. This can be attributed to the strongly developed channel in the central part of the system which was for the most part blocked by vegetation.

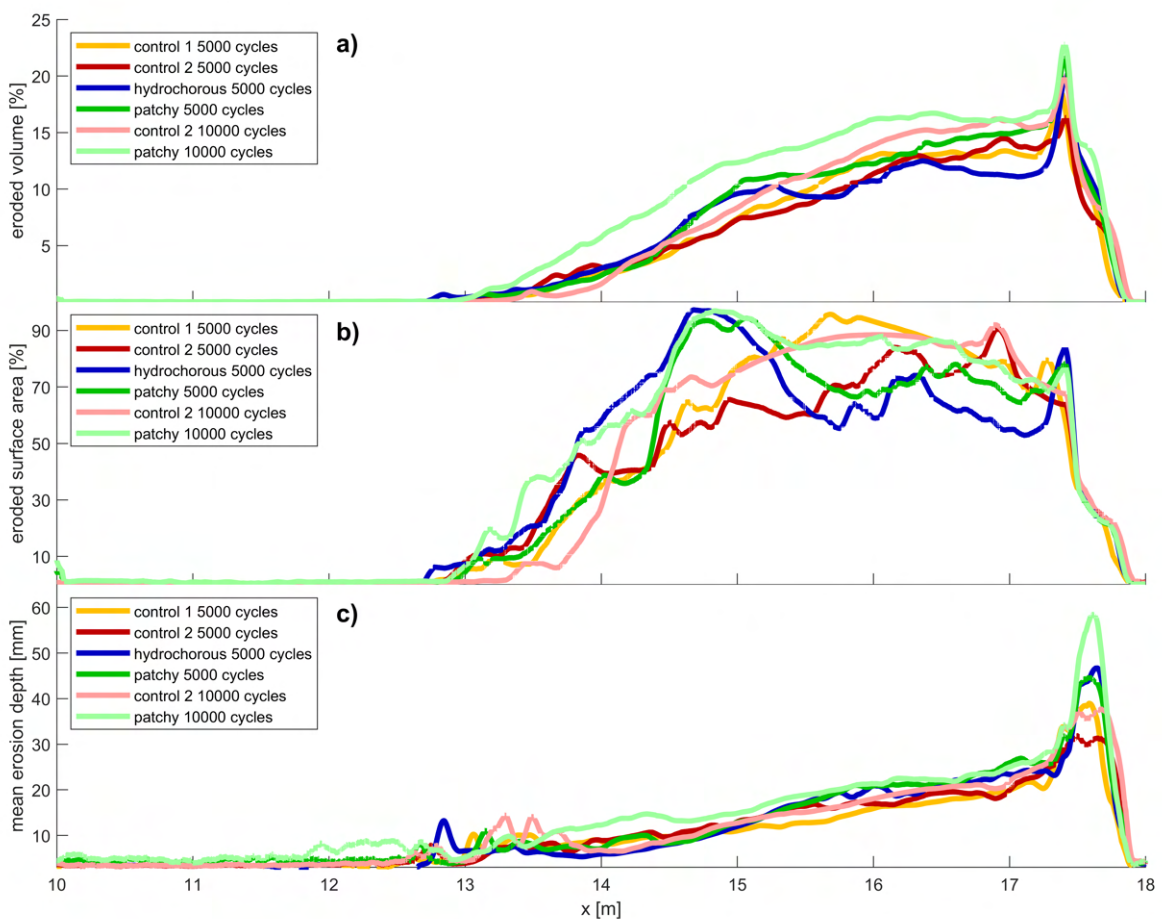


Figure 4.10.: (a) Eroded volume, (b) eroded surface area and (c) average erosion depth along the flume at 5000 cycles in all experiments and at 10 000 cycles in the experiment with patchy seeding. Especially the eroded surface area shows clear differences between vegetated and unvegetated experiments. The eroded volume shows this to a lesser extent as well. Mean erosion depth is mainly dependent on the distance from the inlet but shows some minor variations between experiments, too.

From 5000 cycles to 10 000 cycles, the eroded volume increased over the entire length of the system in the experiment with patchy seeding. Where it was still possible, also the eroded surface area increased. The mean erosion depth increased mainly in the upstream part (see fig. 4.10). The second control experiment showed a similar trend in eroded volume but to a lesser degree, little change in mean erosion depth and a seaward increase and landward decrease in eroded surface area (see fig. 4.10).

All variables were very close to zero in the most landward part up to roughly 12.8 m. This was due to the water flow over the sand bed not reaching velocities sufficiently high for the beginning of motion here. The only exception was formed by the mean erosion depth in the experiment with patchy seeding at 10 000 cycles, which represents the development of one relatively deep channel.

4.3. Vegetation cover and biogeomorphic interactions

While the erosion variables mainly show differences between vegetated and unvegetated experiments, differences between the colonisation patterns can be shown by analysis of the vegetation cover. Fig. 4.11 provides a map of vegetation establishment and erosion in both experiments. It shows the hydrochorous settling of eroded manually sown vegetation between patches around 12 m to 13 m in the later stages of the experiment with patchy seeding and also illustrates the concentric growth of the patches as well as the continuous erosion of patches from one side (see fig. 4.11). A striking difference between the two experiments is, that there was much more erosion of vegetation in the experiment with patchy seeding (see fig. 4.11). Even though the patches determined certain morphological features earlier and also fixed some of them for some time, they were eventually eroded, mainly in the seaward part of the system (see fig. 4.11).

In both vegetation experiments, the vegetation cover increased exponentially over time as long as seeds were added regularly (see fig. 4.12). The experiment with hydrochorous seed spreading reached a vegetation cover of around 12 % at 5500 cycles. The cover was very low during the first 2000 cycles in which already three sowing events took place. After that, the vegetation cover increased exponentially despite the amount of seeds that were added staying constant, which would theoretically imply a linear increase. The exponential increase can be explained by the slow down of the morphological development (see fig. 4.9), which allows for the establishment of a higher share of the same amount of seeds. The amount of eroded vegetation also increased over time, however not as strong as the newly settled vegetation (see fig. 4.12).

The exponential increase was even clearer in the experiment with patchy seeding (see fig. 4.12), mainly due to the exponential increase of sown seeds. After 5000 cycles, the total vegetation cover stayed almost constant. The cover percentage of manually sown vegetation decreased however. The cover that was eroded here (red in fig. 4.12), closely mirrored the newly settled hydrochorously spread vegetation (blue in fig. 4.12), implying that eroded manually sown vegetation was not removed from the system but transported elsewhere within the system.

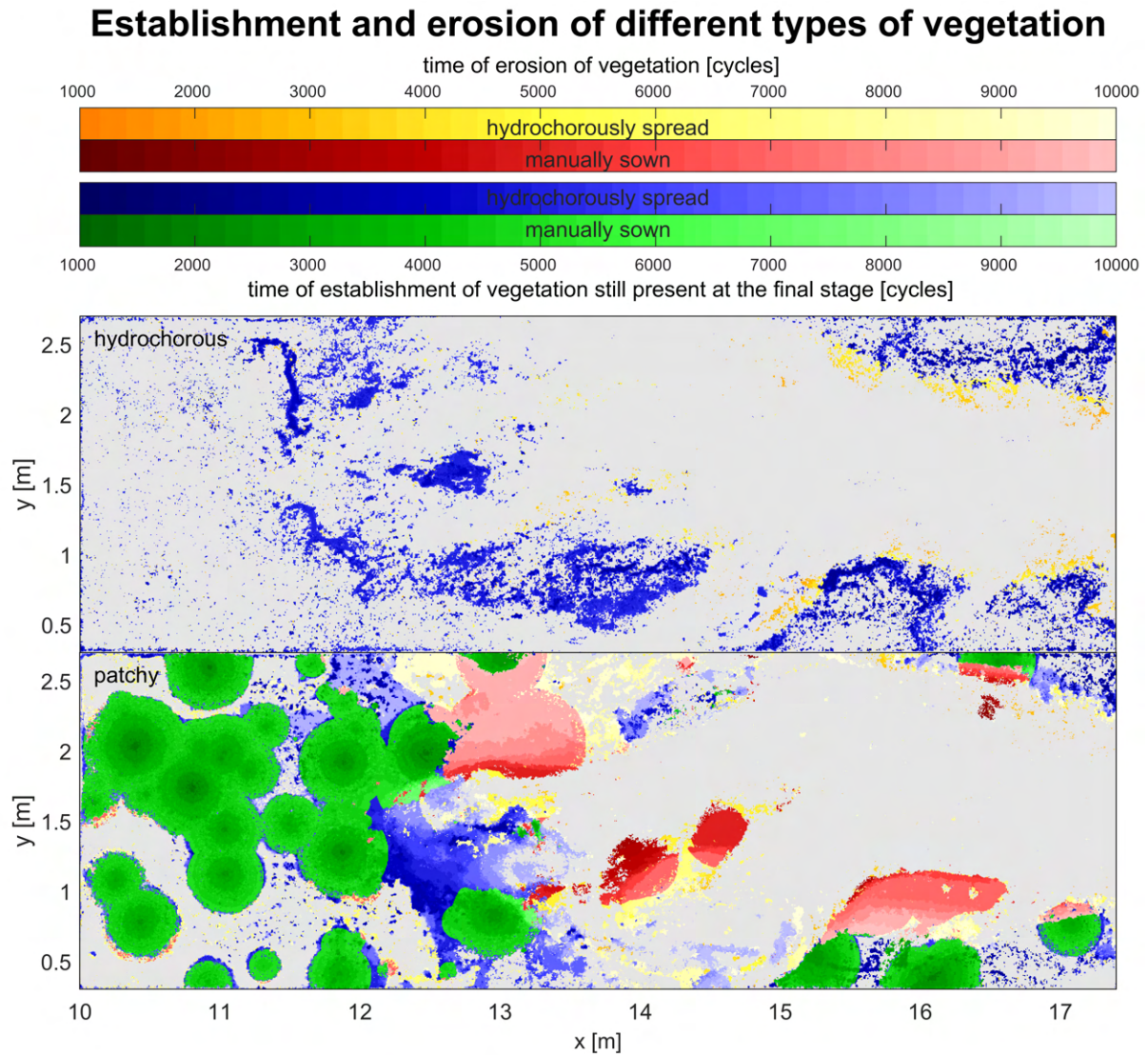


Figure 4.11.: Map of vegetation age and type in both vegetated experiments. Shades of green indicate existing manually sown vegetation with darker colours hinting at a higher age, shades of blue indicate existing hydrochorously spread vegetation with darker colours showing earlier establishment and shades of red and yellow indicate eroded vegetation, established by manual sowing or hydrochorous spreading, respectively. Darker colours correlate with earlier erosion. Grey indicates areas where vegetation has never settled. The experiment with hydrochorous seed spreading is shown in the top panel while the bottom panel shows the experiment with patchy seeding. Hydrochorously spread vegetation in the experiment with patchy seeding is vegetation that was eroded from patches and then deposited by the flow at a different location within the system.

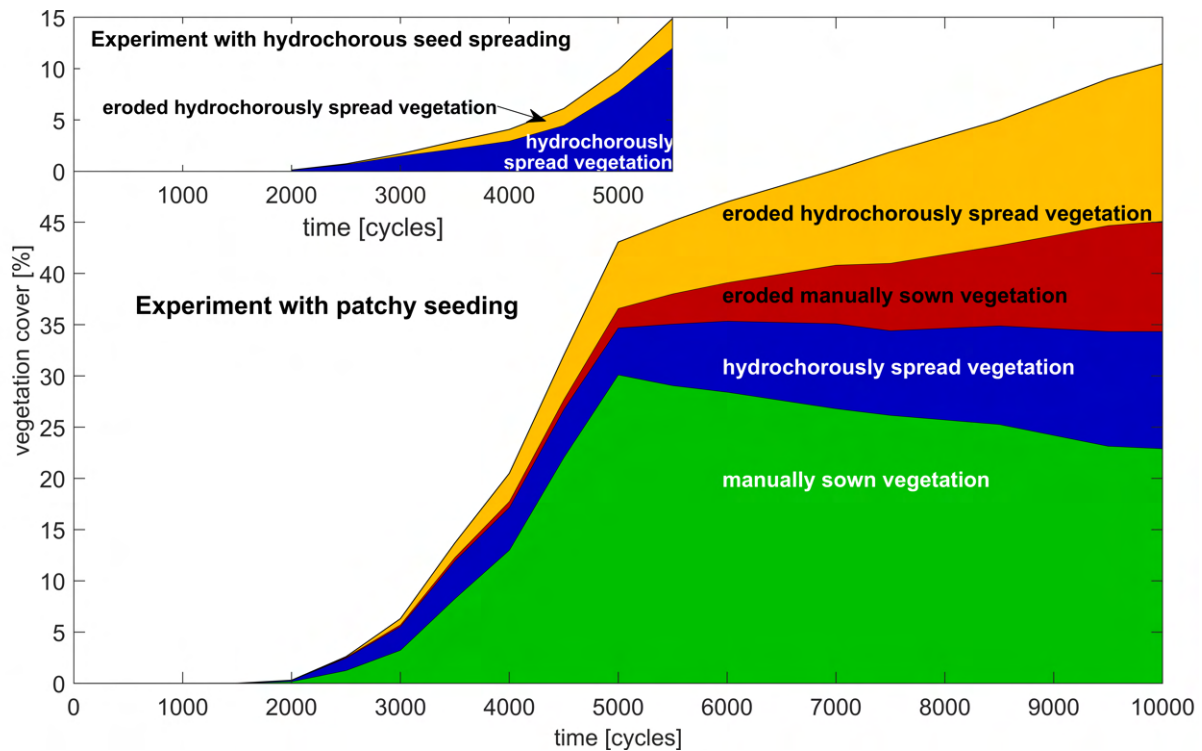


Figure 4.12.: Vegetation cover of different types over time. Green indicates existing manually sown vegetation, blue indicates existing hydrochorously spread vegetation whereas red and yellow indicate eroded vegetation, established by manual sowing or hydrochorous spreading, respectively. The experiment with hydrochorous seed spreading is shown in the inset while the main plot shows the data for the experiment with patchy seeding. The scale is the same in both plots. Hydrochorously spread vegetation in the experiment with patchy seeding is vegetation that was eroded from patches and then deposited by the flow at a different location within the system.

The growing vegetation of course also interacted with the flow and had some significant effects on the morphology. For example, it can determine the positioning and expansion direction of channels by stabilising one of its banks and therefore hindering erosion (see fig. 4.13 a)). Vegetation can slow down flow velocities and thereby focus flow (see fig. 4.13 c)) or even block it (see fig. 4.13 b)). By blocking the flow of water, it can also cut off side channels (see fig. 4.13 f)). The increased flow resistance by vegetation and the resulting focus of flow around it, often leads to scouring (see fig. 4.13 e) and also c)). This can initiate new channel development between vegetated areas as well (see fig. 4.13 d)). The stabilisation of channel banks (see fig. 4.13 h)) can fix certain morphological features, like bifurcations (see fig. 4.13 g)) for a longer time.

These local effects were especially visible in the experiment with patchy seeding due to the very dense vegetation in the patches. One channel in the central part was, roughly between 12.8 m and 14.7 m on one side lined with several patches. This is shown in fig. 4.13 a) as well. These patches slowed down its lateral migration but could not stop it in the end. This balance between channel migration and stabilisation due to vegetation, also due to the systematic expansion of the patches, was in place from around 3000 cycles to 4500 cycles. For an even longer time, the bifurcation

shown in fig. 4.13 g) on the side of the main trunk channel was kept in place by a patch. But also this patch was eventually eroded by the lateral expansion of the main channel.

In the most upstream part, where morphological action did usually not take place due to insufficient flow velocities for the sediment to reach the beginning of motion, some very small channels developed in narrow areas between patches (see fig. 4.13 d)) in the latest stages when a lot water accumulated here due to the blockade of outflow by vegetation (see fig. 4.13 b)). Vegetation blocked the flow on the sides already further seaward. This also led to the side channels being almost completely morphologically inactive (see fig. 4.7). The central channel grew deeper but its landward expansion was hindered by vegetation. However, the flow in the channel was energetic enough to uproot the vegetation but not to remove it as the individual plants were woven together very densely. Deposition of sediment took place under the uprooted vegetation while the plants were floating on the water surface, plants were therefore not buried. The slow lateral migration of this channel eventually led to the breaching of the vegetation which then allowed for further expansion of the channel (see fig. 4.7).

These strong local effects were not as pronounced in the experiment with hydrochorous seed spreading while the overall morphology of this system showed more differences compared to the control experiments than in the experiment with patchy seeding (see also fig. 4.14). The experiment with hydrochorous seed spreading was characterised by a long and straight main channel following the inlet. Unlike in the unvegetated control experiments, the system does not split up into several channels already shortly landward of the inlet but is confined into one channel. This single channel focuses flow more efficiently which enables the system to expand further landward. This confinement is created by vegetation on the banks of the main channel which hinder erosion of the channel banks.

The first split-up of the main channel often occurred around 16 m (see fig. 4.1, 4.3, 4.5 and 4.7). In the unvegetated systems, the two or more channels then quickly expanded laterally and migrated seaward. This resulted in the wide systems with several channels in the downstream part. However, in the experiment with hydrochorous seed spreading, and, to a lesser extent, in the experiment with patchy seeding, this seaward migration did not take place. Instead, the channels expanded landward and became longer. This was likely facilitated by vegetation settlement on the main channel banks in the downstream part which focuses flow in certain areas instead of a more homogeneous flow like in the control experiments. The vegetation cover on these banks was around 4% at the stage where the first differences to the control experiment occurred (around 2500 cycles). The landward expanding channels did not get as wide, instead there were several smaller channels landward of the split-up point. This split-up point between the main trunk channel and smaller channels in the upstream part was eventually found around 15 m (see fig. 4.5).

This behaviour was especially visible in the experiment with hydrochorous seed spreading. In the experiment with patchy seeding, the trunk channel was not as clear and confined but still visible in comparison to the control experiments. The split-up into smaller channels also occurred a bit

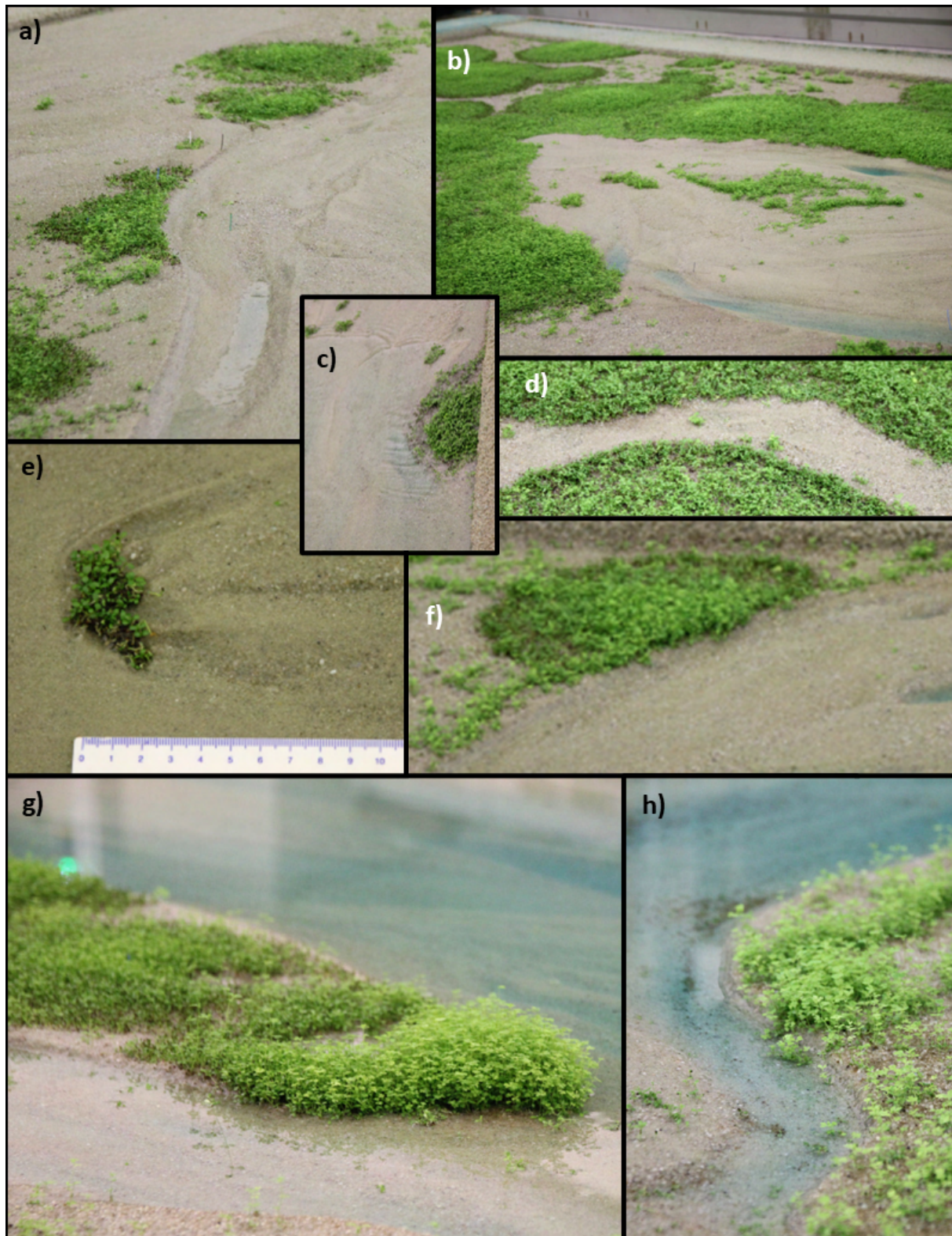


Figure 4.13.: Different local effects of vegetation in the experiments. Examples are: (a) Determining channel position and expansion direction, (b) blocking flow, (c) focusing flow, (d) channel initiation, (e) scouring, (f) cutting off side channels, (g) fixing morphological features and (h) bank stabilisation.

more seaward than in the experiment with hydrochorous seed spreading. The main channel also was wider already at an earlier stage. This was mainly due to erosion on one side as there were several dense patches on the other side and only little vegetation on the side that was eroded (see fig. 4.11). The more densely vegetated bank was eventually eroded as well, but only at a later stage (see fig. 4.7). The concentrated vegetation in certain places also caused the more landward channels to be less in number but larger and more sinuous, so that the upstream part in the experiment with patchy seeding was less branched (see fig. 4.7).

The reason for the stronger vegetation effects on the overall scale in the experiment with hydrochorous seed spreading is most likely the completeness of biogeomorphic feedback loops. Hydrochorously spread vegetation establishes only in areas where flow velocities are low and then further reduces them, enabling more vegetation to settle. This positive feedback is active as a complete feedback loop in the experiment with hydrochorous seed spreading whereas it is not in the experiment with patchy seeding. Here, the locations for vegetation growth are randomly pre-determined, resulting in vegetation also being sown in unsuitable places and not in all places that would be favourable for vegetation growth. Thus, the feedback loop is incomplete, as vegetation might reduce flow velocities but does not necessarily settle in places where flow velocities are low. Only parts of the feedback are therefore in place and dense patches in unsuitable locations might also cause a negative feedback, slowing down flow in areas where it is faster (e.g. side channel cut-off in fig. 4.13 f)) and enhancing flow in areas of previously low flow velocities (e.g. scouring and channel initiation in fig. 4.13 c), d) and e)). This limits the self-organising ability of the landscape.

4.4. Channel network

The developing channel networks closely follow the morphological development described earlier (see fig. 4.1, 4.3, 4.5 and 4.7). First, a straight main channel with lots of small branched side channels forms which then splits up into several channels. A network of ebb- and flood-channels develops which branches out in landward direction (see fig. 4.14 and Appendix A for all network maps).

The digitised channel networks show a similar development in all experiments when overall measures are compared. The total length of channels ΣL shows an exponential increase (see fig. 4.15 a)). Mean unchannelled path length m_{UPL} shows an exponential decrease (see fig. 4.15 b)). The evolution of drainage density D_d closely follows the one of ΣL since the basin area is almost constant and nearly the same in all experiments and timesteps (see fig. 4.15 c)). Geometric efficiency e_g decreases in the beginning and then stays roughly constant between 0.5 and 1 or even slightly increases (see fig. 4.15 d)). The differences between the experiments mainly represent the different speeds of development, seen in other variables like the eroded volume as well (see fig. 4.9). Differences between vegetated or unvegetated experiments or the different colonisation patterns are insignificant because the differences between the two control experiments are usually higher.

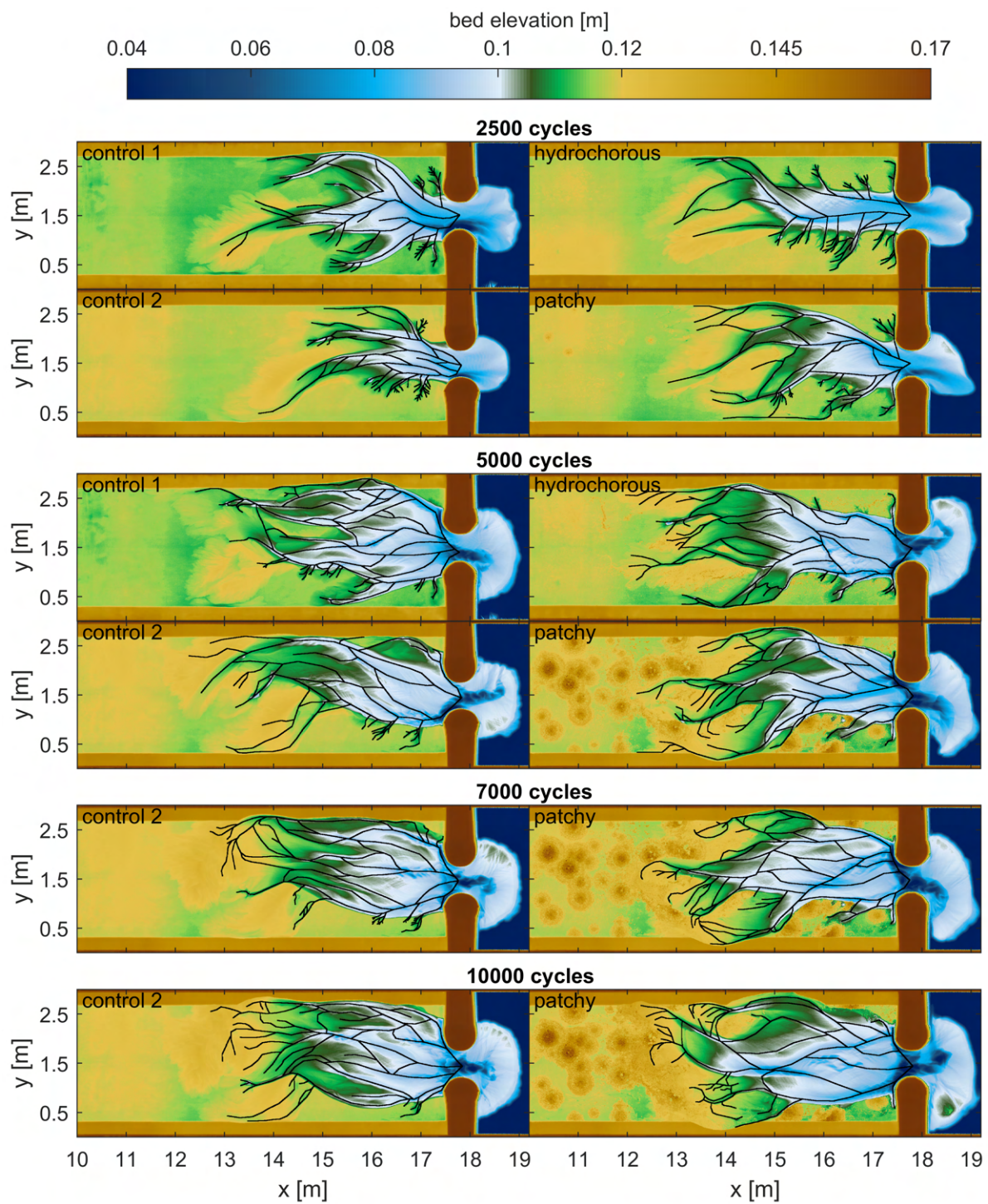


Figure 4.14.: Exemplary maps of the channel network at 2500 cycles and 5000 cycles for all experiments and at 7000 cycles and 10 000 cycles for the second control experiment and the experiment with patchy seeding. Black lines indicate the channels.

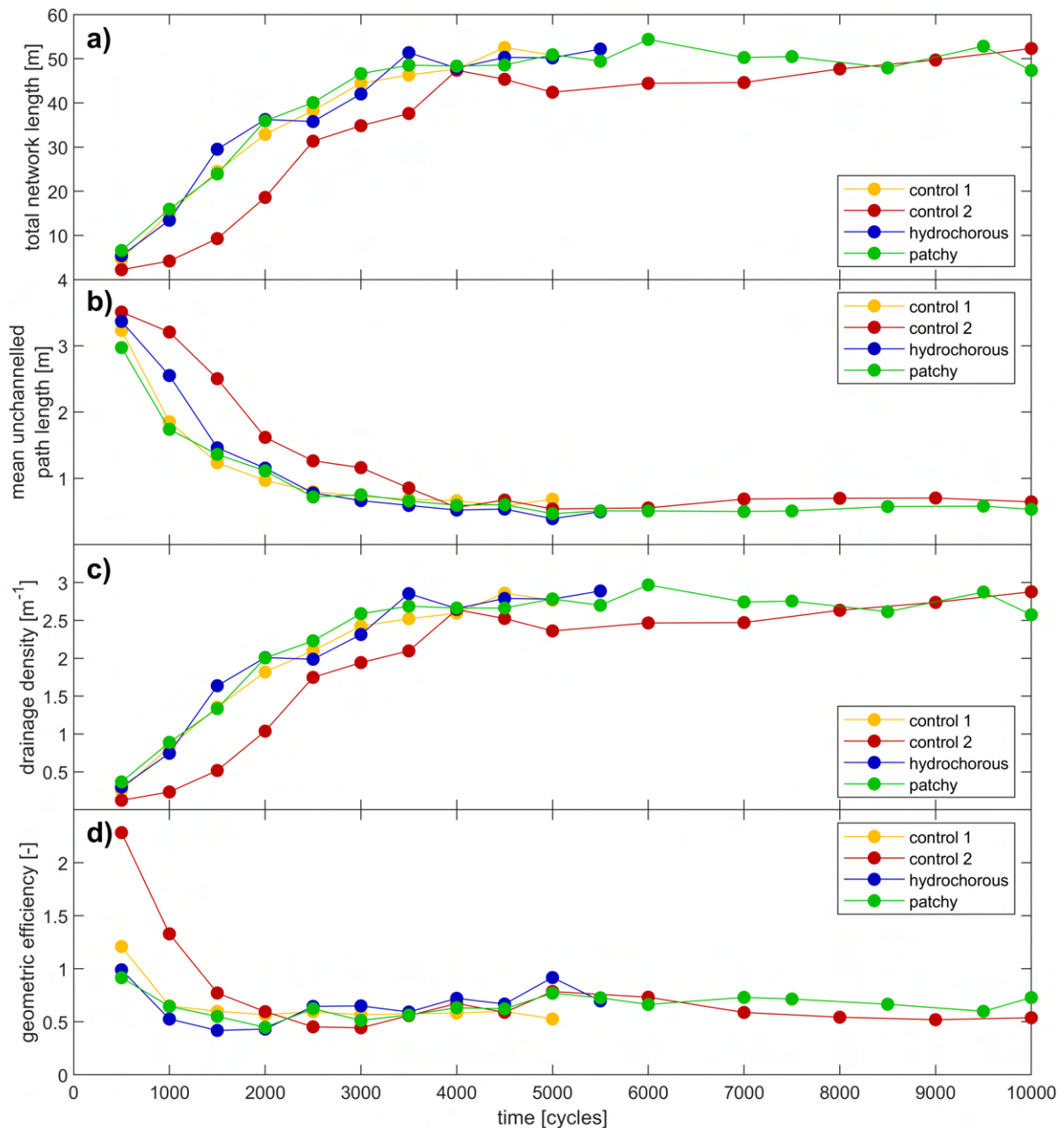


Figure 4.15.: Evolution over time of (a) total length of channels ΣL , (b) mean unchannelled path length m_{UPL} , (c) drainage density D_d and (d) geometric efficiency e_g over time in all experiments.

Just like in the erosion variables (see fig. 4.10), differences are only visible when variables are broken down along the flume (see fig. 4.16). The further landward expansion of the experiments with vegetation also shows in the network measures. The peak in channel network length per cross-section lies further landward in the two vegetated experiments than in the control experiments (see fig. 4.16 a)). Also the number of channels per cross-section has its peak further landward (see fig. 4.16 d)). These peaks are in line with the peak in eroded surface area (see fig. 4.10 b)). Since

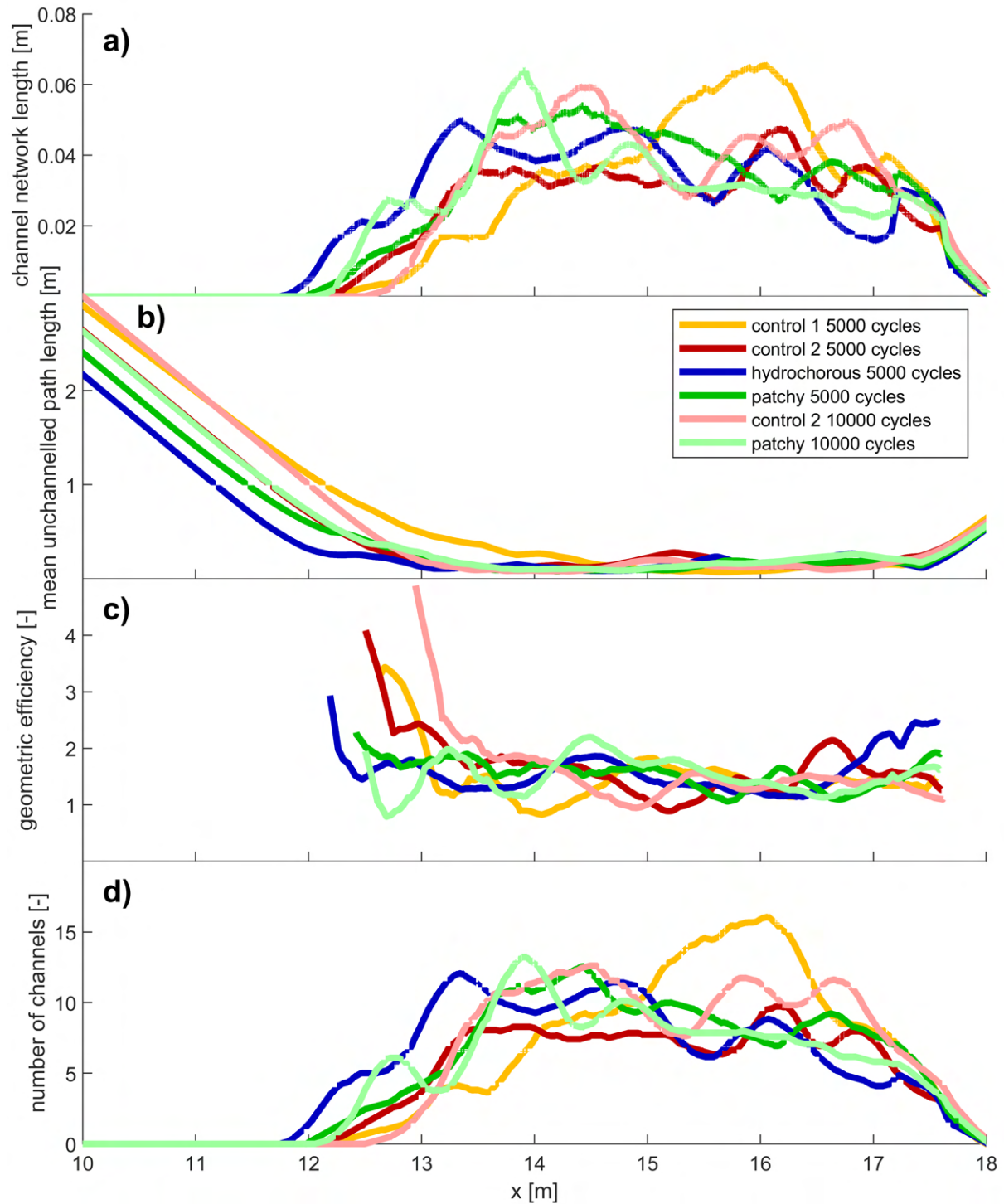


Figure 4.16.: Different variables characterising the channel network at 5000 cycles for all experiments and at 10 000 cycles for the second control experiment and the experiment with patchy seeding along the flume: (a) total length of channels ΣL , (b) mean unchannelled path length m_{UPL} , (c) geometric efficiency e_g and (d) number of channels per cross-section. The legend in panel b) is valid for all panels.

the channels are formed by the erosion of sediment, the number and length of channels logically correlates with the surface area that is affected by erosion.

The mean unchannelled path length generally strongly increases at the landward end of the system as the channel network ends at a certain point (see fig. 4.16 b)). m_{UPL} is lower in the most landward part for the vegetated experiments as their networks extend further landward. Even though the mean unchannelled path length is higher here, the geometric efficiency shows the highest values at the landward end of the systems due to the short network lengths in this area (see fig. 4.16 c)). This behaviour correlates to the high values of e_g for the early development stages of the experiments with short ΣL (see fig. 4.15 c)).

4.5. Water level measurements

The water level measurements showed some similarities in all experiments. The high and low water levels generally lie closer to each other towards the landward end of the system, and this shifts landward as the system expands (see fig. 4.17). The highest high water level always seem to occur at a similar distance from the landward end as well. They also shift landward over time. At the beginning, they lie shortly behind the inlet and then move upstream, making room for a minimum in high water levels in the seaward part of the system (see fig. 4.17). This results in the banks along the major channels in the seaward part of the system becoming supratidal with progressing system growth, even though their elevation does not change and the morphology is barely affected by the flowing water here.

Maps of the sub-, inter- and supratidal area were created for all four experiments based on water level measurements (see fig. 4.18 and Appendix B for all maps). Not all maps are of equal quality due to the number, position and quality of measurements. This causes the sometimes significant differences between two consecutive time steps. The maps that were evaluated as reasonable (medium and good quality as shown in Appendix B) were used in fig. 4.19. This figure shows the evolution of the percentages of areas of different elevation relative to the tidal frame. A clear trend is only visible in supratidal area which increases over time (see fig. 4.19 a)) and high intertidal area which decreases over time (see fig. 4.19 b)). Differences between the different experiments seem to be insignificant as the scatter is high. For the supratidal area, some more analysis was done. The height of the vegetation favours the classification as supratidal as it also appears in the DEMs but does not represent the sand bed elevation. This is especially true for the dense patches. Therefore, the supratidal area that is bare was plotted as well (see fig. 4.19 a)). In the second control experiment, significant areas in the landward part of the system were classified as supratidal which does not match the visual observations during the experiment. Therefore, supratidal area only seaward of 14 m is shown as well.

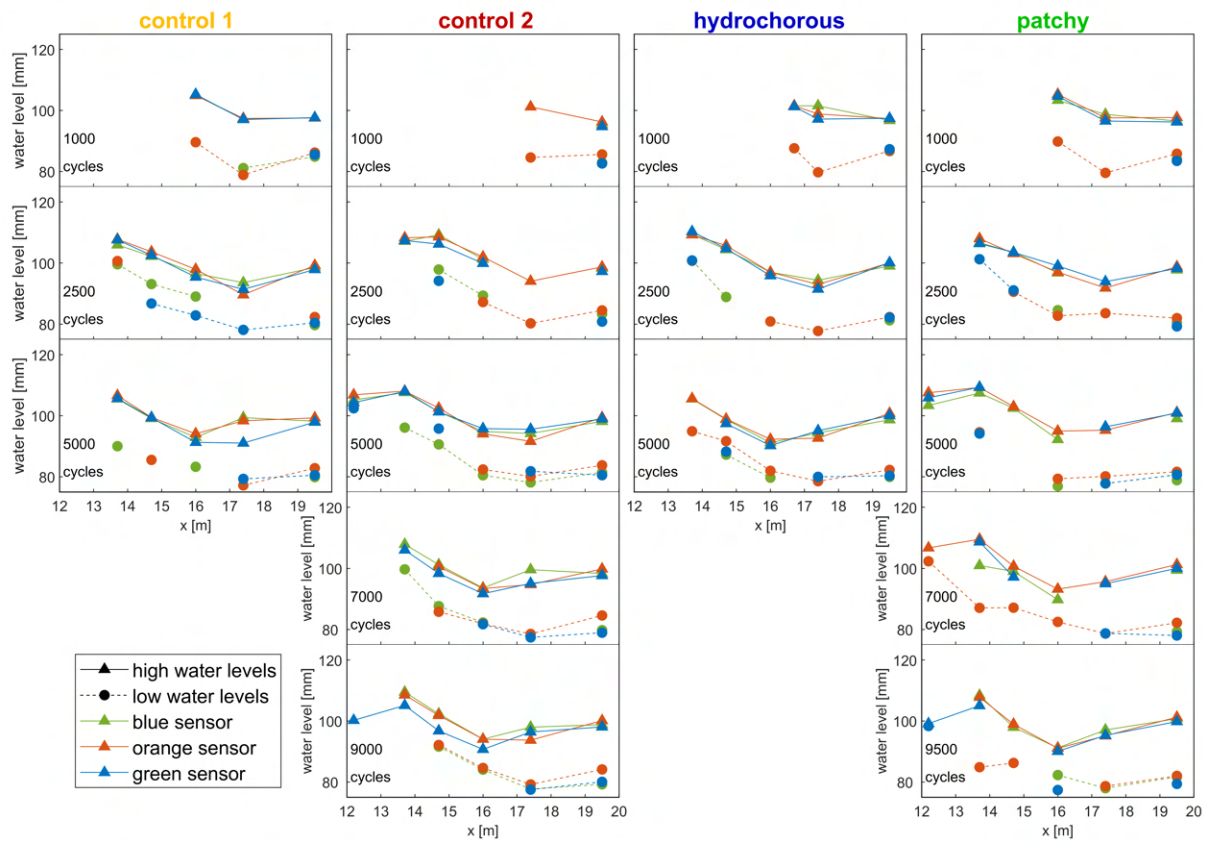


Figure 4.17.: Water surface elevation at different stages during the experiments. Green, orange and blue indicate the different sensors. Triangles and circles indicate the measured high and low water levels, respectively. Solid and dashed lines connect the measured high and low water levels. Only the measurements that were evaluated as reliable are included (see Appendix C).

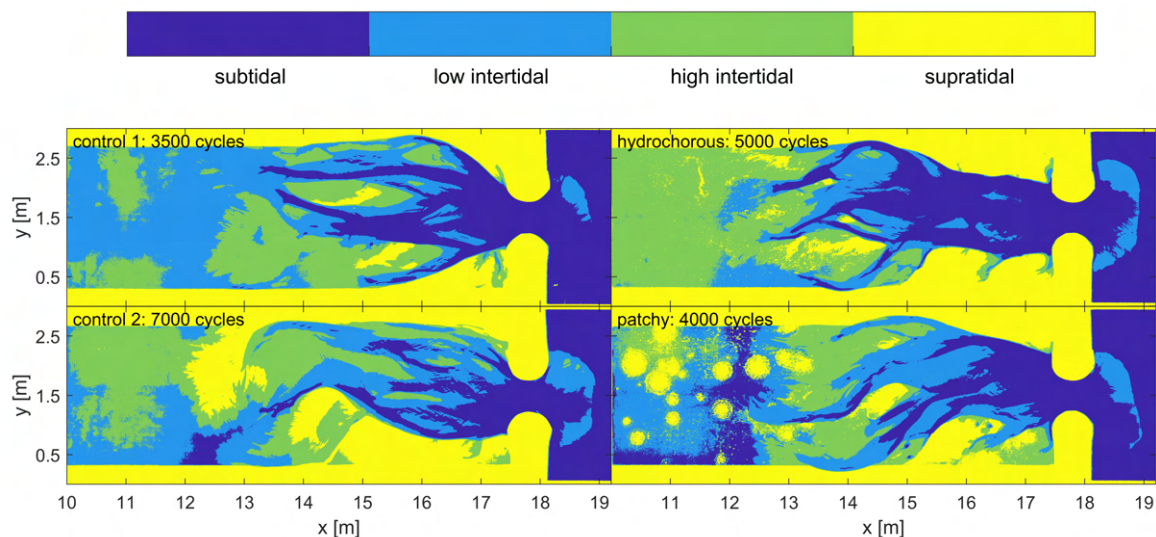


Figure 4.18.: Exemplary maps of sub-, inter- and supratidal areas from different stages of the experiments. Dark blue indicates subtidal areas, light blue and light green indicate low and high intertidal areas, respectively and yellow indicates supratidal areas. These maps give reasonable results, which is not true for all maps.

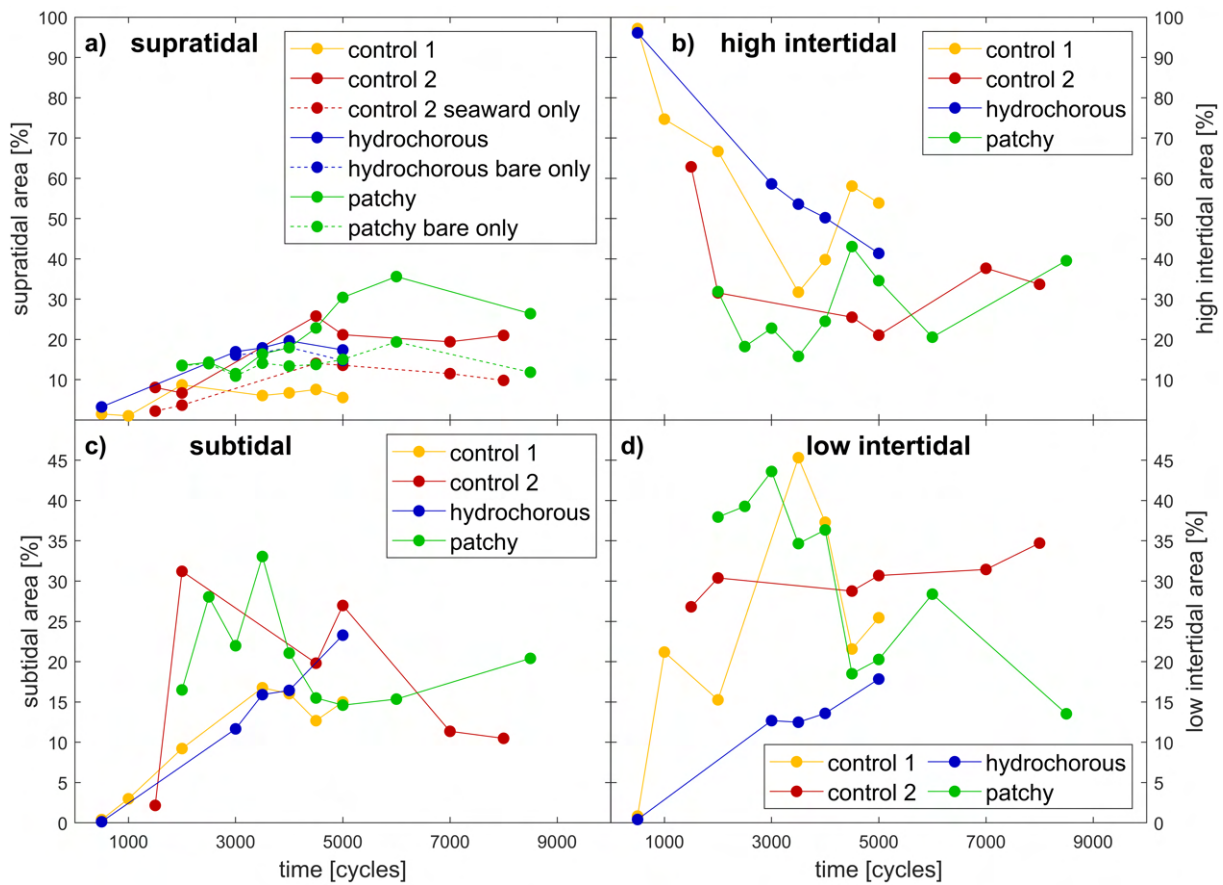


Figure 4.19.: Evolution of sub- (c), low inter- (d), high inter- (b) and supratidal (a) area over time in all experiments, based on the water level measurements. Not all timesteps were taken into account, only the ones where the maps were evaluated as reasonable (medium and good quality in Appendix B).

5. Discussion

5.1. Role of initial conditions and experiment comparability

The four experiments all showed a similar development, starting with a slow adjustment to the boundary conditions which then sped up and eventually came close to an equilibrium (see fig. 4.9). Differences between the experiments are visible in the speed of development. This differs most likely due to small differences in the initial conditions. In physical experiments, the initial conditions can never be exactly the same even though this is tried to achieve. However, small differences in elevation, compactness or local grain size distribution cannot be ruled out, especially in the area close to the inlet, that had to be shaped by hand. These small differences can form perturbations large enough to affect the chaotic development of the channel pattern (Phillips, 2006). While the overall size and growth of the system is governed by the boundary conditions and, at least in the later stages, forms an (almost) equilibrium with these (Phillips, 2006), the exact bar and channel pattern is an instable and chaotic system (Phillips, 2006) which shows continuous adjustments (see fig. 4.1, 4.3, 4.5 and 4.7). This chaotic system is sensitive to initial conditions and the emerging pattern is characterised by a high path dependency (Stallins, 2006).

But since this only characterises the exact bar and channel pattern and not the overall size and characteristics of the system as a whole, the different experiments are still very comparable to each other. They show a clear response to the boundary conditions and the similar outcomes concerning erosion variables (see fig. 4.9) and network measures (see fig. 4.15) underline that. While the exact configuration of bars and channels cannot be attributed to the boundary conditions or one specific variable due to their chaotic nature (Phillips, 2006), a change in the overall distribution of channels under the same hydrodynamic boundary conditions, as observed in the experiments (see fig. 4.10, 4.14 and 4.16), can be attributed to the variables that were changed between the experiments, being the presence and colonisation pattern of vegetation.

Not only can the experiments of this study be compared to each other, but also to other experiments in literature. Earlier experiments in tilting flumes showed similar emerging networks and dendritic systems growing by backward erosion (Kleinhans et al., 2012). Most other experiments in a tilting flume however aimed at simulating different environments, usually entire estuaries. The therefore different settings did not lead to the development of the characteristic channel growth by backward erosion but to a similarly dynamic bar and channel pattern (Kleinhans et al., 2022; Kleinhans et al., 2017; van Dijk et al., 2021; Weisscher et al., 2022). The backward erosion of the channels and

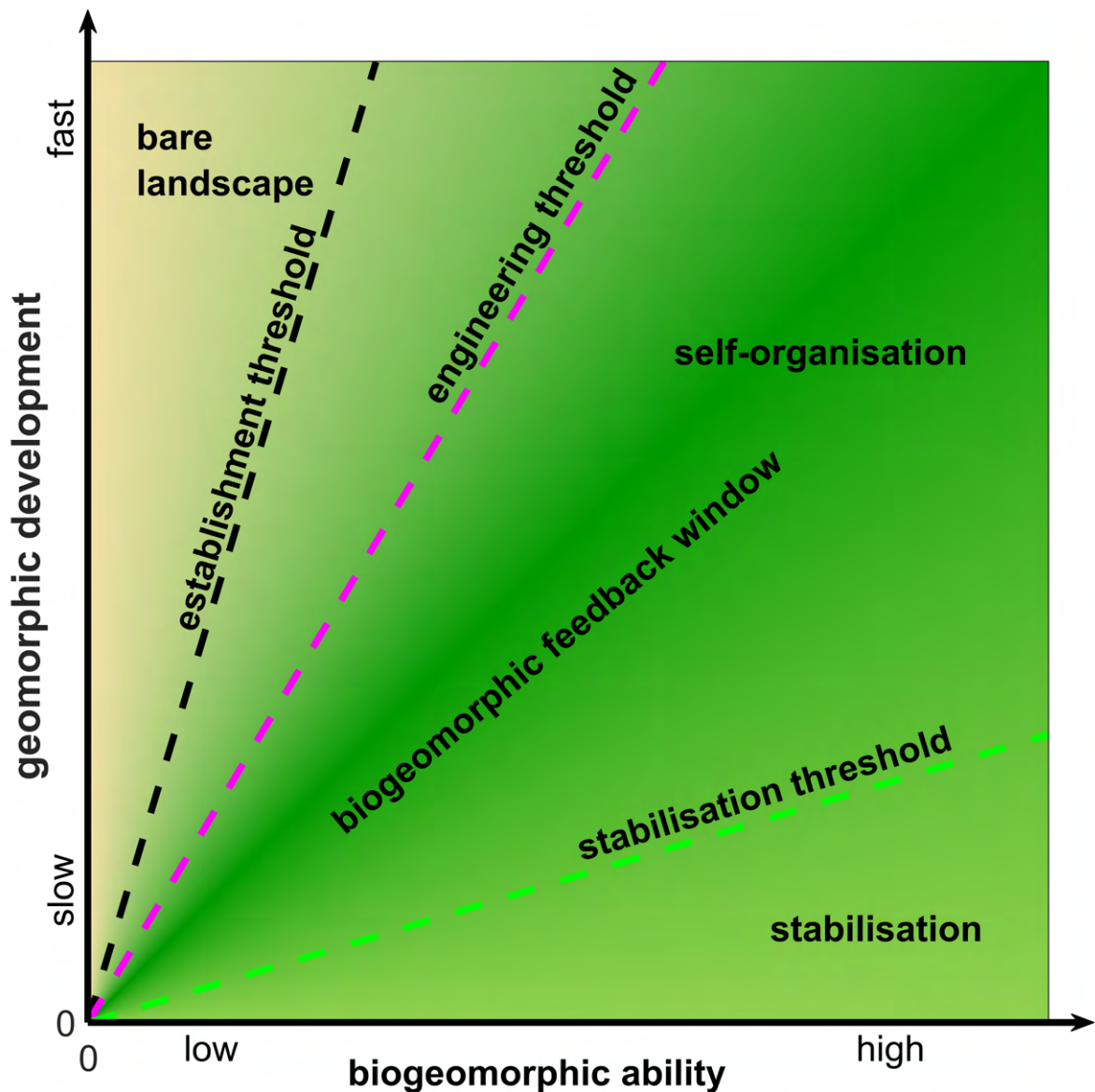
expansion in landward direction is found in natural tidal flats and salt marshes (Kleinhans et al., 2009) as well as in other experiments on tidal basins without tilting and only periodic water level fluctuations (Stefanon et al., 2012).

5.2. Biogeomorphic feedback window in experimental salt marshes

5.2.1. Integration of concepts

The concepts on the conditions for biogeomorphic interaction by Eichel et al. (2016) (see fig. 2.1) and Schwarz et al. (2018) (see fig. 2.2) both have some important similarities and can therefore be integrated into one concept (see fig. 5.1). This concept keeps the timescale of geomorphic development on the y-axis like in the concept of Schwarz et al. (2018). On the x-axis it plots the biogeomorphic ability of plants (see fig. 5.1). This parameter is affected by many different aspects and integrates those. As all these aspects affect the biogeomorphic effects of vegetation, a single one of these parameters would be insufficient to represent the different effects. While being more difficult to quantify, the biogeomorphic ability is able to represent the often existing multiple causality in biogeomorphic systems (Stallins, 2006).

This biogeomorphic ability is affected by the vegetation cover and density, the colonisation pattern and distribution of vegetation, the plants' resilience and resistance to disturbances and other specific plant traits as well as possibly other things, depending on the exact environment and species. Vegetation cover and density generally increase the biogeomorphic ability as more vegetation has a stronger effect. This effect is however most likely not linear, but rather logarithmically, so that the same absolute increase has a stronger impact for a lower vegetation cover or density than if already very much vegetation is present. This is in line with the behaviour of the equation by Baptist et al. (2007) for flow resistance of vegetation, which was used in many studies on biogeomorphic interactions (e.g. Brückner et al., 2019; Oorschot et al., 2016). However, the same vegetation cover can have stronger or weaker effects, depending on its distribution, resulting from e.g. the colonisation pattern of the dominant plant species at a certain site (Schwarz et al., 2014; Schwarz et al., 2018). If the vegetation is concentrated in certain areas, e.g. patches, its biogeomorphic effects are also scale dependent. Local flow velocity reduction can lead to erosion and channel initiation around the patch, as described by Temmerman et al. (2007) and also seen in the experiments (see fig. 4.13 c, d) and e)). Also other individual characteristics of plants than the colonisation pattern play an important role. Not all species can act as eco-engineer, i.e. due to an insufficient resistance or resilience (Eichel et al., 2016; Eichel et al., 2013). Salt marsh vegetation can act as eco-engineer not only by affecting flow velocities but for example also by regulating sedimentation (Marani et al., 2013). The biogeomorphic ability is therefore affected by many different aspects on itself and on their interactions combined and does not necessarily correlate linearly with the individual parameters, accounting for the complex nature of biogeomorphically shaped systems (Stallins, 2006).



affected by: vegetation cover and density, distribution,
colonisation pattern, establishment speed,
plant resilience and resistance, other plant traits

Figure 5.1.: Concept on the conditions for biogeomorphic interactions depending on the speed of the geomorphic development and the biogeomorphic ability of plants.

Within the two axes defined by the geomorphic development and the biogeomorphic ability, different zones are placed which are separated by thresholds (see fig. 5.1). The zones are similar to the different boxes in the concept of Schwarz et al. (2018) (see fig. 2.2) whereas the thresholds are taken from the concept of the biogeomorphic feedback window by Eichel et al. (2016) (see fig. 2.1). The first zone is the zone of bare landscape (see fig. 5.1). A bare landscape emerges when

the geomorphic development is too fast, so that the available vegetation is unable to colonise the system. If the biogeomorphic ability of a species is high enough for a given geomorphic development speed, the establishment threshold is crossed and the vegetation can settle (see fig. 5.1). The same vegetation might not be able to settle for a faster geomorphic development whereas a slower development can enable also species with a lower biogeomorphic ability to establish. When the biogeomorphic ability of the vegetation in the system increases, for example by a higher coverage, the engineering threshold can be crossed (see fig. 5.1). The vegetation then actively shapes the landscape in interaction with the abiotic characteristics. The crossing of the engineering threshold cannot only be achieved by an increase in biogeomorphic ability but for a given biogeomorphic ability also by a reduction in geomorphic development speed (see fig. 5.1).

If the biogeomorphic ability is high in relation to the geomorphic development, the stabilisation threshold can be crossed (see fig. 5.1). Then, the vegetation stabilises the landscape strongly enough, so that the abiotic processes cannot or only barely alter it. This is often achieved by the roots of the plants stabilising the soil and preventing erosion. But not only a high biogeomorphic ability, for example due to a high coverage and/or density, can lead to stabilisation, also a slow geomorphic development can enhance this (see fig. 5.1). Stabilisation of the landscape can enable other plant species to colonise the system and lead to a succession. Such plants can have competitive advantages over the engineering species in stable landscapes. Therefore, this threshold is called the competition threshold by Eichel et al. (2016) (see fig. 2.1). In the context of salt marshes, stabilisation can however also occur with the same species that also act as eco-engineer (Schwarz et al., 2014; Schwarz et al., 2018). Stabilisation is thus the more suitable term than competition.

The zone in between the engineering threshold and the stabilisation threshold marks the conditions under which a self-organised landscape can emerge (see fig. 5.1). This is the biogeomorphic feedback window (Eichel et al., 2016). Here, the landscape is shaped by the feedbacks between abiotic drivers of the geomorphology and the impacts of the colonising plant species on it. This zone can be entered and left via changes in the speed of geomorphic development or the biogeomorphic ability of the colonising vegetation (see fig. 5.1). Outside of this window, the landscape evolution is either dominated only by abiotic processes or only by the vegetation itself but not by the feedbacks between the two.

All the thresholds in this concept emerge from the origin where both geomorphic development and biogeomorphic ability are zero (see fig. 5.1). From here on they expand and the separation between them increases. This is different from the concept of Schwarz et al. (2018) (see fig. 2.2), where the separation between the zones was roughly parallel. The radial separation is more suitable as a landscape where the geomorphic development is zero, is always stable no matter how this is affected by biogeomorphic interactions. Similarly, a landscape where the biogeomorphic ability is zero, which equals no vegetation, is always bare. The zones in between the thresholds, like the biogeomorphic feedback window, become wider with increasing geomorphic development speed

and/or biogeomorphic ability. More combinations can then lead to a self-organised landscape and biogeomorphic feedbacks. All the transitions between the zones and the thresholds are not fixed of course. The transitions are likely smooth and a landscape does not jump from one state to another if a certain vegetation variable surpasses a certain value. The thresholds are thus rather threshold ranges and mixed-type landscapes can occur.

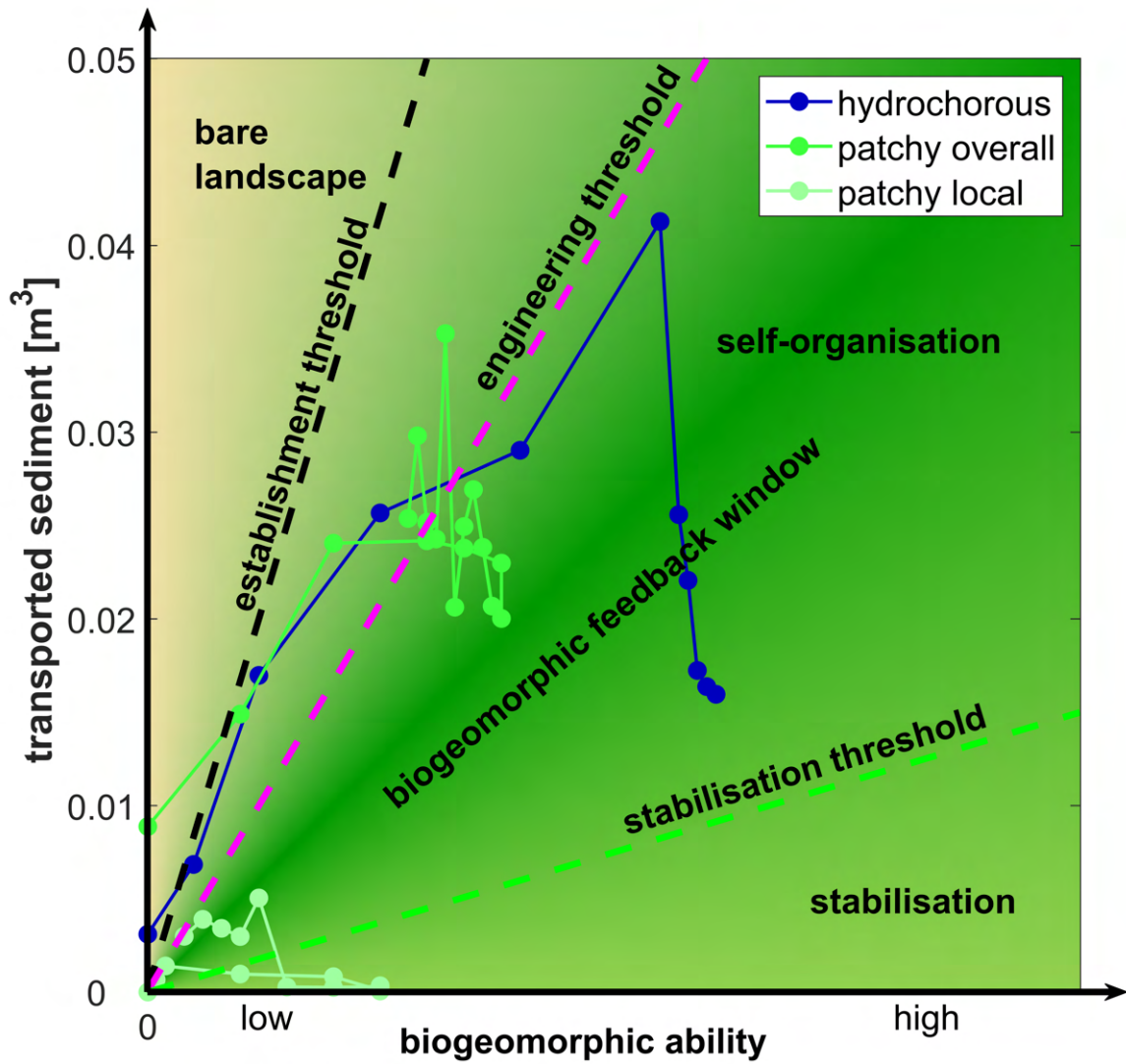
5.2.2. Quantified conceptual representation of the experiments

For the classification of the experiments in the concept on the conditions for biogeomorphic interactions, a semi-quantitative approach was used. As proxy for the geomorphic development speed, the sediment that was transported between two consecutive DEMs was used (see fig. 5.2). This is calculated as the volume of sediment that was eroded from the system in comparison to the previous DEM. It is therefore not the eroded volume that is showcased in fig. 4.9 a), as this is the eroded volume in comparison to the initial condition. The biogeomorphic ability was quantified manually on an arbitrary scale (see fig. 5.2). Although it is subjective, the manual quantification is necessary as many different variables and their individual feedbacks and combinations have effect on the biogeomorphic ability.

The two vegetated experiments were both classified on the overall scale and the patchy experiments also on the local scale to showcase scale-dependent differences (see fig. 5.2). For this local scale, the area between 15.5 m and 17.5 m in x-direction and between 0.3 m and 1 m in y-direction was used. This is the bank along the main channel where one vegetation patch fixed a bifurcation between the main channel and a side channel for several thousand cycles (see fig. 4.7 and 4.13 g)). The consecutive points with the respective values for the transported sediment and biogeomorphic ability are connected by lines, so that they form a trajectory of the experiment over time (see fig. 5.2). All experiments are characterised by a biogeomorphic ability of zero in the beginning as no vegetation was present at the start.

The hydrochorous experiment shows a steep increase in geomorphic development speed, represented by the transported sediment, until 3000 cycles. Sowing started at 1000 cycles but only very few seeds could settle, so that the biogeomorphic ability was still very low, but already sufficient to just cross the establishment threshold. 500 cycles later, biogeomorphic ability was already higher, but still only very few seeds could settle as also the geomorphic development speed increased. This is represented by the two dots both being only very close over the establishment threshold (see fig. 5.2). After that, more seeds could settle, so that the biogeomorphic ability is increased significantly. At 2500 cycles, the engineering threshold is crossed (see fig. 5.2). At this stage, the morphology also starts to develop differently from the control experiments (see fig. 4.5 and 4.14). The vegetation cover on the banks along the main channel was around 4 %, as mentioned earlier. Such a low cover can thus be already sufficient to reach the engineering threshold, however it has to occur in the right configuration. The cover was rather uniformly spread over the banks along the main channel (see fig. 4.11) and therefore slowed down flow velocities here significantly,

resulting in the flow being focused completely into the central main channel. This would have been much less efficient, if the cover was concentrated in one place or not located on the main channel banks at all, but e.g. in the landward part of the system. This highlights the importance of the combined measure of biogeomorphic ability, since one parameter, like for example vegetation cover, is insufficient to represent the strength of the vegetation’s biogeomorphic effects.



affected by: vegetation cover and density, distribution, colonisation pattern, establishment speed, plant resilience and resistance, other plant traits

Figure 5.2.: Quantitative representation of the experiments in the concept on the conditions for biogeomorphic interactions. The sediment that was transported between two consecutive DEMs was used as proxy for the geomorphic development. The biogeomorphic ability was quantified on an arbitrary scale. The experiment with hydrochorous seed spreading showed more self-organisation than the patchy experiment on the overall scale. Locally however, the patches could even stabilise the landscape, at least for a certain time.

After the peak at 3000 cycles, the transported sediment drastically decreases and in combination with a further increased biogeomorphic ability, the trajectory of the experiment with hydrochorous seed spreading leads from the edges and an only slightly self-organised landscape to the centre of the biogeomorphic feedback window (see fig. 5.2). This is most likely the result of the eco-engineering activities of the vegetation. The settling of vegetation in areas with low flow velocities and the following further decrease in flow velocities, causes the decrease in transported sediment while increasing the biogeomorphic ability. This positive feedback loop can only come into action if it is closed, which is the case in the experiment with hydrochorous seed spreading. Further development of the system might have brought it into the stabilisation zone but the experiment was stopped at 5500 cycles.

The experiment with patchy seeding showed a different behaviour (see fig. 5.2). Initially, there are similarities, only few seeds/patches can establish at 1000 cycles but it is sufficient to cross the establishment threshold. Later, the trajectory also enters the biogeomorphic feedback window (see fig. 5.2). However, the biogeomorphic ability is lower than in the experiment with hydrochorous seed spreading, even though the vegetation cover is higher (see fig. 4.12). This again emphasises that one aspect alone, like the vegetation cover, is insufficient to represent the vegetation's biogeomorphic ability. A broader set of parameters needs to be represented, unlike in the concept of Schwarz et al. (2018) (see fig. 2.2), which mainly relies on the timescale of vegetation colonisation. While this still is an important factor, it is not the only one affecting the biogeomorphic ability.

The feedback loop between low flow velocities and increased flow resistance by vegetation is not closed in the experiment with patchy seeding, as the patches are placed on randomly pre-determined locations (see fig. 3.3) where they can cause an either positive or negative feedback. This results in the transported sediment not decreasing significantly, but staying in a constant range, though with high scatter (see fig. 5.2). Many patches are eroded (see fig. 4.11), which also adversely affects the biogeomorphic ability, causing it to start decreasing at a certain point (see fig. 5.2). Even though the patches in the experiment form a high resistance due to their density, they have a relatively low resilience, as they are not replanted once eroded. Hydrochorously spread vegetation however can recolonise areas if the hydrodynamic conditions allow for that again. This leads to the trajectory of the experiment with patchy seeding leaving the biogeomorphic feedback window again in the later stages (see fig. 5.2) even though it was entered earlier, similarly to the experiment with hydrochorous seed spreading. Closed feedback loops between abiotic and biotic processes are therefore crucial for the emergence of self-organised landscapes. If only vegetation affects flow velocities by increasing the hydraulic resistance, but the hydrodynamics do not determine where vegetation settles, a self-organised landscape cannot emerge.

This behaviour is however not independent of scale. Since the distribution of vegetation is not uniform in the experiment with patchy seeding, it can cause a much higher biogeomorphic ability locally. If only the part of the system between 15.5 m and 17.5 m in x-direction and 0.3 m and 1 m in y-direction is considered, the transported sediment is generally much lower of course (see

fig. 5.2). At the same time, the biogeomorphic ability is not that much lower than on the overall scale. This results in the area's trajectory leading into the stabilisation zone already very early (see fig. 5.2), which causes the bifurcation in this area to be in place without much alteration for several thousand cycles (see fig. 4.7). In later stages, the transported sediment increases as the main channel starts eroding its banks. The biogeomorphic ability of the plants decreases meanwhile as their high and dense cover only causes a spatially uniform increased flow resistance for water flowing over the area, which barely happens. Instead, the channel bank is eroded from the side where all the plants further away from the channel have no effect. This leads to the trajectory leaving the stabilisation zone again and entering the biogeomorphic feedback window (see fig. 5.2), where the bank stabilisation by plants and erosion driven by the hydrodynamics both determine the landscape evolution. Since the banks are still eroded, the hydrodynamics seem to be the dominant power here, leading to the trajectory eventually coming close to the edge of the biogeomorphic feedback window at the other side, close to the engineering threshold (see fig. 5.2).

This was only one example of the effects on a local scale. There might be other local examples from the experiment with patchy seeding that would end up in the centre of the biogeomorphic feedback window or from the experiment with hydrochorous seed spreading that do not lead there. Both, the biogeomorphic ability and the geomorphic development speed differ in space in the experiments. This results in the biogeomorphic feedback window not only being visible in the system development over time but also in space throughout the system. Different parts can be in different zones and be either stable, bare or self-organised or something in between. Often, the parts closest to the inlet or the main channel remain bare due to the high geomorphic activity whereas sheltered areas and the most landward part are stable and the areas in between can show a self-organised character (see fig. 4.1, 4.3, 4.5, 4.7 and 4.14).

Biogeomorphic feedbacks are therefore highly scale-dependent. The dense patches can have strong local effects (see fig. 4.13) while on the overall scale, the vegetation distribution in the experiment with patchy seeding is less suitable for the given hydrodynamics (see fig. 4.11), resulting in a more self-organised landscape emerging in the experiment with hydrochorous seed spreading (see fig. 4.14). The crucial feedback loop between low flow velocities and increased flow resistance due to vegetation might be closed locally in the patchy experiment, namely where the random patch locations are in line with areas where abiotic processes result in low flow velocities as well, but it does not necessarily have to. Here, the biogeomorphic effects can be even stronger than in local examples of the experiment with hydrochorous seed spreading due to the higher vegetation cover and density. Therefore, many general biogeomorphic effects could be observed more clearly at specific local sites in the experiment with patchy seeding (see fig. 4.13). The positive feedback loop in the experiment with hydrochorous seed spreading is not as enhanced as in some local cases in the experiment with patchy seeding, which makes the observation of clear local vegetation effects more difficult but does result in a more self-organised landscape on the overall scale since the feedback loop is closed everywhere.

If parts of this feedback loop are missing, the biogeomorphic ability of the vegetation is reduced. Its cover, density, resilience, resistance and many other aspects can be the same but its distribution throughout the system will not be ideal for a self-organised landscape to emerge if their location is unsuitable. Only if the landscape can fully self-organise and thus also 'organise' the locations suitable for vegetation growth, it can unfold its full self-organisation potential with all the accompanying benefits like increased resilience to different outer disturbances in a changing climate (Liu et al., 2020; Schwarz et al., 2018).

5.3. Water levels and tidal frame

The maps of sub-, inter- and supratidal areas for all experiments (see Appendix B) are unfortunately not all as reliable as each other or as desired. This is mainly due to the low number of measurements. A maximum of 18 measurements is not able to account for the large morphological variability within the system and therefore not for differences in water level on the local scale. However, the high and low water level still follow a certain trend. They are the highest in the most landward part of the system and decrease in seaward direction (see fig. 4.17). In later development stages of the system, a minimum in high and low water levels occurs landward of the inlet which gets more pronounced and moves landward with further development (see fig. 4.17). The tidal range decreases in landward direction. Since this pattern exists, it was possible to interpolate the few data points over the entire system area. But of course, the interpolation does not perform equally well everywhere. In fig. 4.19, only the somewhat reasonable maps were taken into account. But these also have areas where they are less precise. An example for this are the maps of the second control experiment for 4500, 5000, 7000 and 8000 cycles. These are overall relatively reasonable but show a lot of supratidal area in the landward part, which does not reflect the actual situation. If this is considered when looking at fig. 4.19 a), a difference between vegetated and unvegetated experiments becomes clear. A higher share of the system is supratidal in the experiments with vegetation. This also holds, if only bare areas are considered and the errors in the landward part of the second control experiment are excluded. Taking into account that vegetated areas can be supratidal as well, even if they are not shown in the adjusted graph, the difference is clear (see fig. 4.19 a)). This is in line with findings of earlier experiments (Weisscher et al., 2022) and shows how plants act as eco-engineers. They enhance the creation of their own ideal habitat.

5.4. Comparison and evolution of channel networks

Concerning quantifications of the channel network like ΣL , D_d , m_{UPL} or e_g , all experiments were very similar, regardless of vegetation being present or not or its colonisation pattern (see fig. 4.15). This suggests, that such quantitative measures of channel networks in salt marshes are mainly determined by abiotic factors and not by vegetation colonisation. Even though Kearney and Fagherazzi (2016) found more efficient networks in vegetated salt marshes, newer studies suggest that abiotic

factors play a more important role in the determination of channel network properties (Liu et al., 2022). This is also what was seen in the experiments with equal boundary conditions. Yet, there are differences in the channel network, however, not on the scale of overall measures but on the configuration in detail (see fig. 4.14). Such differences might suffice to make the channel network more efficient in some cases, as found for the five systems compared by Kearney and Fagherazzi (2016) but do not hold in general for all systems, as Liu et al. (2022) showed by analysing 14 systems.

Furthermore, it remains questionable whether the measure of geometric efficiency e_g is the most suitable to describe the efficiency of a channel network, especially in the experiments. It describes efficiency as the ability of the network to supply the system well with a relatively short total network length. It increases for a constant basin area when a lower m_{UPL} is achieved with a constant ΣL , or if ΣL can be lower and m_{UPL} does not increase. In the experiments however, e_g is the highest at the very beginning of the system development and mainly decreases with further system development (see fig. 4.15 d)). The very low ΣL at the start dominates over the high m_{UPL} in the calculation of e_g . This leads to the unintuitive results of the smallest systems being the most efficient. The relation between ΣL and m_{UPL} might therefore need some adjustments to accurately describe efficiency over different stages of development. An adjusted individual weighting of the two main drivers ΣL and m_{UPL} might however result in a dimensional parameter, which limits comparability across different scales.

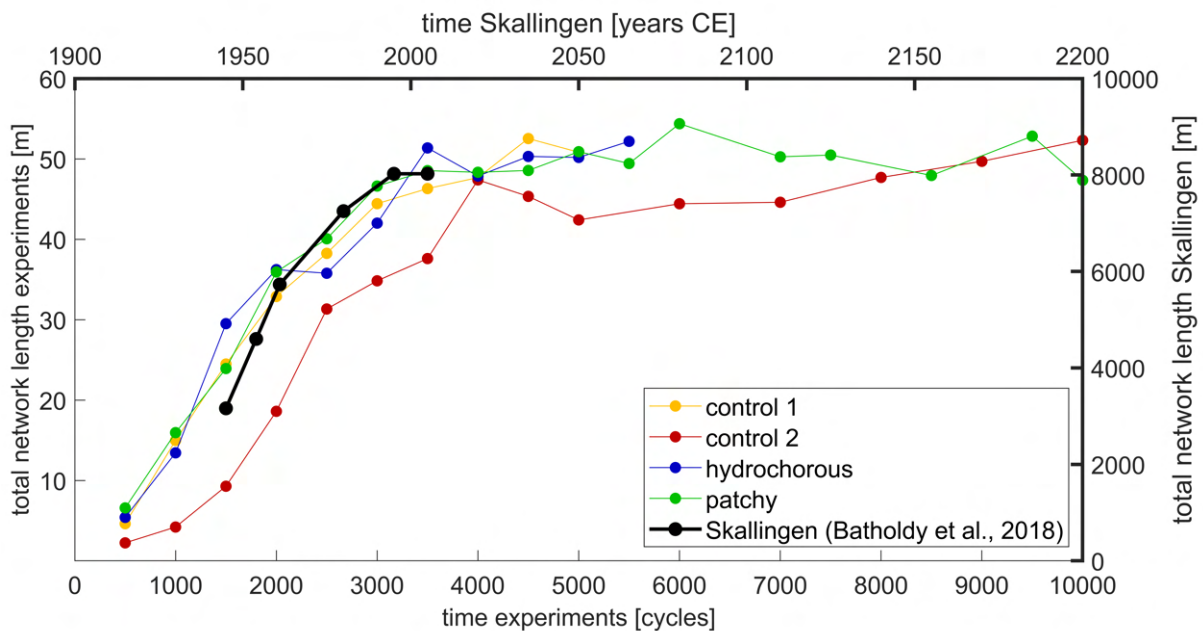


Figure 5.3.: Evolution of the total network length ΣL in the experiments and at Skallingen, Denmark, as found by Bartholdy et al. (2018)

The channel network expansion happens logarithmically (see fig. 4.15 a)). This can also be observed in the development of natural salt marshes (Bartholdy et al., 2018). A comparison of the development of the experiments with the development of the salt marshes at the back-side of the Skallingen spit in Denmark, which started developing around the year 1900 (Bartholdy et al., 2018), shows that the system evolution in the experiments can represent a natural salt marsh development over a few hundred years (see fig. 5.3). But of course, the speed of salt marsh development and channel network expansion can differ significantly between sites in nature.

5.5. Comparison with natural salt marshes

Within this project, experimental salt marshes were successfully created for the first time. The experimental systems, especially the vegetated ones, show some major similarities with real salt marsh systems. Large natural salt marsh systems often have a main trunk channel which penetrates relatively straight far into the system. Several side channels branch off from these main channels and are generally much smaller than the main channel (see also fig. 2.3). This was also visible in both vegetated experiments. Unvegetated intertidal systems on the other hand, often show a split-up into several channels more equally wide already close to the inlet or edge of the system (Kearney & Fagherazzi, 2016). Channels in these systems also do not reach the most landward parts of the system, unlike in vegetated marshes where usually the entire system is dissected by channels of various sizes. This is in line with the differences between vegetated and unvegetated experiments in this study.

But of course there are some major differences between the experimental systems and real world salt marshes as well. A first difference is that the experimental systems emerge by eroding an initially higher surface and carve their channels into the bed, exporting sediment. Natural salt marshes, however, usually are importing systems where sediment is deposited (Bartholdy et al., 2018) and channels emerge where the hydrodynamic conditions do not allow for deposition. But erosion of sediment by channels also occurs, especially with lateral and upstream channel migration and expansion (Bartholdy et al., 2018; Bij de Vaate et al., 2020; Schwarz et al., 2014). This expansion also takes place via backward eroding steps (Kleinhans et al., 2009), similarly to the backward erosion in the experiments. The elevation of the marsh platform is determined by the sediment availability and the species present, as these also actively determine the platform elevation by biogeomorphic feedbacks and biological sedimentation (Marani et al., 2013). Natural salt marsh sediments are usually fine and cohesive (Allen, 2000), which marks another difference to the experiments, where a poorly sorted and relatively coarse sand is used. This is however necessary to limit scale effects (Kleinhans et al., 2017).

The species used in the experiments are another major difference. Studies have shown that biogeomorphic effects can be very species specific (Bij de Vaate et al., 2020). Unfortunately, real salt marsh species like *Spartina anglica* or *Salicornia europaea* are unsuitable for the use in laboratory

experiments. The species used, *Lotus pedunculatus*, has been used successfully in the past and is a suitable plant for scaled landscape experiments (Kleinhans et al., 2022; Lokhorst et al., 2019; Weisscher et al., 2022). Only one species is used, which also does not represent the diversity of natural salt marshes (Allen, 2000; Boorman, 1999). However, when tidal flats are initially colonised by vegetation, this is usually done by a single species and other species follow later (Schwarz et al., 2018). The colonisation by different species is also dependent on elevation and inundation frequency (Allen, 2000). Here, the spring-neap cycle of natural tides can have a significant effect, which is absent as well in the experiments.

A major difference in the resulting morphology is that channels in real salt marsh systems are usually much longer and also much more sinuous. The length of channels in the experimental system is limited by the basin dimensions and the tilting period. Longer systems are unsuitable because not all the water can be drained through the inlet then. Wider inlets are not useful as the width of the flume is limited and the system would reach the hard boundary condition of the flume walls too fast. The lower sinuosity of the channels is likely to be connected to the fact that the tilting of the flume drives the flow. This tilting of course always happens over the same axis and therefore imposes a gradient in a single direction whereas water surface gradients in natural systems are not necessarily oriented in one single direction from landward to seaward. The tilting is, however, generally a suitable method to simulate tidal systems and the one that imposes the least scale effects (Kleinhans et al., 2012; Kleinhans et al., 2017). Another effect of the tilting and the single gradient direction is the emerging shape of the system in the early stages. The channel networks then have a similar shape to a coniferous tree. In natural systems where water surface gradients are theoretically only dependent on distance from the inlet, such a shape would not develop. Instead, a more hemispherical shape would develop (Boechat Albernaz et al., 2021). This effect is especially visible in the early stages but of course continues later as well and might therefore affect the morphology.

The tilting and the erosional character of the experimental systems might not make them perfectly comparable to nature. This shows for example when certain measures and characteristics of the channel network are compared to those of natural systems (Kearney & Fagherazzi, 2016; Liu et al., 2020). The drainage density of the systems is very high, even considering the small scale, the geometric efficiency in the experiments is generally lower than in natural salt marshes and more comparable to unvegetated systems (Kearney & Fagherazzi, 2016). This implies an over-representation of channels and an, in relation, smaller marsh platform. A lower tilting amplitude might lead to a more reasonable channel development if vegetation is added at the same speed. This would however significantly lengthen the duration of one experiment which makes it practically much less feasible, also due to the emergence of mold and other adverse effects like cohesion caused by algae that occur in vegetated experiments over time. This mismatch between the timescale of channel development and that of vegetation colonisation can also be found in the comparison with the salt marsh development at Skallingen (Bartholdy et al., 2018). While the timescale of the channel development might be comparable to a few centuries of natural development, the

vegetation cover that was observed in the experiments (see fig. 4.12) was, even in the experiment with patchy seeding, much lower than that of a centuries-old natural salt marsh, where often the entire system with exception of the narrow channels themselves, is densely vegetated (Bartholdy et al., 2018) (see also fig. 2.3).

While the comparability to nature might thus be limited, the experiments are still very comparable to each other and the main conclusions are still valid. However, there is one important difference to note regarding the main conclusion. The patch locations in the experiment were determined randomly in advance of the experiment, which resulted in the experiment with patchy seeding showing a less self-organised landscape due to missing feedbacks. This does however not imply that natural systems colonised by species like *Spartina anglica*, that tend to grow in a patchy pattern, will be less self-organised as well. In nature, patch locations are determined by the hydrochorous spread of seeds and the establishment of vegetation in suitable conditions. Less self-organised landscapes therefore do not emerge where patchy patterns are dominant but where the feedback loop between hydrodynamics and vegetation growth is not closed. Patchy patterns can even lead to more self-organised landscapes if the necessary conditions concerning geomorphic development speed and biogeomorphic ability are met (Schwarz et al., 2018).

5.6. Implications for salt marsh restoration and future research

While the locations for vegetation growth are always determined by hydrodynamics in completely natural salt marsh systems and feedback loops are therefore closed, this does not necessarily have to be the case in restoration projects. The feedback loop can remain open if locations of vegetation are not determined naturally, for example if vegetation is planted manually, but it is also conceivable that channels are not in the place where they would emerge naturally. This is also suggested by Vaassen (2022). Salt marsh restoration sites are often characterised by pre-existing ditches which serve as initial tidal channels (Vandenbruwaene et al., 2012). In some cases, these can quickly start to meander and migrate (Wolters et al., 2005) and thereby erode already established vegetation. While Wolters et al. (2005) still advocate for the construction of channels to increase the success of restoration measures as they enhance sedimentation rates and nutrient supply, the results of this study suggest that this has to be done very carefully. The result of such man-made channels might otherwise be a less self-organised landscape with a higher share of bare areas. Self-organised landscapes are usually more resilient and are dissected by a more efficient channel network (Kearney & Fagherazzi, 2016; Liu et al., 2020). This is especially important in a changing climate and with rising sea levels, as the sufficient supply of sediment to the salt marshes is highly dependent on the proximity to channels (Temmerman et al., 2005; C. Wang et al., 2021). Artificial channel construction might therefore enhance the initial development, especially in highly consolidated sediments (Wolters et al., 2005) but might have adverse long-term effects as these channels are not necessarily in the place where they would emerge naturally, so that not all natural feedbacks are included.

Further research is necessary to understand the effects of complete and incomplete biogeomorphic feedbacks on the landscape, its development and the implications thereof for the artificial restoration of natural landscapes. As salt marshes can store high amounts of carbon (Mcleod et al., 2011; Mossman et al., 2021; Ouyang & Lee, 2014), their restoration forms a suitable measure to mitigate climate change. In order for this to be successful, the marshes need to be and stay vegetated, for which a suitable channel network is crucial. Factors determining their development and location thus need better understanding.

Possibilities for future experiments in the Metronome include experiments where patch locations are determined by hydrochorous spreading. These patches could then be expanded in a similar way as in the experiment conducted within the scope of this research. The resulting morphology might be more self-organised and shaped by biogeomorphic feedbacks than the experiments presented here. Experiments could also try to mimic restorations measures more closely, for example by creating initial channels and some patches to start with. Further patch locations could then be chosen individually for each sowing event based on the morphological development. The choice might be subjective then but could aim to sow at locations where patch establishment would be likely in nature. In such a way, it could be investigated, whether a restoration measure with artificial channels and intensive monitoring can be as successful as natural development while maybe being able to speed up the initial establishment of salt marsh vegetation.

6. Conclusion

The four experiments studied in this thesis have shown some notable similarities but also differences, depending on the presence and colonisation pattern of vegetation. Vegetation stabilises banks and slows down flow, causing it to be focused in a clear, straight main channel, thereby enhancing the further landward expansion of the system. The split-up into several channels, and thus also the area with the most eroded surface area and channels per cross-section, occurred further landward in the vegetated experiments.

This behaviour was more clearly visible in the experiment with hydrochorous seed spreading than in the experiment with patchy seeding. This can be explained by the positive feedback loop between low flow velocities, the establishment of vegetation and the resulting further reduction of flow velocities. It was complete in the experiment with hydrochorous seed spreading but the loop remained open in the experiment with patchy seeding since the patch locations were randomly pre-determined. A classification in the integrated concept on the conditions for biogeomorphic interactions clarifies these differences. The experiment with patchy seeding is characterised by a lower biogeomorphic ability. In combination with a more active geomorphic development, this results in it reaching only the edge of the biogeomorphic feedback window whereas the experiment with hydrochorous seed spreading reaches the centre of the biogeomorphic feedback window.

This is however not independent of scale. Locally, the experiment with patchy seeding even showed stabilisation, due to the relatively high vegetation cover and density in the patches. Despite that, the locations of the patches are not always ideal and their biogeomorphic ability on the overall scale is lower, shown by the large-scale erosion of patches. The missing feedback between hydrodynamics and the location of vegetation establishment thus results in a less self-organised landscape, showing how crucial complete feedback loops are for biogeomorphic interactions. This needs to be taken into account in possible salt marsh restoration measures. The creation of artificial channels in pre-determined locations might be as sub-optimal as the planting of patches in random locations.

Despite the morphological differences, quantitative measures of the overall systems, like eroded volume, drainage density, mean unchannelled path length or geometric efficiency, were fairly similar. Differences between the experiments were insignificant, showing that these are mainly determined by hydrodynamic boundary conditions, but also underlining the comparability of the experiments. Differences only became visible when the variables mentioned above were analysed along the flume, showing the further landward expansion of the vegetated systems. Vegetation also amplified the emergence of supratidal area, whereas differences in sub- and intertidal area were insignificant.

Appendix

A. Channel network maps

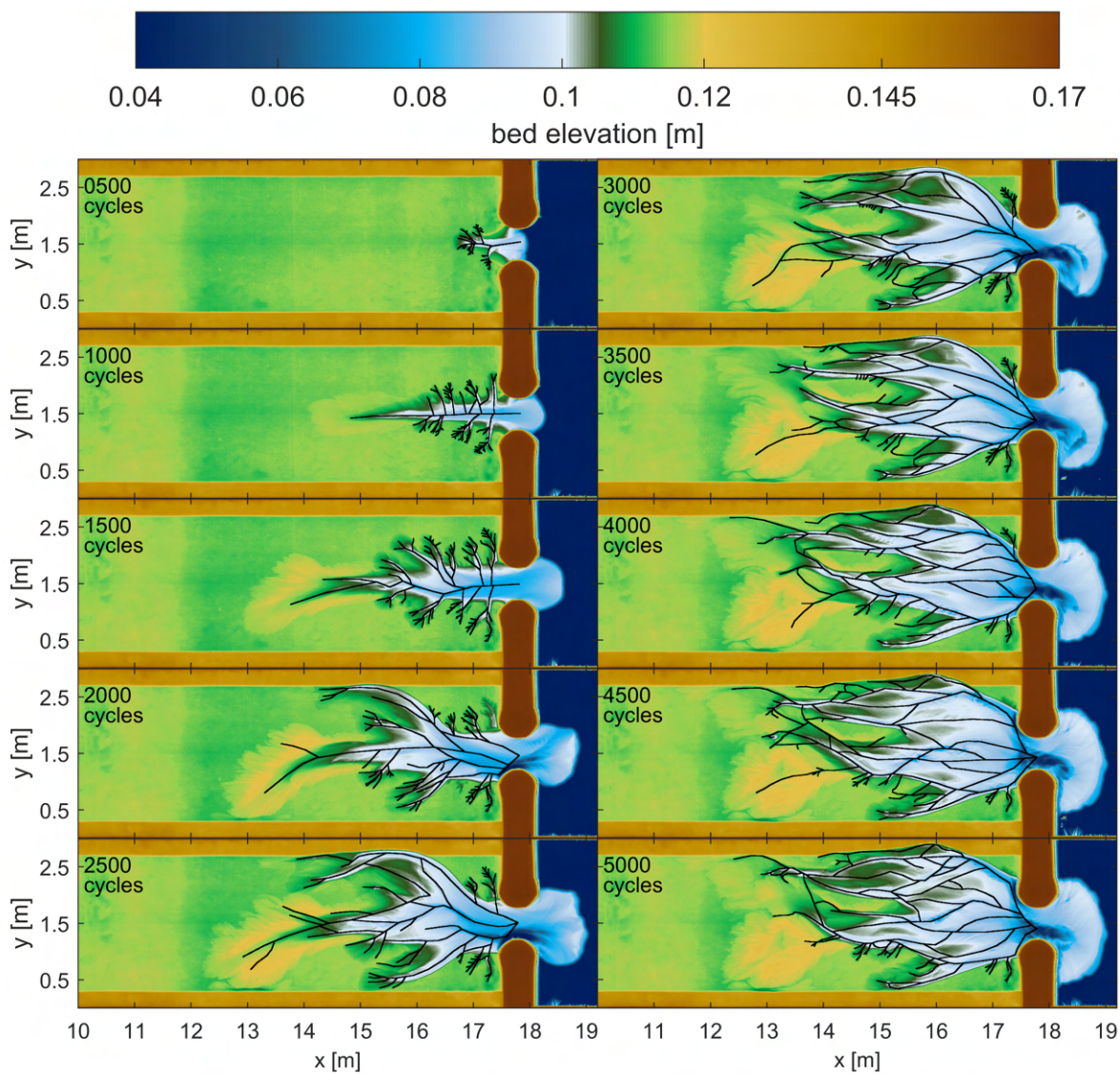


Figure A.1.: Maps of the digitised channel networks in all timesteps of the first unvegetated control experiment. Black lines indicate the channels.

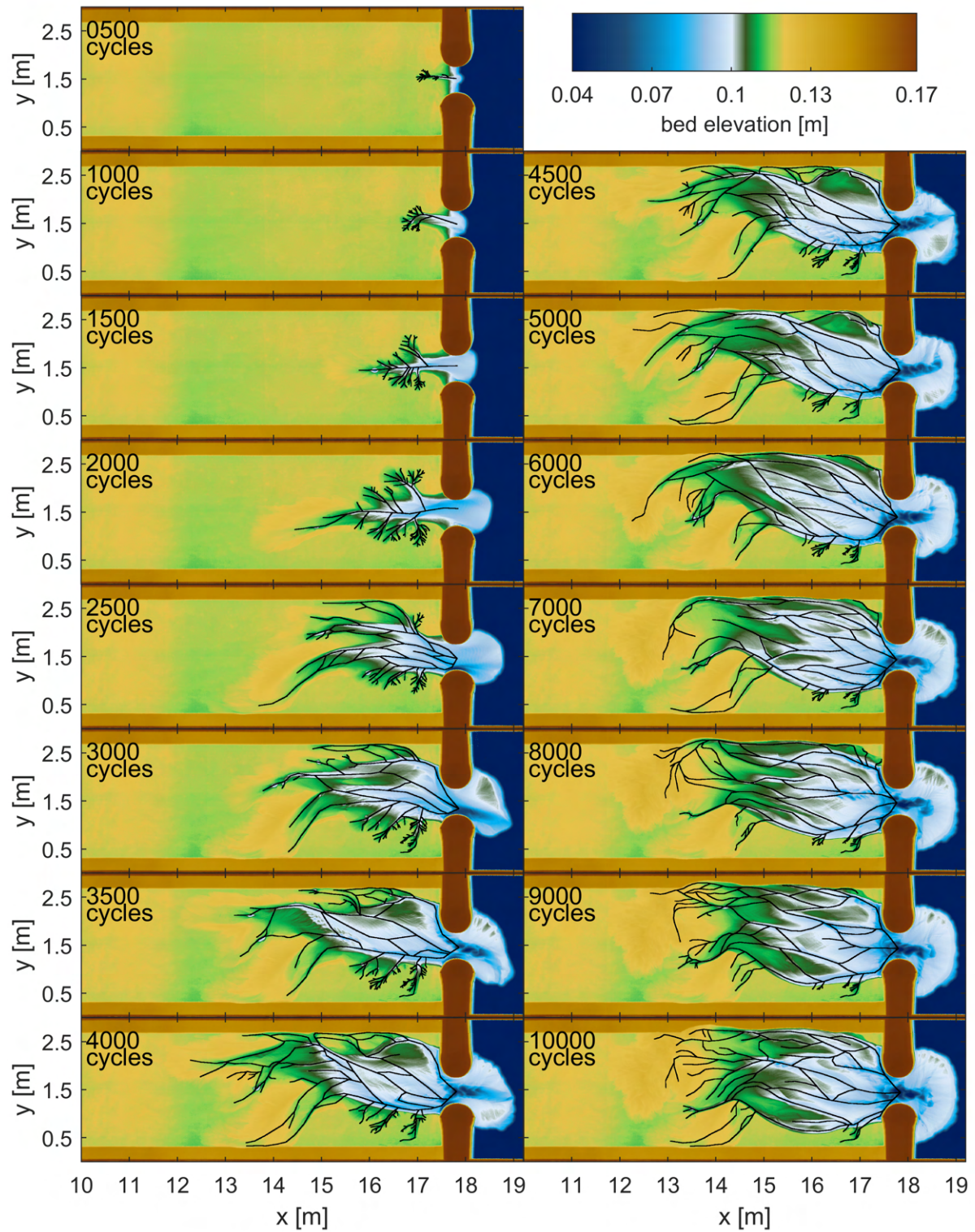


Figure A.2.: Maps of the digitised channel networks in all timesteps of the second unvegetated control experiment. Black lines indicate the channels.

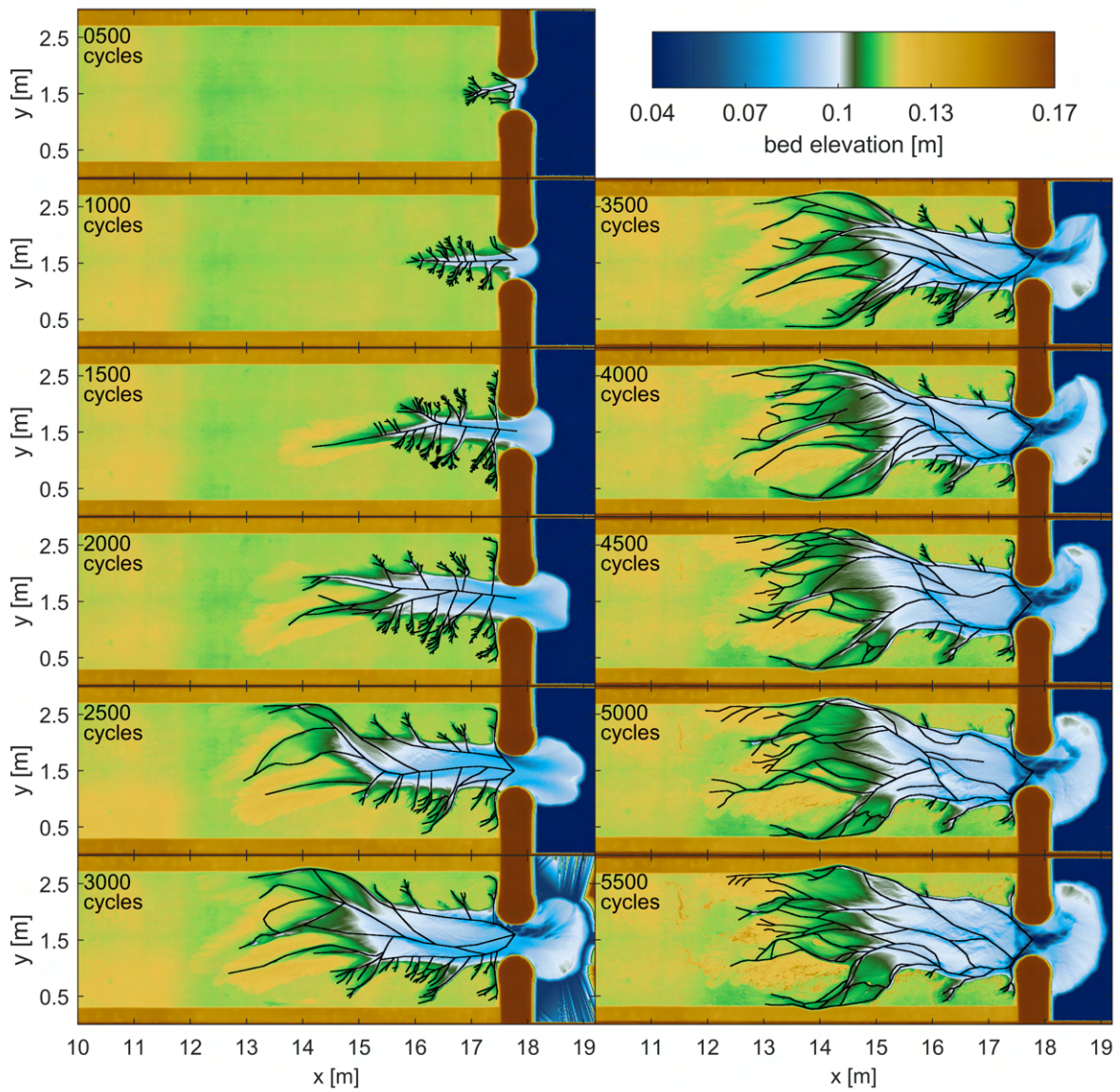


Figure A.3.: Maps of the digitised channel networks in all timesteps of the experiment with hydrochorous seed spreading. Black lines indicate the channels.

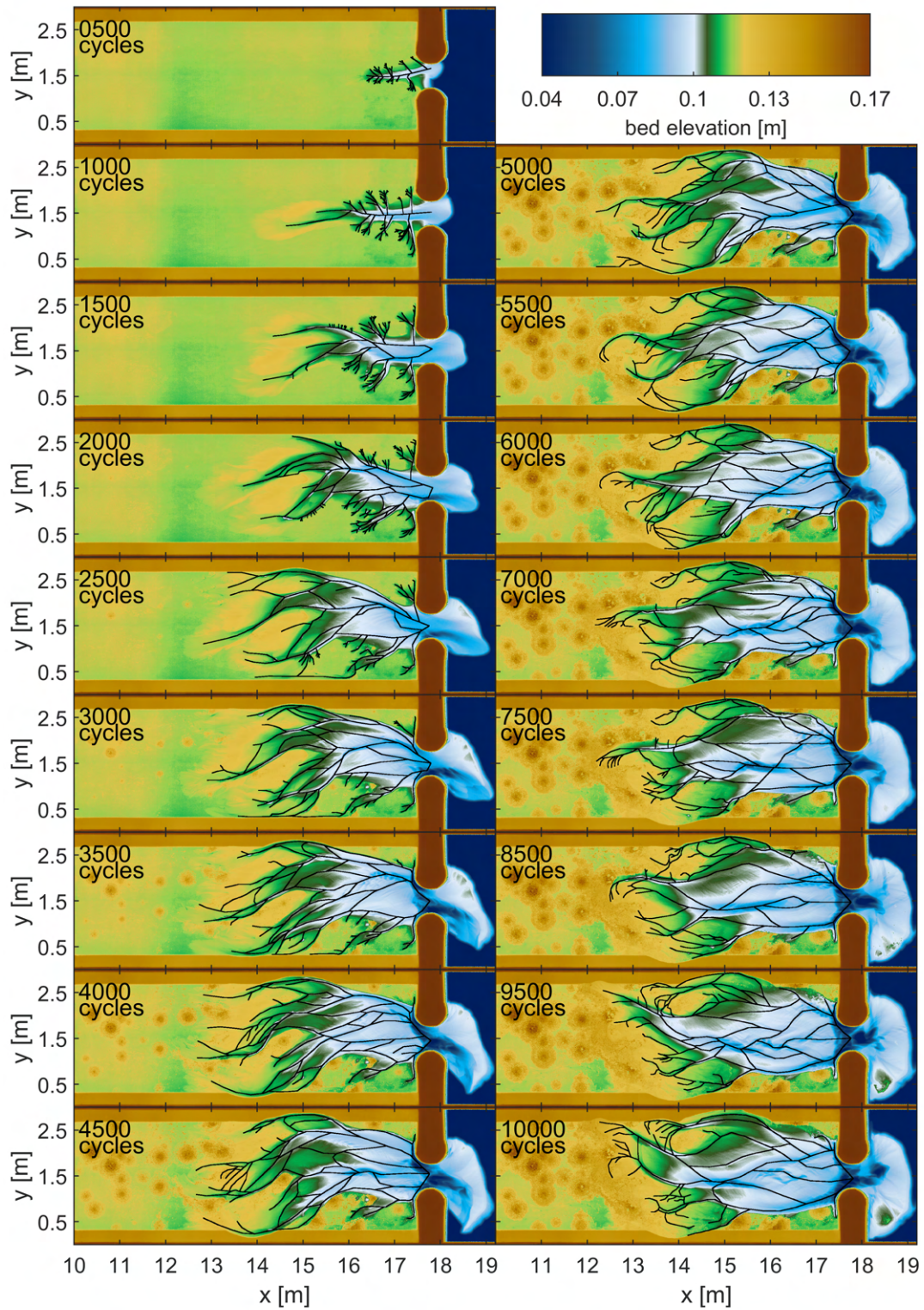


Figure A.4.: Maps of the digitised channel networks in all timesteps of the experiment with patchy seeding. Black lines indicate the channels.

B. Maps of sub-, inter- and supratidal area

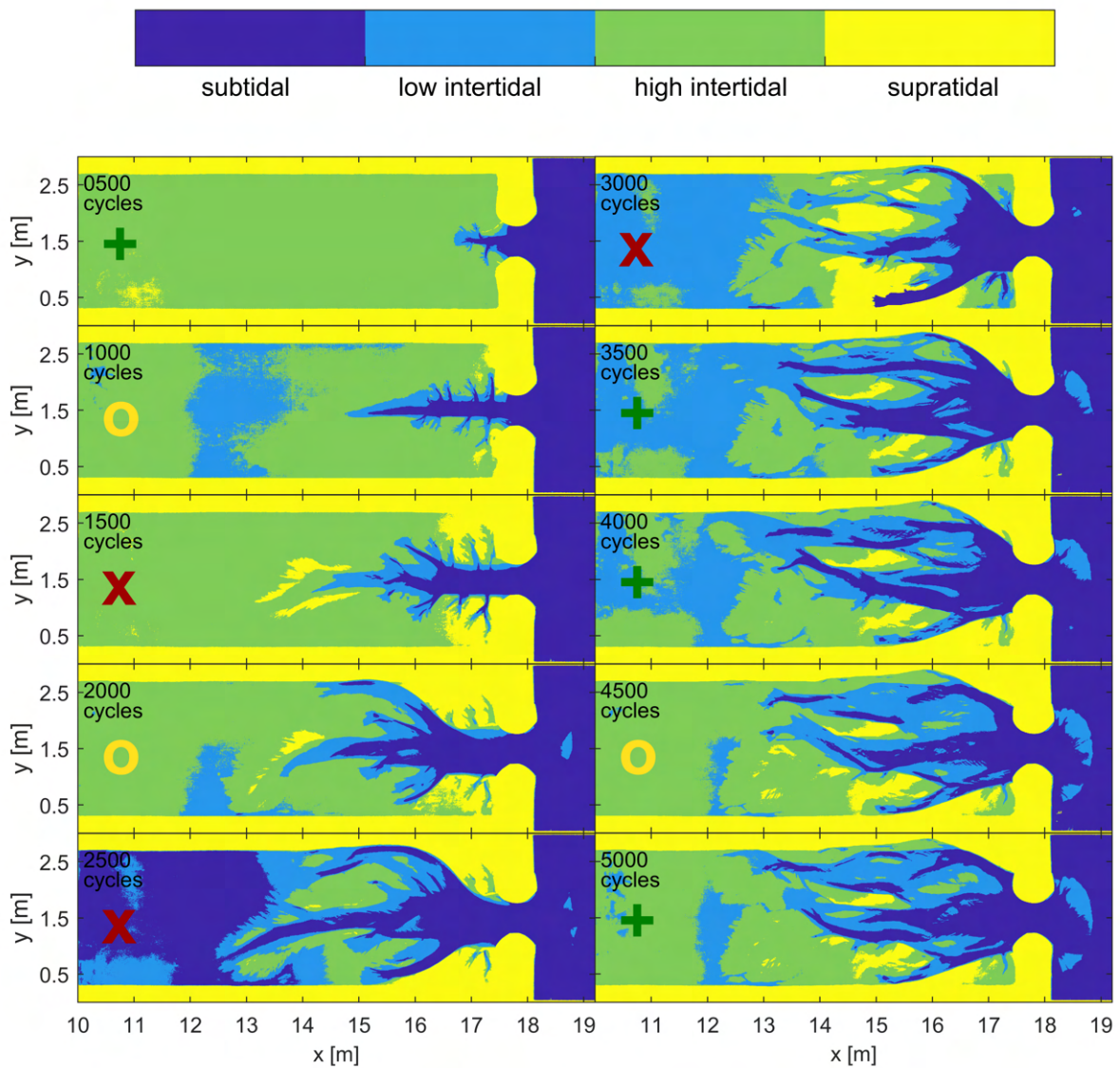


Figure B.1.: Maps of sub-, inter- and supratidal area in the first unvegetated control experiment based on water level measurements. The sign in the landward part indicates the map's quality with a green +, yellow o and red x indicating good, medium and bad quality, respectively.

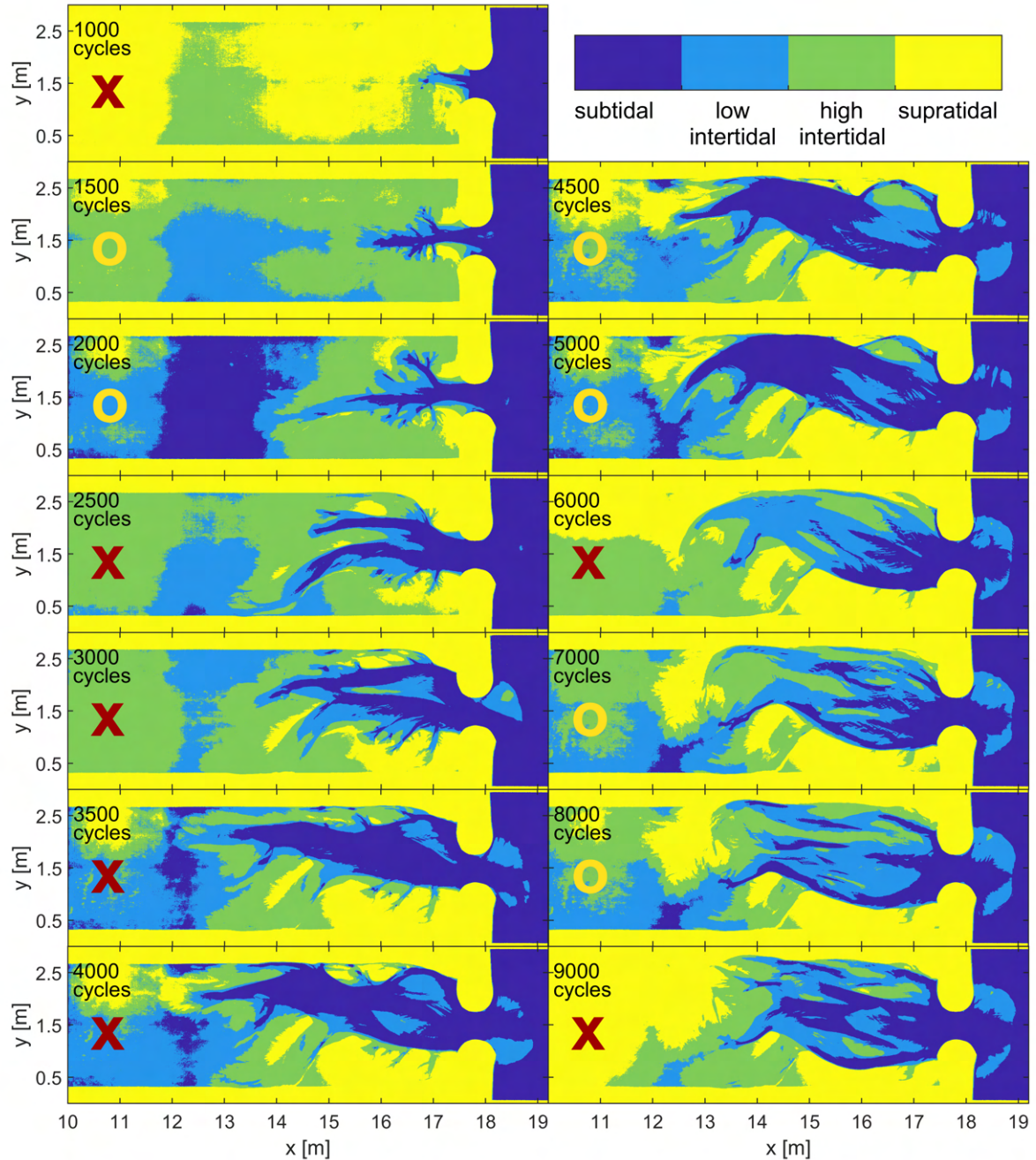


Figure B.2.: Maps of sub-, inter- and supratidal area in the second unvegetated control experiment based on water level measurements. The sign in the landward part indicates the map's quality with a green +, yellow o and red x indicating good, medium and bad quality, respectively. The map for 500 cycles is not shown because all measurements were of poor quality.

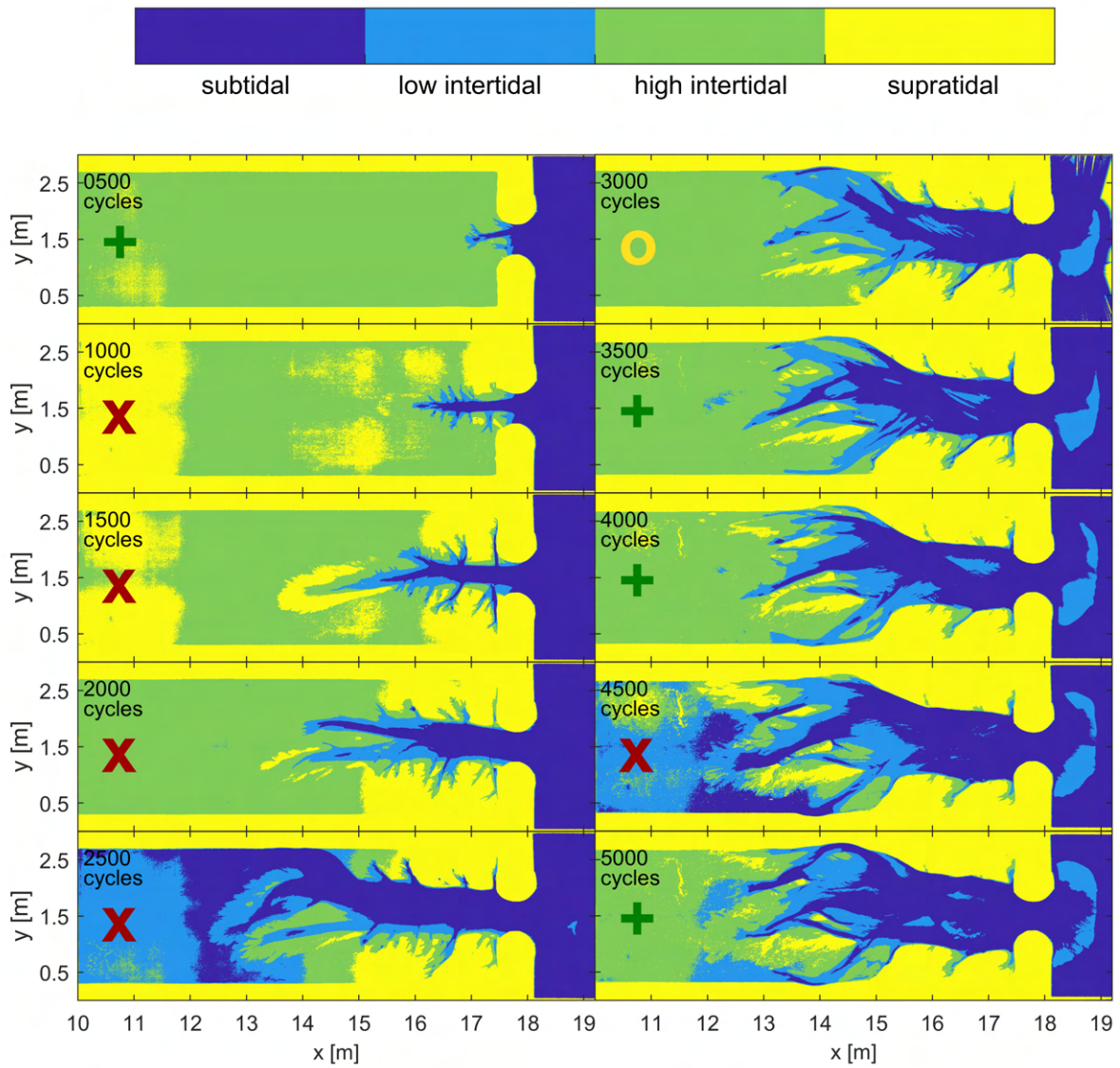


Figure B.3.: Maps of sub-, inter- and supratidal area in the experiment with hydrochorous seed spreading based on water level measurements. The sign in the landward part indicates the map's quality with a green +, yellow o and red x indicating good, medium and bad quality, respectively.

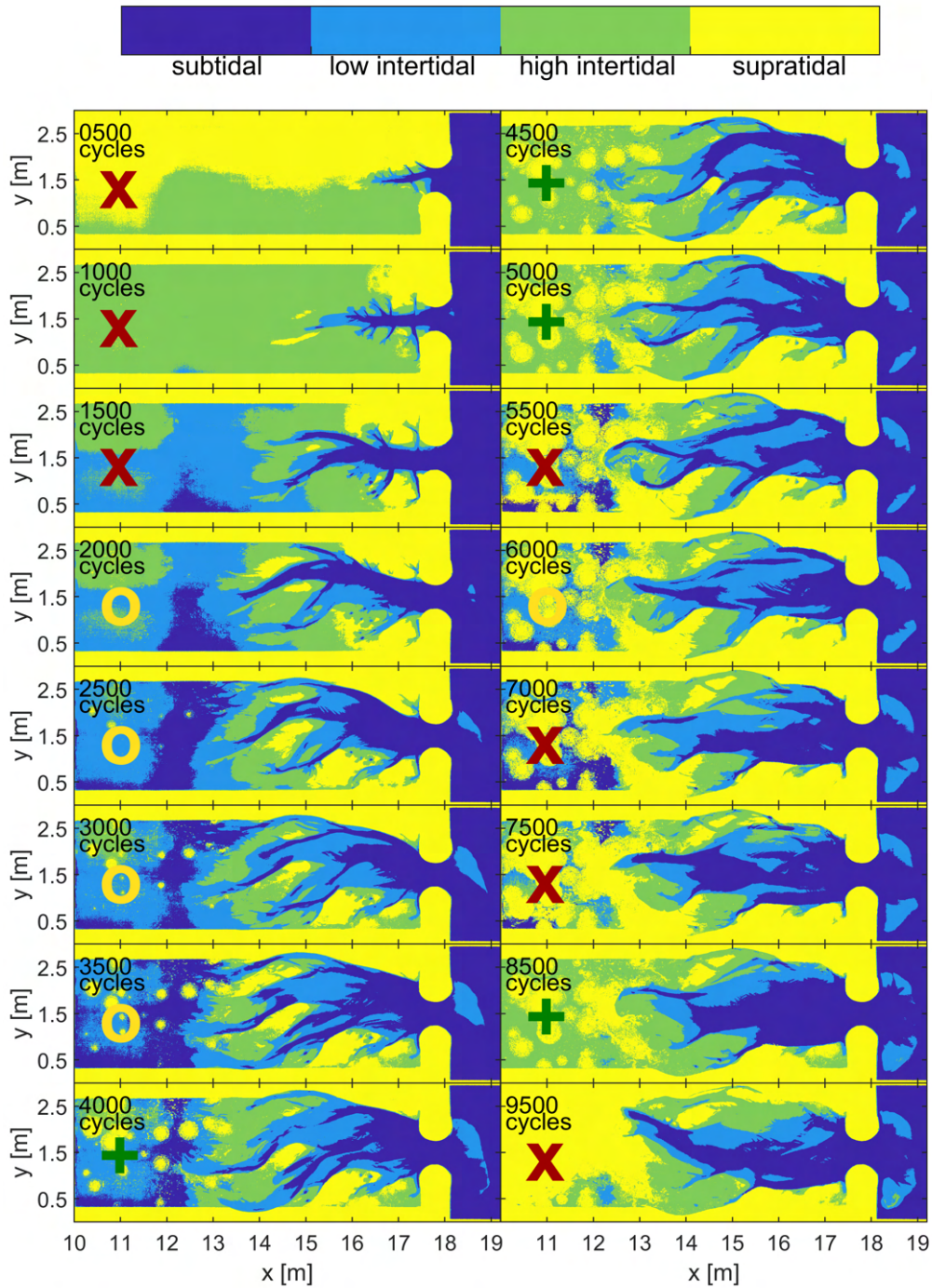


Figure B.4.: Maps of sub-, inter- and supratidal area in the experiment with patchy seeding based on water level measurements. The sign in the landward part indicates the map's quality with a green +, yellow o and red x indicating good, medium and bad quality, respectively.

C. Positions and reliability of water level measurements

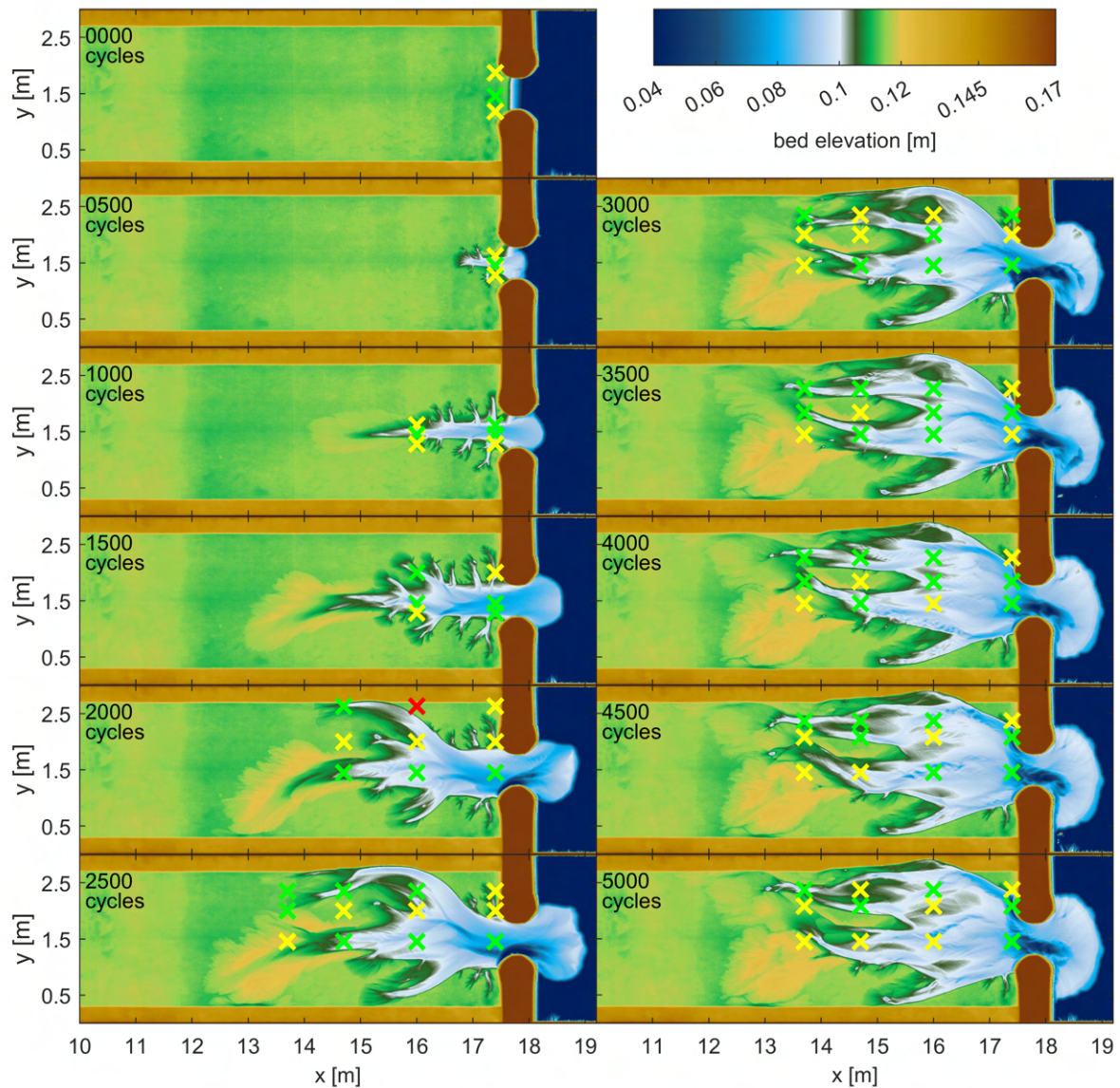


Figure C.1.: Positions and reliability of water level measurements in the first unvegetated control experiment. The positions of the measurements are marked by crosses. Their colour indicates the evaluated reliability. Green indicates reliable high and low water levels, yellow only reliable high water levels and red indicates that both, high and low water levels, are not reliable. There were no measurements where only the low water level was reliable. Additional measurements were conducted seaward of the delta at 19.5 m in x-direction with the same respective positions in y-direction in the corresponding time step. These measurements almost always gave reliable high and low water levels. The measurements in the last time step were conducted shortly before the DEM was taken, instead of afterwards.

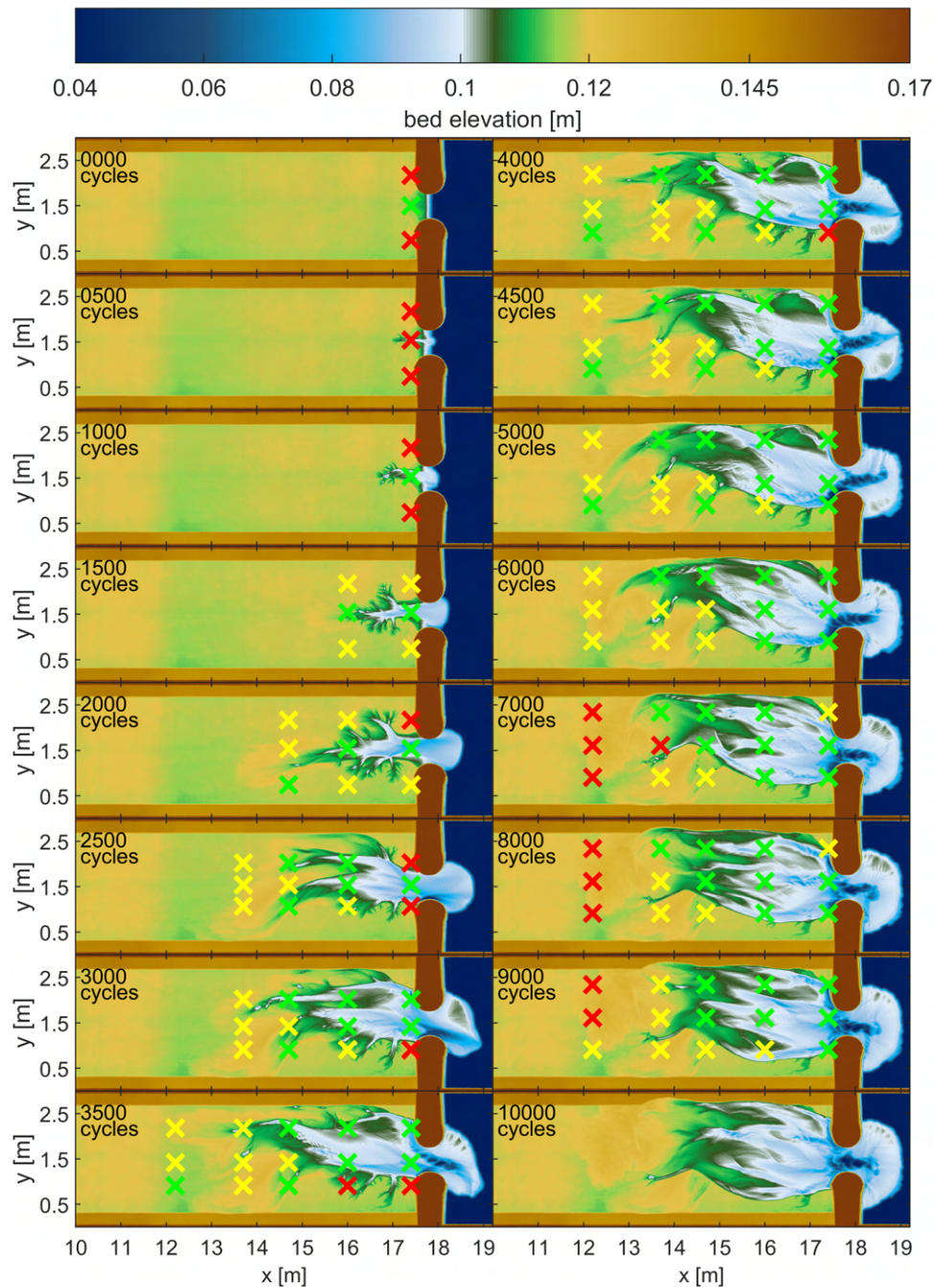


Figure C.2.: Positions and reliability of water level measurements in the second unvegetated control experiment. The positions of the measurements are marked by crosses. Their colour indicates the evaluated reliability. Green indicates reliable high and low water levels, yellow only reliable high water levels and red indicates that both, high and low water levels, are not reliable. There were no measurements where only the low water level was reliable. Additional measurements were conducted seaward of the delta at 19.5 m in x-direction with the same respective positions in y-direction in the corresponding time step. These measurements almost always gave reliable high and low water levels. There are no measurements in the last time step since measurements were always done when the experiment was continued after a DEM was taken.

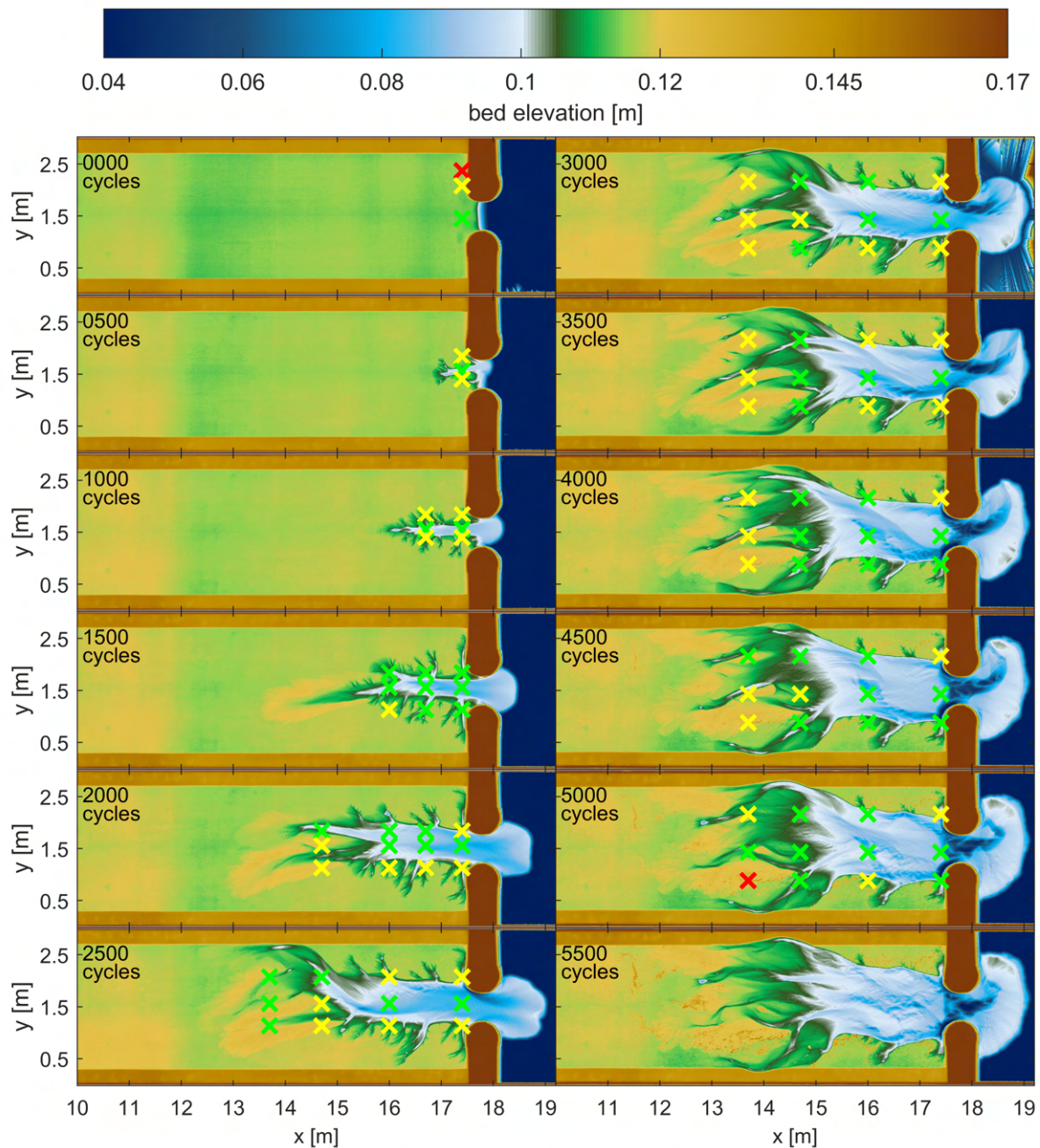


Figure C.3.: Positions and reliability of water level measurements in the experiment with hydrochorous seed spreading. The positions of the measurements are marked by crosses. Their colour indicates the evaluated reliability. Green indicates reliable high and low water levels, yellow only reliable high water levels and red indicates that both, high and low water levels, are not reliable. There were no measurements where only the low water level was reliable. Additional measurements were conducted seaward of the delta at 19.5 m in x-direction with the same respective positions in y-direction in the corresponding time step. These measurements almost always gave reliable high and low water levels. There are no measurements in the last time step since measurements were always done when the experiment was continued after a DEM was taken.

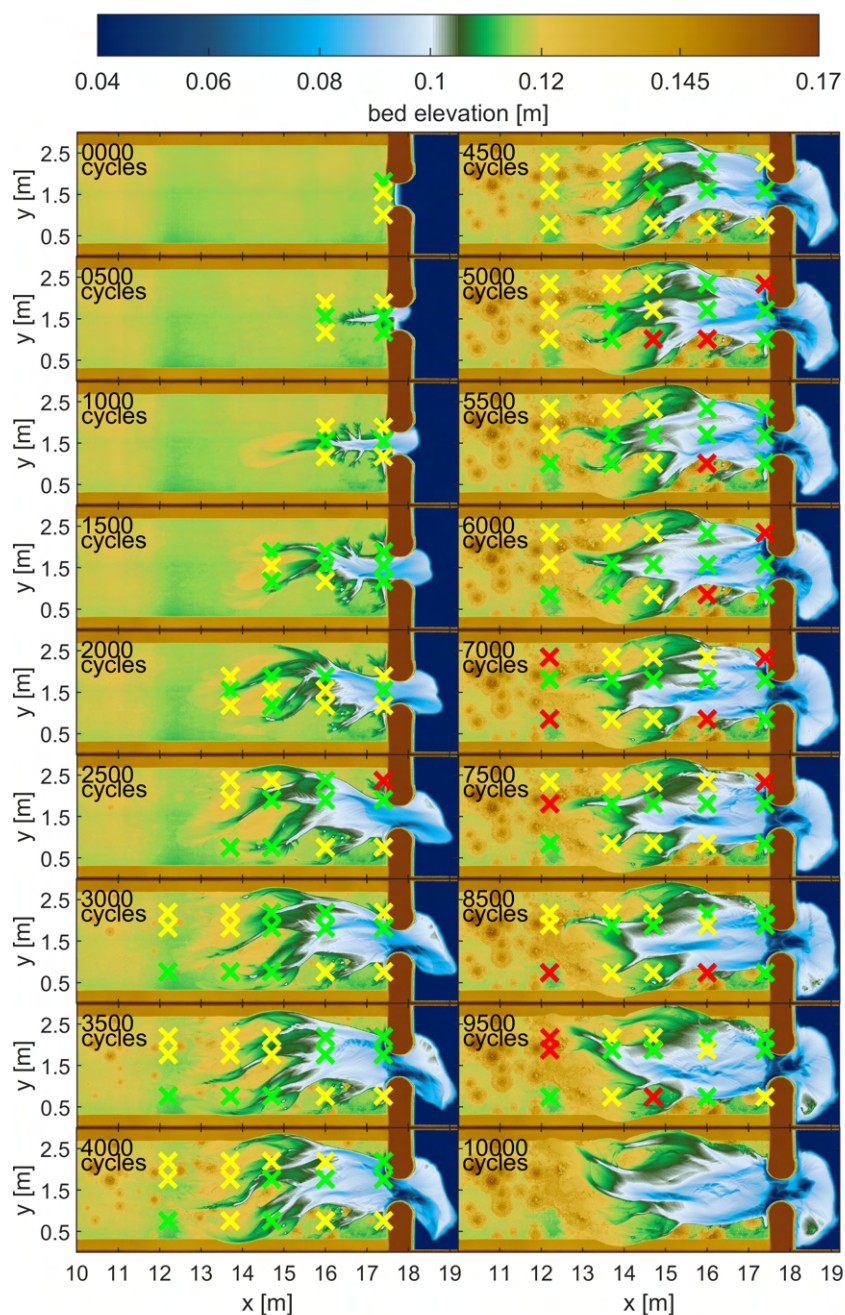


Figure C.4.: Positions and reliability of water level measurements in the experiment with patchy seeding. The positions of the measurements are marked by crosses. Their colour indicates the evaluated reliability. Green indicates reliable high and low water levels, yellow only reliable high water levels and red indicates that both, high and low water levels, are not reliable. There were no measurements where only the low water level was reliable. Additional measurements were conducted seaward of the delta at 19.5 m in x-direction with the same respective positions in y-direction in the corresponding time step. These measurements almost always gave reliable high and low water levels. There are no measurements in the last time step since measurements were always done when the experiment was continued after a DEM was taken.

References

- Allen, J. R. L. (2000). Morphodynamics of holocene salt marshes: A review sketch from the atlantic and southern north sea coasts of europe. *Quaternary Science Reviews*, 19(12), 1155–1231. [https://doi.org/10.1016/S0277-3791\(99\)00034-7](https://doi.org/10.1016/S0277-3791(99)00034-7)
- Baker, R., Taylor, M. D., Able, K. W., Beck, M. W., Cebrian, J., Colombano, D. D., Connolly, R. M., Currin, C., Deegan, L. A., Feller, I. C., Gilby, B. L., Kimball, M. E., Minello, T. J., Rozas, L. P., Simenstad, C., Turner, R. E., Waltham, N. J., Weinstein, M. P., Ziegler, S. L., ... Staver, L. W. (2020). Fisheries rely on threatened salt marshes. *Science*, 370(6517), 670–671. <https://doi.org/10.1126/science.abe9332>
- Baptist, M., Babovic, V., Rodríguez Uthurburu, J., Keijzer, M., Uittenbogaard, R., Mynett, A., & Verwey, A. (2007). On inducing equations for vegetation resistance. *Journal of Hydraulic Research*, 45(4), 435–450. <https://doi.org/10.1080/00221686.2007.9521778>
- Bartholdy, J., Brivio, L., Bartholdy, A., Kim, D., & Fruergaard, M. (2018). The skallingen spit, denmark: Birth of a back-barrier saltmarsh. *Geo-Marine Letters*, 38(2), 153–166. <https://doi.org/10.1007/s00367-017-0523-5>
- Bij de Vaate, I., Brückner, M. Z. M., Kleinhans, M. G., & Schwarz, C. (2020). On the impact of salt marsh pioneer species-assemblages on the emergence of intertidal channel networks. *Water Resources Research*, 56(3), e2019WR025942. <https://doi.org/10.1029/2019WR025942>
- Boechat Albernaz, M., Brückner, M. Z. M., van Maanen, B., van der Spek, A. J. F., & Kleinhans, M. G. (2021). Vegetation reconfigures barrier coasts and affects tidal basin infilling under sea level rise. *Unpublished manuscript*.
- Boorman, L. A. (1999). Salt marshes – present functioning and future change. *Mangroves and Salt Marshes*, 3(4), 227–241. <https://doi.org/10.1023/A:1009998812838>
- Braat, L., Leuven, J. R. F. W., Lokhorst, I. R., & Kleinhans, M. G. (2019). Effects of estuarine mudflat formation on tidal prism and large-scale morphology in experiments. *Earth Surface Processes and Landforms*, 44(2), 417–432. <https://doi.org/10.1002/esp.4504>
- Braudrick, C. A., Dietrich, W. E., Leverich, G. T., & Sklar, L. S. (2009). Experimental evidence for the conditions necessary to sustain meandering in coarse-bedded rivers. *Proceedings of the National Academy of Sciences*, 106(40), 16936–16941. <https://doi.org/10.1073/pnas.0909417106>
- Brückner, M. Z. M., Schwarz, C., van Dijk, W. M., van Oorschot, M., Douma, H., & Kleinhans, M. G. (2019). Salt marsh establishment and eco-engineering effects in dynamic estuaries determined by species growth and mortality. *Journal of Geophysical Research: Earth Surface*, 124(12), 2962–2986. <https://doi.org/10.1029/2019JF005092>

- Cao, H., Zhu, Z., van Belzen, J., Gourgue, O., van de Koppel, J., Temmerman, O. S., Herman, P. M. J., Zhang, L., Yuan, L., & Bouma, T. J. (2021). Salt marsh establishment in poorly consolidated muddy systems: Effects of surface drainage, elevation, and plant age. *Ecosphere*, *12*(9), e03755. <https://doi.org/10.1002/ecs2.3755>
- Childress, N. (2021, September 20). *Bluwhitered*. Retrieved September 20, 2021, from <https://www.mathworks.com/matlabcentral/fileexchange/4058-bluewhitered>
- Corenblit, D., Baas, A. C. W., Bornette, G., Darrozes, J., Delmotte, S., Francis, R. A., Gurnell, A. M., Julien, F., Naiman, R. J., & Steiger, J. (2011). Feedbacks between geomorphology and biota controlling earth surface processes and landforms: A review of foundation concepts and current understandings. *Earth-Science Reviews*, *106*(3), 307–331. <https://doi.org/10.1016/j.earscirev.2011.03.002>
- Costanza, R., de Groot, R., Sutton, P., van der Ploeg, S., Anderson, S. J., Kubiszewski, I., Farber, S., & Turner, R. K. (2014). Changes in the global value of ecosystem services. *Global Environmental Change*, *26*, 152–158. <https://doi.org/10.1016/j.gloenvcha.2014.04.002>
- D’Alpaos, A., Da Lio, C., & Marani, M. (2012). Biogeomorphology of tidal landforms: Physical and biological processes shaping the tidal landscape. *Ecohydrology*, *5*(5), 550–562. <https://doi.org/10.1002/eco.279>
- D’Alpaos, A., Lanzoni, S., Marani, M., & Rinaldo, A. (2007). Landscape evolution in tidal embayments: Modeling the interplay of erosion, sedimentation, and vegetation dynamics. *Journal of Geophysical Research: Earth Surface*, *112*. <https://doi.org/10.1029/2006JF000537>
- D’Alpaos, A., Lanzoni, S., Marani, M., & Rinaldo, A. (2010). On the tidal prism–channel area relations. *Journal of Geophysical Research: Earth Surface*, *115*. <https://doi.org/10.1029/2008JF001243>
- Davidson, K. E., Fowler, M. S., Skov, M. W., Doerr, S. H., Beaumont, N., & Griffin, J. N. (2017). Livestock grazing alters multiple ecosystem properties and services in salt marshes: A meta-analysis. *Journal of Applied Ecology*, *54*(5), 1395–1405. <https://doi.org/10.1111/1365-2664.12892>
- de Groot, R., Brander, L., van der Ploeg, S., Costanza, R., Bernard, F., Braat, L., Christie, M., Crossman, N., Ghermandi, A., Hein, L., Hussain, S., Kumar, P., McVittie, A., Portela, R., Rodriguez, L. C., ten Brink, P., & van Beukering, P. (2012). Global estimates of the value of ecosystems and their services in monetary units. *Ecosystem Services*, *1*(1), 50–61. <https://doi.org/10.1016/j.ecoser.2012.07.005>
- Dijkema, K. S. (1987). Geography of the salt marshes in europe. *Zeitschrift für Geomorphologie*, *31*(4), 489–499. Retrieved April 8, 2022, from <https://www.vliz.be/nl/personen-opzoeken?module=ref&refid=250059>
- Duarte, C. M., Dennison, W. C., Orth, R. J. W., & Carruthers, T. J. B. (2008). The charisma of coastal ecosystems: Addressing the imbalance. *Estuaries and Coasts*, *31*(2), 233–238. <https://doi.org/10.1007/s12237-008-9038-7>

- Eichel, J., Corenblit, D., & Dikau, R. (2016). Conditions for feedbacks between geomorphic and vegetation dynamics on lateral moraine slopes: A biogeomorphic feedback window. *Earth Surface Processes and Landforms*, 41(3), 406–419. <https://doi.org/10.1002/esp.3859>
- Eichel, J., Krautblatter, M., Schmidlein, S., & Dikau, R. (2013). Biogeomorphic interactions in the turtmann glacier forefield, switzerland. *Geomorphology*, 201, 98–110. <https://doi.org/10.1016/j.geomorph.2013.06.012>
- Fagherazzi, S., Bortoluzzi, A., Dietrich, W. E., Adami, A., Lanzoni, S., Marani, M., & Rinaldo, A. (1999). Tidal networks: 1. automatic network extraction and preliminary scaling features from digital terrain maps. *Water Resources Research*, 35(12), 3891–3904. <https://doi.org/10.1029/1999WR900236>
- Fagherazzi, S., Mariotti, G., Leonardi, N., Canestrelli, A., Nardin, W., & Kearney, W. S. (2020). Salt marsh dynamics in a period of accelerated sea level rise. *Journal of Geophysical Research: Earth Surface*, 125(8), e2019JF005200. <https://doi.org/10.1029/2019JF005200>
- Gillespie, A. R., Kahle, A. B., & Walker, R. E. (1987). Color enhancement of highly correlated images. II. channel ratio and “chromaticity” transformation techniques. *Remote Sensing of Environment*, 22(3), 343–365. [https://doi.org/10.1016/0034-4257\(87\)90088-5](https://doi.org/10.1016/0034-4257(87)90088-5)
- Gourgue, O., van Belzen, J., Schwarz, C., Vandenbruwaene, W., Vanlede, J., Belliard, J.-P., Fagherazzi, S., Bouma, T. J., van de Koppel, J., & Temmerman, S. (2021). Biogeomorphic modeling to assess resilience of tidal marsh restoration to sea level rise and sediment supply. *Earth Surface Dynamics Discussions*, 1–38. <https://doi.org/10.5194/esurf-2021-66>
- Greene, C. (2022, March 10). *Circle plotter*. Retrieved March 10, 2022, from <https://www.mathworks.com/matlabcentral/fileexchange/45952-circle-plotter>
- Horton, R. E. (1932). Drainage-basin characteristics. *Eos, Transactions American Geophysical Union*, 13(1), 350–361. <https://doi.org/10.1029/TR013i001p00350>
- Horton, R. E. (1945). Erosional development of streams and their drainage basins; hydrophysical approach to quantitative morphology. *GSA Bulletin*, 56(3), 275–370. [https://doi.org/10.1130/0016-7606\(1945\)56\[275:EDOSAT\]2.0.CO;2](https://doi.org/10.1130/0016-7606(1945)56[275:EDOSAT]2.0.CO;2)
- Hughes, S. A. (2002). Equilibrium cross sectional area at tidal inlets. *Journal of Coastal Research*, 18(1), 160–174. Retrieved April 11, 2022, from <https://www.jstor.org/stable/4299062>
- Jones, C. G., Lawton, J. H., & Shachak, M. (1996). Organisms as ecosystem engineers. In F. B. Samson & F. L. Knopf (Eds.), *Ecosystem management: Selected readings* (pp. 130–147). https://doi.org/10.1007/978-1-4612-4018-1_14
- Kearney, W. S., & Fagherazzi, S. (2016). Salt marsh vegetation promotes efficient tidal channel networks. *Nature Communications*, 7(1), 12287. <https://doi.org/10.1038/ncomms12287>
- Kelleway, J. J., Cavanaugh, K., Rogers, K., Feller, I. C., Ens, E., Doughty, C., & Saintilan, N. (2017). Review of the ecosystem service implications of mangrove encroachment into salt marshes. *Global Change Biology*, 23(10), 3967–3983. <https://doi.org/10.1111/gcb.13727>
- Kirwan, M. L., & Murray, A. B. (2007). A coupled geomorphic and ecological model of tidal marsh evolution. *Proceedings of the National Academy of Sciences*, 104(15), 6118–6122. <https://doi.org/10.1073/pnas.0700958104>

- Kleinhans, M. G., Vegt, M. v. d., Scheltinga, R. T. v., Baar, A. W., & Markies, H. (2012). Turning the tide: Experimental creation of tidal channel networks and ebb deltas. *Netherlands Journal of Geosciences*, *91*(3), 311–323. <https://doi.org/10.1017/S0016774600000469>
- Kleinhans, M. G., Roelofs, L., Weisscher, S. A. H., Lokhorst, I. R., & Braat, L. (2022). Estuarine morphodynamics and development modified by floodplain formation. *Earth Surface Dynamics*, *10*(2), 367–381. <https://doi.org/10.5194/esurf-10-367-2022>
- Kleinhans, M. G., Schuurman, F., Bakx, W., & Markies, H. (2009). Meandering channel dynamics in highly cohesive sediment on an intertidal mud flat in the westerschelde estuary, the netherlands. *Geomorphology*, *105*(3), 261–276. <https://doi.org/10.1016/j.geomorph.2008.10.005>
- Kleinhans, M. G., van der Vegt, M., Leuven, J., Braat, L., Markies, H., Simmelink, A., Roosendaal, C., van Eijk, A., Vrijbergen, P., & van Maarseveen, M. (2017). Turning the tide: Comparison of tidal flow by periodic sea level fluctuation and by periodic bed tilting in scaled landscape experiments of estuaries. *Earth Surface Dynamics*, *5*(4), 731–756. <https://doi.org/10.5194/esurf-5-731-2017>
- Leonardi, N., Carnacina, I., Donatelli, C., Ganju, N. K., Plater, A. J., Schuerch, M., & Temmerman, S. (2018). Dynamic interactions between coastal storms and salt marshes: A review. *Geomorphology*, *301*, 92–107. <https://doi.org/10.1016/j.geomorph.2017.11.001>
- Leuven, J. R. F. W., Braat, L., van Dijk, W. M., de Haas, T., van Onselen, E. P., Ruessink, B. G., & Kleinhans, M. G. (2018). Growing forced bars determine nonideal estuary planform. *Journal of Geophysical Research: Earth Surface*, *123*(11), 2971–2992. <https://doi.org/10.1029/2018JF004718>
- Liu, Z., Fagherazzi, S., She, X., Ma, X., Xie, C., & Cui, B. (2020). Efficient tidal channel networks alleviate the drought-induced die-off of salt marshes: Implications for coastal restoration and management. *Science of The Total Environment*, *749*, 141493. <https://doi.org/10.1016/j.scitotenv.2020.141493>
- Liu, Z., Gourgue, O., & Fagherazzi, S. (2022). Biotic and abiotic factors control the geomorphic characteristics of channel networks in salt marshes. *Limnology and Oceanography*, *67*(1), 89–101. <https://doi.org/10.1002/lno.11977>
- Loconsole, D., Cristiano, G., & De Lucia, B. (2019). Glassworts: From wild salt marsh species to sustainable edible crops. *Agriculture*, *9*(1), 14. <https://doi.org/10.3390/agriculture9010014>
- Lokhorst, I. R., de Lange, S. I., van Buiten, G., Selaković, S., & Kleinhans, M. G. (2019). Species selection and assessment of eco-engineering effects of seedlings for biogeomorphological landscape experiments. *Earth Surface Processes and Landforms*, *44*(14), 2922–2935. <https://doi.org/10.1002/esp.4702>
- Marani, M., Belluco, E., D’Alpaos, A., Defina, A., Lanzoni, S., & Rinaldo, A. (2003). On the drainage density of tidal networks. *Water Resources Research*, *39*(2). <https://doi.org/10.1029/2001WR001051>

-
- Marani, M., Lio, C. D., & D'Alpaos, A. (2013). Vegetation engineers marsh morphology through multiple competing stable states. *Proceedings of the National Academy of Sciences*, *110*(9), 3259–3263. <https://doi.org/10.1073/pnas.1218327110>
- Martínez-Cagigal, V. (2022, January 11). *Custom colormap*. Retrieved January 11, 2022, from <https://www.mathworks.com/matlabcentral/fileexchange/69470-custom-colormap>
- Mcleod, E., Chmura, G. L., Bouillon, S., Salm, R., Björk, M., Duarte, C. M., Lovelock, C. E., Schlesinger, W. H., & Silliman, B. R. (2011). A blueprint for blue carbon: Toward an improved understanding of the role of vegetated coastal habitats in sequestering CO₂. *Frontiers in Ecology and the Environment*, *9*(10), 552–560. <https://doi.org/10.1890/110004>
- McMahon, W. J., & Davies, N. S. (2018). The shortage of geological evidence for pre-vegetation meandering rivers. *Fluvial meanders and their sedimentary products in the rock record* (pp. 119–148). <https://doi.org/10.1002/9781119424437.ch5>
- Mcowen, C., Weatherdon, L., Bochove, J.-W., Sullivan, E., Blyth, S., Zockler, C., Stanwell-Smith, D., Kingston, N., Martin, C., Spalding, M., & Fletcher, S. (2017). A global map of salt-marshes. *Biodiversity Data Journal*, *5*, e11764. <https://doi.org/10.3897/BDJ.5.e11764>
- Möller, I., Kudella, M., Rupprecht, F., Spencer, T., Paul, M., van Wesenbeeck, B. K., Wolters, G., Jensen, K., Bouma, T. J., Miranda-Lange, M., & Schimmels, S. (2014). Wave attenuation over coastal salt marshes under storm surge conditions. *Nature Geoscience*, *7*(10), 727–731. <https://doi.org/10.1038/ngeo2251>
- Mossman, H. L., Pontee, N., Born, K., Lawrence, P. J., Rae, S., Scott, J., Serato, B., Sparkes, R. B., Sullivan, M. J. P., & Dunk, R. M. (2021, October 12). *Rapid carbon accumulation at a saltmarsh restored by managed realignment far exceeds carbon emitted in site construction*. bioRxiv. <https://doi.org/10.1101/2021.10.12.464124>
- Nelson, J. L., & Zavaleta, E. S. (2012). Salt marsh as a coastal filter for the oceans: Changes in function with experimental increases in nitrogen loading and sea-level rise. *PLOS ONE*, *7*(8), e38558. <https://doi.org/10.1371/journal.pone.0038558>
- Oorschot, M. v., Kleinhans, M., Geerling, G., & Middelkoop, H. (2016). Distinct patterns of interaction between vegetation and morphodynamics. *Earth Surface Processes and Landforms*, *41*(6), 791–808. <https://doi.org/10.1002/esp.3864>
- Ouyang, X., & Lee, S. Y. (2014). Updated estimates of carbon accumulation rates in coastal marsh sediments. *Biogeosciences*, *11*(18), 5057–5071. <https://doi.org/10.5194/bg-11-5057-2014>
- Phillips, J. D. (2006). Deterministic chaos and historical geomorphology: A review and look forward. *Geomorphology*, *76*(1), 109–121. <https://doi.org/10.1016/j.geomorph.2005.10.004>
- Reijers, V. C., Siteur, K., Hoeks, S., van Belzen, J., Borst, A. C. W., Heusinkveld, J. H. T., Govers, L. L., Bouma, T. J., Lamers, L. P. M., van de Koppel, J., & van der Heide, T. (2019). A lévy expansion strategy optimizes early dune building by beach grasses. *Nature Communications*, *10*(1), 2656. <https://doi.org/10.1038/s41467-019-10699-8>
-

- Rinaldo, A., Fagherazzi, S., Lanzoni, S., Marani, M., & Dietrich, W. E. (1999). Tidal networks: 2. watershed delineation and comparative network morphology. *Water Resources Research*, 35(12), 3905–3917. <https://doi.org/10.1029/1999WR900237>
- Rupprecht, F., Möller, I., Paul, M., Kudella, M., Spencer, T., van Wesenbeeck, B. K., Wolters, G., Jensen, K., Bouma, T. J., Miranda-Lange, M., & Schimmels, S. (2017). Vegetation-wave interactions in salt marshes under storm surge conditions. *Ecological Engineering*, 100, 301–315. <https://doi.org/10.1016/j.ecoleng.2016.12.030>
- Schuerch, M., Spencer, T., Temmerman, S., Kirwan, M. L., Wolff, C., Lincke, D., McOwen, C. J., Pickering, M. D., Reef, R., Vafeidis, A. T., Hinkel, J., Nicholls, R. J., & Brown, S. (2018). Future response of global coastal wetlands to sea-level rise. *Nature*, 561(7722), 231–234. <https://doi.org/10.1038/s41586-018-0476-5>
- Schwarz, C., Ye, Q. H., van der Wal, D., Zhang, L. Q., Bouma, T., Ysebaert, T., & Herman, P. M. J. (2014). Impacts of salt marsh plants on tidal channel initiation and inheritance. *Journal of Geophysical Research: Earth Surface*, 119(2), 385–400. <https://doi.org/10.1002/2013JF002900>
- Schwarz, C., Gourgue, O., van Belzen, J., Zhu, Z., Bouma, T. J., van de Koppel, J., Ruessink, G., Claude, N., & Temmerman, S. (2018). Self-organization of a biogeomorphic landscape controlled by plant life-history traits. *Nature Geoscience*, 11(9), 672–677. <https://doi.org/10.1038/s41561-018-0180-y>
- Silvestri, S., Defina, A., & Marani, M. (2005). Tidal regime, salinity and salt marsh plant zonation. *Estuarine, Coastal and Shelf Science*, 62(1), 119–130. <https://doi.org/10.1016/j.ecss.2004.08.010>
- Sonnentag, O., Hufkens, K., Teshera-Sterne, C., Young, A. M., Friedl, M., Braswell, B. H., Milliman, T., O’Keefe, J., & Richardson, A. D. (2012). Digital repeat photography for phenological research in forest ecosystems. *Agricultural and Forest Meteorology*, 152, 159–177. <https://doi.org/10.1016/j.agrformet.2011.09.009>
- Stallins, J. A. (2006). Geomorphology and ecology: Unifying themes for complex systems in biogeomorphology. *Geomorphology*, 77(3), 207–216. <https://doi.org/10.1016/j.geomorph.2006.01.005>
- Stefanon, L., Carniello, L., D’Alpaos, A., & Rinaldo, A. (2012). Signatures of sea level changes on tidal geomorphology: Experiments on network incision and retreat. *Geophysical Research Letters*, 39(12). <https://doi.org/10.1029/2012GL051953>
- Tal, M., & Paola, C. (2010). Effects of vegetation on channel morphodynamics: Results and insights from laboratory experiments. *Earth Surface Processes and Landforms*, 35(9), 1014–1028. <https://doi.org/10.1002/esp.1908>
- Temmerman, S., Bouma, T. J., Govers, G., & Lauwaet, D. (2005). Flow paths of water and sediment in a tidal marsh: Relations with marsh developmental stage and tidal inundation height. *Estuaries*, 28(3), 338–352. <https://doi.org/10.1007/BF02693917>

- Temmerman, S., Bouma, T., Van de Koppel, J., Van der Wal, D., De Vries, M., & Herman, P. (2007). Vegetation causes channel erosion in a tidal landscape. *Geology*, 35(7), 631–634. <https://doi.org/10.1130/G23502A.1>
- Townend, I., Fletcher, C., Knappen, M., & Rossington, K. (2011). A review of salt marsh dynamics. *Water and Environment Journal*, 25(4), 477–488. <https://doi.org/10.1111/j.1747-6593.2010.00243.x>
- Vaassen, S. (2022). [report on effects of artificially created channels in salt marsh restoration projects] (Internship report). Koninklijk Nederlands Instituut voor Onderzoek der Zee (NIOZ).
- Valiela, I., Lloret, J., Bowyer, T., Miner, S., Remsen, D., Elmstrom, E., Cogswell, C., & Robert Thieler, E. (2018). Transient coastal landscapes: Rising sea level threatens salt marshes. *Science of The Total Environment*, 640-641, 1148–1156. <https://doi.org/10.1016/j.scitotenv.2018.05.235>
- Vandenbruwaene, W., Meire, P., & Temmerman, S. (2012). Formation and evolution of a tidal channel network within a constructed tidal marsh. *Geomorphology*, 151-152, 114–125. <https://doi.org/10.1016/j.geomorph.2012.01.022>
- Vandenbruwaene, W., Bouma, T. J., Meire, P., & Temmerman, S. (2013). Bio-geomorphic effects on tidal channel evolution: Impact of vegetation establishment and tidal prism change. *Earth Surface Processes and Landforms*, 38(2), 122–132. <https://doi.org/10.1002/esp.3265>
- van Dijk, W. M., Teske, R., van de Lageweg, W. I., & Kleinhans, M. G. (2013). Effects of vegetation distribution on experimental river channel dynamics. *Water Resources Research*, 49(11), 7558–7574. <https://doi.org/10.1002/2013WR013574>
- van Dijk, W. M., Cox, J. R., Leuven, J. R., Cleveringa, J., Taal, M., Hiatt, M. R., Sonke, W., Verbeek, K., Speckmann, B., & Kleinhans, M. G. (2021). The vulnerability of tidal flats and multi-channel estuaries to dredging and disposal. *Anthropocene Coasts*, 4(1), 36–60. <https://doi.org/10.1139/anc-2020-0006>
- Wang, C., Schepers, L., Kirwan, M. L., Belluco, E., D’Alpaos, A., Wang, Q., Yin, S., & Temmerman, S. (2021). Different coastal marsh sites reflect similar topographic conditions under which bare patches and vegetation recovery occur. *Earth Surface Dynamics*, 9(1), 71–88. <https://doi.org/10.5194/esurf-9-71-2021>
- Wang, F., Sanders, C. J., Santos, I. R., Tang, J., Schuerch, M., Kirwan, M. L., Kopp, R. E., Zhu, K., Li, X., Yuan, J., Liu, W., & Li, Z. (2021). Global blue carbon accumulation in tidal wetlands increases with climate change. *National Science Review*, 8(9), nwaa296. <https://doi.org/10.1093/nsr/nwaa296>
- Weisscher, S. a. H., Van den Hoven, K., Pierik, H. J., & Kleinhans, M. G. (2022). Building and raising land: Mud and vegetation effects in infilling estuaries. *Journal of Geophysical Research: Earth Surface*, 127(1), e2021JF006298. <https://doi.org/10.1029/2021JF006298>
- Wiberg, P. L., Fagherazzi, S., & Kirwan, M. L. (2020). Improving predictions of salt marsh evolution through better integration of data and models. *Annual Review of Marine Science*, 12, 389–413. <https://doi.org/https://doi.org/10.1146/annurev-marine-010419-010610>

- Woebbecke, D. M., Meyer, G. E., Von Bargen, K., & Mortensen, D. A. (1995). Color indices for weed identification under various soil, residue, and lighting conditions. *Transactions of the ASAE (USA)*, *38*(1), 259–269. <https://doi.org/https://doi.org/10.13031/2013.27838>
- Wolters, M., Garbutt, A., & Bakker, J. P. (2005). Salt-marsh restoration: Evaluating the success of de-embankments in north-west europe. *Biological Conservation*, *123*(2), 249–268. <https://doi.org/10.1016/j.biocon.2004.11.013>

Acknowledgements

First of all, I want to thank my supervisors Maarten Kleinhans and Jana Eichel for the opportunity of writing this thesis, insightful discussions and the helpful comments on earlier versions of this thesis.

Verder ben ik dankbaar voor de uitgebreide technische ondersteuning door de technici van de Metronoom, Marcel, Henk en Arjan en het altijd flexibele bedenken van toegepaste oplossingen voor een hele hoop problemen. Zonder deze technische kennis waren de experimenten nooit mogelijk geweest.

Nooit mogelijk geweest waren de experimenten natuurlijk ook zonder Sarah en Tim, die met mij de experimenten hebben doorgevoerd. In het begin was het tijdens de pilots wel even uitvogelen hoe we schorren het beste kunnen simuleren, maar daarna was het ook wel veel routine werk, die in me eentje zeker minder leuk en ook nauwelijks mogelijk was geweest. Sarah was hier een grote hulp en gezellige collega, hartelijk bedankt daarvoor en ook voor het tegenlezen van mijn scriptie! Ook Thomas, die het tweede controle experiment, dat we samen waren begonnen, nog zonder mij heeft afgemaakt, mag hier niet ongenoemd blijven.

I am also grateful for the productive discussions on the planning and interpretation of the experiments with Olivier and Stijn from Antwerp, not to forget about the provision of the patch locations.

Sowing those patches proved to be a very time consuming but in turn also not very enjoyable task, which is why I am very thankful for all the help that we received here from many people: Maarten, Jana, the other Jana, Max, Dennis, Tim and Lonneke. Some of these people also helped with shoveling the countless cubic metres of sand in and out of the Metronome, many thanks for that.

The other Jana, along with Steven, deserves special thanks for introducing me to the Metronome and showing me how it works, and how it sometimes doesn't, and how to overcome such problems. I am also thankful for some pieces of code I could make use of.

Verdere ervaring met de Metronoom en verschillende experimentele settings heb ik dan met Josephien en Pelle opgedaan. Dit was vaak heel gezellig en later zeker hulpzaam voor de schor-experimenten, vooral tijdens de pilots.

Danken möchte ich selbstverständlich auch meinem Freund Chris, nicht nur fürs Korrekturlesen, sondern vor allem auch für die moralische Unterstützung und das Festhalten an unserer Beziehung,

obwohl ich in die Niederlande gegangen bin. Danken möchte ich auch Chris' ehemaligem Mitbewohner Leon für die ein oder andere aufmunternde Unterhaltung in der Küche, wenn ich mal wieder an meinem Matlab-Code verzweifelt bin. Sowohl Chris als auch Leon bin ich außerdem dankbar für das Bereitstellen von L^AT_EX-Templates und die Beratung diesbezüglich, ohne die die Erstellung des Layouts dieser Arbeit sicherlich deutlich zeitintensiver gewesen wäre.

Besonders großer Dank gebührt natürlich auch meinen Eltern - fürs Korrekturlesen, aber vor allem auch für moralische und finanzielle Unterstützung im gesamten Studium und trotz meiner Entscheidung, meinen Master im Ausland zu machen. Vielen, vielen Dank dafür!

Statement of originality

I declare that:

1. this is an original report, which is entirely my own work,
2. where I have made use of the ideas of other writers, I have acknowledged the source in all instances,
3. where I have used any diagram or visuals I have acknowledged the source in all instances,
4. this report has not and will not be submitted elsewhere for academic assessment in any other academic course.

Student data:

Name: Jan-Eike Rossius

Registration number: 7062052

Date: August 12, 2022

Signature:

